Regulating Interlayer Spacing and Defects on Nitrogen-Doped Hard Carbon Anodes from Waste Plastic for Sodium-Ion Batteries

by

Qiran Lu

A thesis

presented to the University of Waterloo

in fulfillment of the

thesis requirement for the degree of

Master of Applied Science

in

Chemical Engineering

Waterloo, Ontario, Canada, 2025

© Qiran Lu 2025

Author's Declaration

This thesis consists of material all of which I authored or co-authored: see Statement of Contributions included in the thesis. This is a true copy of the thesis, including any required final revisions, as accepted by my examiners.

I understand that my thesis may be made electronically available to the public.

Statement of Contributions

The body of this thesis is based upon unpublished works.

Chapter 1, 2, 3, 4 of this thesis contain paragraphs from an unpublished review paper of which I am the first author. I conceptualized study design, collected data, and wrote manuscript under the supervision of Dr. Aiping Yu.

Chapter 5 of this thesis contain paragraphs from an unpublished research work of which I am the first author. I conceptualized study design, performed data collection, and constructed the manuscript under the supervision of Dr. Aiping Yu.

Abstract

Sodium-ion batteries (SIBs) are regarded as a promising option among rechargeable batteries for energy storage systems (ESS) due to low-cost and abundant sodium source. One of the key bottleneck problems constraint their commercialization progress is the lack of suitable anode. As a potential choice, hard carbons emerge because of their unique microstructure and sustainable precursors. Nevertheless, capacity and cycling performance of hard carbons are not satisfactory for market needs. The performance of hard carbon is linked to three key microstructural parameters: interlayer spacing, pore architecture, and defect. Suitable interlayer distance enables sodium ions intercalation, while closed pores allow sodium ions fill into. Defect sites on surface facilitate the adsorption of sodium ions. Lasted researches indicate element doping affects both interlayer spacing and defect concentration in hard carbons. It is worth mentioning that waste plastics is a global issue, while these carbon-contained waste are possible to be used as hard carbon precursor. In this thesis, we employed waste polyethylene terephthalate (PET) as raw material, combining with nitrogen doping technique, synthesized nitrogen-doped hard carbon (NHC) as anode for SIBs. This hard carbon contains expanded interlayer and various defect sites, enhancing overall electrochemical performance. Using as anode, it delivers a reversible capacity of 340.4 mAh g^{-1} at 20 mA g^{-1}. At the same time, the complex sodium storage behavior is unveiled by a series of electrochemical measurements. This research not only fulfills the demand of high-performance SIBs anodes, but also promotes a sustainable future.

Acknowledgements

This work has been supported by the University of Waterloo.

I would like to express my sincere gratitude to my supervisor, Dr. Aiping Yu, for her guidance and support during my MASc studies.

I would also like to acknowledge and thank the readers of this thesis: Dr. Aiping Yu, Dr. Tizazu Mekonnen, Dr. Eric Croiset.

Table of Contents

Author’s Declaration ii

Statement of Contributions iii

Abstract iv

Acknowledgements v

List of Figures viii

List of Tables xi

List of Abbreviations xii

Chapter1: Introduction 1

Chapter2: Fundamental and Sodium Storage Mechanism of Hard Carbon Anodes for Sodium-Ion Batteries 3

2.1 Microstructural Characteristics of Hard Carbon 3

2.2 Theoretical Models for Na^+ Storage Mechanisms 4

2.3 Key Structural Parameters for Optimization 7

Chapter3: Literature review: Synthesis Strategies for Hard Carbon 9

3.1 Polymer-Derived Hard Carbon 9

3.1.1 Phenolic resins 9

3.1.2 Waste plastics 10

3.1.3 Other synthetic polymers 11

3.2 Biomass-Derived Hard Carbon 12

3.2.1 Cellulose-based precursors 13

3.2.2 Lignin-based precursors 14

3.2.3 Other biomass sources 14

3.3 Alternative Carbon Sources and Composites 16

3.3.1 Pitch-based hard carbon 16

3.3.2 Templated synthesis of porous hard carbon 17

3.3.3 Hybrid carbon materials 18

Chapter4: Literature review: Structure-Performance Correlation on Hard Carbon 23

4.1 Interlayer Spacing Control 23

4.2 Pore Structure Engineering 26

4.3 Defects and Functional Groups 29

4.4 Future Perspectives 35

Chapter5: Regulating Interlayer Spacing and Defects on Nitrogen-Doped Hard Carbon Anodes from Waste Plastic for Sodium-Ion Batteries 38

5.1 Introduction 38

5.2 Experimental Section 40

5.2.1 Materials and Chemicals 40

5.2.2 Synthesis of Reduced Graphene Oxide (rGO) 40

5.2.3 Synthesis of Multi Walled Carbon Nanotubes (MWCNTs-COOH) 41

5.2.4 Synthesis of Hard Carbon (HC) 41

5.2.5 Synthesis of Nitrogen-doped Hard Carbons (NHC) 41

5.2.6 Material Characterization 41

5.2.7 Electrode Fabrication and Electrochemical Testing 42

5.3 Results and Discussion 42

5.3.1 Morphological and Structural Characterization 42

5.3.2 Surface Chemistry and Defect Engineering 49

5.3.3 Electrochemical Performance Comparison 50

5.3.4 Kinetic and Mechanistic Insights 52

Chapter6: Conclusion 59

Letter of Copyright Permission 61

References 85

List of Figures

Figure 1. (a) Abundance of element in the earth crust. Reproduced with permission[4]. (b) Schematic illustration of SIBs ' work mechanism. Reproduced with permission[4]. (c) Operation voltages and theoretical specific capacities of anode materials for SIBs. Reproduced with permission[6]. 2

Figure 2. The evolution of sodium ions storage mechanisms for hard carbons. Reproduced with permission[16a, 18a, 19, 21a, 22]..... 7

Figure 3. (a) Reversible specific capacities contributed by the plateau and slope regions of epoxy phenol novolac resin hard carbons. Reproduced with permission[34]. (b) Computational simulation model of free volumes in phenolic resin precursor. Reproduced with permission[35]. (c) Synthesis route of resin gel. Reproduced with permission[36]. (d) Charge/discharge curves of PC-hard carbon and PET-hard carbon at different carbonization temperatures. Reproduced with permission[37]. (e) Schematic illustration of nitrogen-doped hard carbon synthesis procedure. Reproduced with permission[38]. (f) Illustration of the information of hollow multicavity carbon spheres. Reproduced with permission[39]. (g) Cycling performance of hyper cross-linked polymers-based hard carbon at 0.5 A g^{-1}. Reproduced with permission[40]. 12

Figure 4. (a) Schematic illustration of the sodium-ion insertion mechanism into nanovoids through micropores based on NMR analysis. Reproduced with permission[46]. (b) Rate performances of carbon anodes at various current densities. Reproduced with permission[47]. (c) HRTEM image of sample from cellulose separator. Reproduced with permission[49]. (d) Rate performance of samples from 25 to 500 mA g^{-1}. Reproduced with permission[51]. (e) Schematic illustration of flash joule heating method. Reproduced with permission[52]. (f) Schematic synthesis route of oxygen-doped carbon microspheres (ONCM) and their cycling performance. Reproduced with permission[54]. (g) Rate performance and capacity retention of hard carbon materials under different current densities. Reproduced with permission[59]. (h) Charge and discharge curves (first cycle) for bamboo-based hard carbons (BP). Reproduced with permission[60]. (i) Cycling performance at 20 mAh g^{-1} for CHC prepared in different heating rates. Reproduced with permission[57]. 16

Figure 5. (a) Cycling performance of KOH - added pitch-derived hard carbon. Reproduced with permission[70]. (b) Modeling of organic groups in carbon layers. Reproduced with permission[71]. (c) Cycling performance of different pitch fractions-derived hard carbons. Reproduced with permission[72]. (d) Rate performance of the N-rich porous carbon nanosheets. Reproduced with permission[62]. (e) SEM image of flower-like MnP-ZnP_2 composites. Reproduced with permission[63]. (f) Cycling performance of hard carbon and vanadium nitride/hard carbon composites. Reproduced with permission[64]. (g) SEM image of Fe_7S_8/N-doped carbonized silk textile. Reproduced with permission[65]. 19

Figure 6. (a) The sloping and plateau regions capacities of hard carbons from celluloses with different crystallinities. Reproduced with permission[77]. (b) Schematic illustration of the sodiation process in hard carbon and hard carbons from crosslinked precursors. Reproduced with permission[78]. (c) ICE comparison of hard carbons from different pyrolysis temperatures.

Reproduced with permission[80]. (d) HRTEM image for hard carbon. Reproduced with permission[84]. (e) Cycling performance of phenolic resin-based hard carbons. Reproduced with permission[85]. (f) Schematic illustration of K-doped hard carbon. Reproduced with permission[86]. 26

Figure 7. (a) Schematic diagram of the closed-pore formation mechanism in the pyrolysis process. Reproduced with permission[11b]. (b) Schematic diagram of the preparation of CVD hard carbon. Reproduced with permission[92]. (c) The comparison of reversible specific capacity and ICE of CVD hard carbon with previous reported hard carbon anodes. Reproduced with permission[93]. (d) Capacity contributions from the plateau and slope regions. Reproduced with permission[94]. (e) Comparison of rate capability between A-2.25-6-T and recently reported hard carbon anode. Reproduced with permission[95]. (f) Cycling performance of RFSH-1400 and RF-1400 in ether-based electrolyte. Reproduced with permission[35]..... 29

Figure 8. (a) Schematic diagram of the optimization mechanism of NP-CNS-T. Reproduced with permission[102]. (b) Schematic diagram of sodium ions absorption/desorption mechanisms in MPTZ-700. Reproduced with permission[103]. (c) Rate performance of all samples from 0.1 to 50 A g^{-1}. Reproduced with permission[104]. (d) The initial charge – discharge curves of D-CSHC and CSHC. Reproduced with permission[105]. (e) Rate performance of the HC-CA-15% anode with reported hard carbon anodes. Reproduced with permission[108]. (f) Cycling performance of BC-1300, L-1300, and A-1300 at 0.1 C. Reproduced with permission[109]. .. 32

Figure 9. (a-c) SEM images of rGO, MWCNTs-COOH and HC; (d) HRTEM and FFT images of NHC-800. 44

Figure 10. (a) N_2 adsorption-desorption isotherms of hard carbons; (b) Pore size distribution of hard carbons. 44

Figure 11. (a) Raman spectra of hard carbons; (b)XRD patterns of hard carbons. 46

Figure 12. Raman fitting curves of hard carbons. 47

Figure 13. XRD fitting curves of hard carbons. 48

Figure 14. (a) XPS survey spectra of NHCs; (b) High-resolution N 1s spectra for NHC-700; (c) High-resolution N 1s spectra for NHC-800; (d) High-resolution N 1s spectra for NHC-900. 50

Figure 15. (a) Cycling performance of rGO, MWCNTs-COOH and HC; (b) Rate performance of rGO, MWCNTs-COOH and HC from 10 mAh g^{-1} to 200 mAh g^{-1} (c) The initial galvanostatic charge-discharge curves of NHCs; (d) Cycling performance of NHCs; (e) Rate performance of NHCs from 10 mAh g^{-1} to 200 mAh g^{-1}. 52

Figure 16. (a) Cyclic voltammograms of rGO; (b) MWCNTs-COOH; (c) HC; (d) NHC-800 at 0.1 mV s^{-1}..... 53

Figure 17. (a) CV curves of rGO at various scan rates from 0.1 to 1 mV s^{-1}; (b) The correlations of current scan rate (v) and peak current (i) of rGO; (c) Capacitive contributions of rGO at various scanning rates; (d) CV curves of MWCNTs-COOH at various scan rates from 0.1 to 1 mV s−1; (e) The correlations of current scan rate (v) and peak current (i) of MWCNTs-COOH; (f) Capacitive contributions of MWCNTs-COOH at various scanning rates; (g) CV curves of

HC at various scan rates from 0.1 to 1 mV s−1; (h) The correlations of current scan rate (v) and peak current (i) of HC; (i) Capacitive contributions of HC at various scanning rates. 55

Figures 18. (a) CV curves of NHC-700 at various scan rates from 0.1 to 1 mV s^{-1}; (b) The correlations of current scan rate (v) and peak current (i) of NHC-700; (c) Capacitive contributions of NHC-700 at various scanning rates; (d) CV curves of NHC-800 at various scan rates from 0.1 to 1 mV s^{-1}; (e) The correlations of current scan rate (v) and peak current (i) of NHC-800; (f) Capacitive contributions of NHC-800 at various scanning rates; (g) CV curves of NHC-900 at various scan rates from 0.1 to 1 mV s^{-1}; (h) The correlations of current scan rate (v) and peak current (i) of NHC-900; (i) Capacitive contributions of NHC-900 at various scanning rates. 56

Figures 19. (a) Diffusion coefficients of sodium ions during the sodiation and desodiation process of HC; (b) Diffusion coefficients of sodium ions during the sodiation and desodiation process of NHC-800; (c) Potential-time curve of NHC-800 for GITT test; (d) EIS of rGO, MWCNTs-COOH, HC and NHC-800. 58

List of Tables

Table 1. Summary of Classification and Properties of Hard Carbon Anodes for SIBs..... 19

Table 2. Summary of Optimization Strategies and Properties of Hard Carbon Anodes for SIBs. 32

Table 3. Physical parameters of the hard carbon samples from Raman spectra..... 48

Table 4. Physical parameters of the hard carbon samples from XRD patterns. 48

Table 5. Relative percentage of different nitrogen species for NHCs. 50

List of Abbreviations

DMC	dimethyl carbonate
EC	ethylene carbonate
EDS	energy-dispersive X-ray spectroscopy
EIS	electrochemical impedance spectroscopy
EVs	electric vehicles
FFT	fast fourier transform
GITT	galvanostatic intermittent titration technique
HC	hard carbon
HRTEM	high-resolution transmission electron microscope
LIBs	lithium-ion batteries
MWCNTs-COOH	multi walled carbon nanotubes
NHC	nitrogen-doped hard carbon
NMP	N-methyl-2-pyrrolidone
PVDF	polyvinylidene fluoride
rGO	reduced graphene oxide
SEI	solid-electrolyte interphase
SEM	scanning electron microscope
SIBs	sodium-ion batteries
XPS	X-ray photoelectron spectroscopy
XRD	X-ray diffraction

Chapter1: Introduction

As modern society evolves, the need for energy resources skyrockets due to the increase in electric vehicles (EVs) and portable electronic devices. At the same time, environmental concerns and the sustainability movement are increasing the need for renewable energy sources. This is where electrical energy storage systems on a large scale come in to enable the equal balance of supply and demand[1]. Rechargeable batteries are considered one of the most efficient technologies in storing and converting electrochemical energy, and they offer portable and stationary solutions.

Lithium-ion batteries (LIBs) maintain their status as the most popular option from the rechargeable battery family due to their successful commercialization, high energy density, and long cycle life, among other factors. However, their long-term prospects are constrained by the uneven distribution and scarcity of lithium resources, thus requiring the hunt for other alternatives to stored energy. On the other hand, sodium is one of the most abundant elements in the Earth's crust(Figure 1a)[2], having been explored as a candidate for batteries since the 1970s and 1980s[3]. In recent years, the development of sodium-ion batteries (SIBs) regained focus after being abandoned for a while, because they are cheaper and more sustainable than LIBs, which makes them useful for large-scale stored energy and electronic devices.

Essentially, an SIB system has two main parts, a positive electrode, or cathode, and a negative electrode or anode, which are separated by an electrolyte that allows for sodium-ion transport(Figure 1b). During charging stages, sodium ions will deintercalate from the positive electrode store and move through the electrolyte to the anode, where they are collected. These ions will travel back to the positive electrode during discharge, completing the electrochemical cycle while outputting electrical energy[4]. Achieving high performance SIBs directly depends on the selection of appropriate electrode materials. SIBs cathodes are quite diverse, usually composed of prussian blue analogues, organic compounds, and transition metal oxides[5].

On the anode side, developing effective sodium storage materials has received the highest attention. To this date, five main mechanisms of sodium-ion storage have been identified: intercalation, which is dominant in carbon materials; conversion; and alloying, conversion-alloy, and organics(Figure 1c)[6]. The merit of carbon materials is their great electrochemical conductivity coupled with long-term chemical stability, in addition to lower cost. The collection of characteristics offered by these materials

makes them extremely useful as SIB anodes. The opposing side includes metals and other potential anode materials such as oxides, sulfides, phosphides, and alloys. These materials are severely hindered by an aggressive volume expansion coupled with particle aggregation which makes them difficult to use in reality[7].

The graphite anode is still the most common type used in LIBs as it has the cheapest market price and offers a high cycle lifespan. On the other hand, even though both lithium and sodium are part of the alkali metals, sodium ions have an ionic radius larger than that of lithium ions, which makes intercalation into the graphite structure very challenging[1]. This obstacle has driven a lot of efforts aimed at non-graphitic carbon materials as SIB anode substitutes. Generally, these materials can be divided into four groups: hard carbon, soft carbon, graphene, and carbon nanotubes. Hard carbon has the ability to endure a disordered structure even at elevated temperatures above 3000 °C and shows promise in sodium storage[8]. On the contrary, soft carbon is able to transform into graphite at high temperature. Additionally, two-dimensional graphene exhibits remarkable electronic conductivity as well as one-dimensional carbon nanotubes which offer a distinct advantage to ion transport.

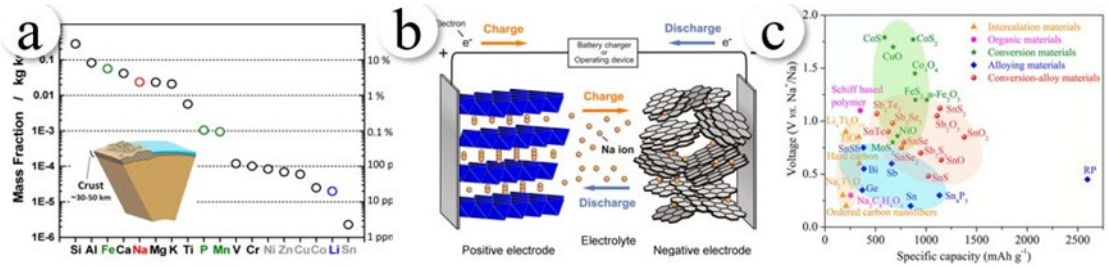


Figure 1. (a) Abundance of element in the earth crust. Reproduced with permission[4]. (b) Schematic illustration of SIBs' work mechanism. Reproduced with permission[4]. (c) Operation voltages and theoretical specific capacities of anode materials for SIBs. Reproduced with permission[6].

Chapter2: Fundamental and Sodium Storage Mechanism of Hard Carbon Anodes for Sodium-Ion Batteries

2.1 Microstructural Characteristics of Hard Carbon

The performance characteristics of sodium-ion storage in anode materials are deeply influenced by the material’ s microstructure. Unlike graphite which has a highly organized layered structure, hard carbon has a microscopic disordered structure which are extensively studied. This disorder is important for how sodium is stored in the material. In hard carbon, graphitized nanodomains, pores and structural defects are incorporated irregularly into the matrix. Some hard carbons contain dopants like nitrogen, boron, sulfur, and phosphorus, which also determines the storage mechanisms of sodium ions and the electrochemical performance of the material.

Graphite-like nanodomains within hard carbon are akin to active sites for the intercalation of sodium ions, much like the processes occurring within lithium-ion intercalated in graphite. The possibility of Na^+ insertion between carbon layers is limited by two factors: interlayer distance (d-spacing) and microcrystallite’s size. They both play an important role. With their highly turbostratic structure, hard carbons tend to have greater interlayer distances than graphite, encountering a greater ease of sodium-ion diffusion and intercalation. The carbon microstructure can be classified into three regimes based on d-spacing: (i) graphite-like ($d < 0.36$ nm), (ii) pseudo-graphitic (0.36 – 0.4 nm), and (iii) highly disordered ($d > 0.4$ nm)[9]. Of these, the pseudo-graphitic phase is best known for its availability and flexibility in hosting reversible Na-ion intercalation, as it offers optimal structural openness and energetic favorable conditions. It is, thus, essential to optimize the proportion of such domains in order to improve plateau capacity and cycling stability over extended periods.

Sodium storage in hard carbon materials is significantly affected by mechanisms such as surface adsorption and geometric filling. Surface-open and closed pores have very different electrochemical behaviors. Pores that are open and accessible to electrolyte solution are generally associated with surface-driven capacitive storage mechanisms, helping to form the sloping region of charge/discharge curves and appearing as quasi-rectangle signatures in cyclic voltammetry (CV) profiles[10]. Furthermore, high specific surface area improves the rate performance due to the rapid Na^+ adsorption and short diffusion pathways.

There are trade-offs, however, too much surface area increases solid electrolyte interphase (SEI) formation and decreases initial Coulombic efficiency (ICE). Closed pores, which are typically created by the coalescence of nanopores or the folding of curved carbon layers during high-temperature pyrolysis, tend to dominate a bulk diffusion-controlled storage process. Also, internal voids can house sodium in ionic or metallic forms such that they primarily contribute to low-voltage plateau capacity[11]. Although advancements have been achieved in designing pore architectures, the fundamental understanding of the relationship between pore type, size distribution, connectivity, and Na-storage behavior remains insufficient and requires further study with in situ and operando characterization techniques.

Defects are integral to hard carbon materials and they significantly assist in sodium-ion storage. These features may include atomic vacancies, edge sites, Stone–Wales defects and other disorder on the local level[12]. These types of defect sites act as centers of high energy adsorption for sodium ion, usually making the sloping region of the high-voltage zone during electrochemical cycling[13]. The pseudocapacitive character of these sites allows for rapid sodium adsorption which therefore increases the rate capability of defect-bearing hard carbon anodes.

Achieving precise control over these defects and measurement of their quantities remains problematic due to their complex and heterogeneous patterns. It is even more difficult to disentangle microstructure and electrochemical behavior because it is a mixture of intrinsic (deriving from the precursor or synthesis path) and extrinsic (added by doping or post treatment) defects. Defect study using Raman spectroscopy is well known, as many parameters, for example, D/G band intensity ratio, peak width, height, and D and G band position shift, convey information regarding one’s degree of disorder and defect density[14]. Supplementary techniques like electron paramagnetic resonance (EPR), X-ray photoelectron spectroscopy (XPS), and high-resolution transmission electron microscopy (HRTEM) such can form a clearer image on the role of defects on sodium storage together with Raman[15].

2.2 Theoretical Models for Na^+ Storage Mechanisms

To electrochemically enhance the performance of hard carbon anodes in sodium-ion batteries (SIBs), a thorough comprehension of the mechanisms behind sodium storage is of utmost importance. Even though considerable work has been done towards the tailoring and making of hard carbon materials, the exact mechanism of sodium storage is still an open question and, along with many researchers, remains actively under investigation. As described in the earlier section, three groups of active sites are mostly

accepted to facilitate sodium storage: the graphitic nanodomain, the pores, and the structural defects of the carbonaceous material. Over time, several theoretical models have been developed to account for the intricate electrochemical behavior of hard carbon, each offering different opinions about the roles of these sites (Figure 2).

One of the earliest and most formally cited mechanisms is the "insertion – filling" mechanism[16], which was introduced in 2000 as part of a landmark study on pyrolyzed glucose derived hard carbon[16a]. This mechanism was accompanied by the now-famous "House of Cards" structural model where they hypothesized that disordered and randomly oriented carbon layers formed weakly packed microstructures. Based on this hypothesis, sodium ions undertake a two-step process to store: first, they are inserted to be fixed between graphitic layers during the higher voltage nearing discharge (sloping region) and afterwards, they gradually fill the nanopores within the carbon matrix at lower voltages (plateau region).

A set of ex situ characterization techniques aided in supporting this interpretation. Structural analyses during charge–discharge cycles in 2011 showed that interlayer spacing undergoes reversible expansion in the sloping region, which was confirmed by a shift of the broad XRD peak to lower angles[17]. Additionally, SAXS measurements showed that changes in pore-related scattering intensities within the plateau region were occupied by sodium. This hypothesis was further confirmed by Raman spectroscopy, which showed that the red shift of the G-band induced by interlayer insertion over the sloping region indicates structural relaxation due to interlayer insertion.

From 2013 onward, an alternative explanation referred to as the "adsorption–intercalation" mechanism became more popular[18]. This mechanism, rooted in BET surface area measurements and XRD data, proposes a chronologically inverted order of events. Marked by the sloping region, sodium ions are proposed to initially adsorb to the surface defects and edge sites leading to the capacitive behavior. When the voltage is decreased further, the ions are posited to intercalate into graphitic domains with appropriate interlayer spacing which gives rise to the low potential plateau.

Experimental evidence supports that theory. It was noted by Ding et al. that the reduction of porosity in hard carbons increased the plateau capacity—this was contrary to the expectation based on the "insertion - filling model." Furthermore, Ex-situ XRD investigations showed that the interlayer distance expanded when sodium was inserted at sub-0.1 V, directly assigning graphitic domains reasoning for the plateau formation[18b]. In 2017, Qiu's group applied in-situ XRD to keep track of phase changes during the discharge - charge cycles. The results obtained showed a total of six unique

stages, where the splitting and merging peaks signified the active intercalation and deintercalation of sodium into the carbon layers[18a].

The "adsorption–filling" model remains the third one and stems from the research conducted in 2018 on hard carbon filled with sulfur. This mechanism refuted the widely accepted explanation for the origin of the plateau region as intercalation. The low-voltage plateau was vanished when the micropores of hard carbon was occupied. Meanwhile, the Raman spectra showed almost no change of G peak during the discharge process, thereby proving intercalation into the graphitic nanodomains was minimal[19]. In 2020, a study based on biomass-derived hard carbon nanotubes provided more evidence. It posited that during deep discharge, clusters of metallic sodium form within closed nanopores, which is what causes the plateau. Extensive data were collected using X-ray photoelectron spectroscopy (XPS) and transmission electron microscopy (TEM), which showed strong proof that sodium was present in an ionic state with above 0.1 V and reversibly transformed into metallic clusters below this value[20].

To explain the increasing behavior intricacies, some researchers have blended previous models into multistage frameworks. An example is the "three-phase" model, which portrays the discharge process as comprising three regions: surface adsorption at high voltages, interlayer intercalation at intermediate voltages, and nanopore filling at low voltages[21]. Studies utilizing the galvanostatic intermittent titration technique (GITT) s suggested that the sodium diffusion coefficients were distinct for each phase and the lowest intercalation kinetics were due to energy barriers between the carbon layers[21a].

This multistage approach was broadened in 2021 into a four-step model as "adsorption–intercalation–pore filling–metallic deposition." The authors, using in situ Raman spectroscopy paired with GITT, demonstrated that sodium fills sites to the pore openings first and thereafter accumulates in excess in clusters as if through deposition[22]. This interpretation articulates the phenomena associated with the gradual capacity increase in the plateau region and highlights the sodium behavior's complexity within disordered carbon matrices.

Collectively, these developing sophisticated mechanisms highlight the complex hard carbon host's sodium storage characteristics. While each model has its own distinct perspective, it is becoming more apparent that no single mechanism is able to explain the diversity of behaviors observed across different carbon architectures. Understanding the relation between different sodiation/desodiation processes using the combination of in situ and operando techniques such as XRD, Raman, and TEM as well

as advanced electrochemical techniques will be critical. A single cohesive theory is needed that integrates all these factors, defect chemistry, structural variabilities, as well as other acts within and around the materials to provide a model suitable for guiding research on hard carbon materials.

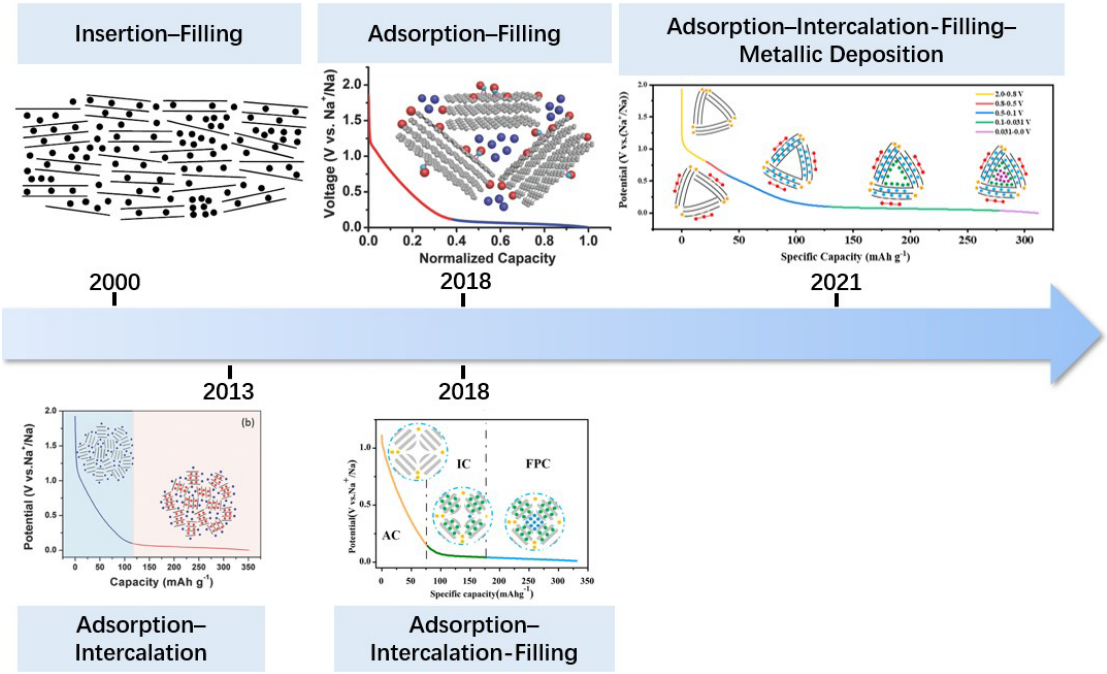


Figure 2. The evolution of sodium ions storage mechanisms for hard carbons. Reproduced with permission[16a, 18a, 19, 21a, 22].

2.3 Key Structural Parameters for Optimization

As described previously, sodium ions interact with hard carbon anodes by intercalation into graphitic nanodomains, pore filling, and adsorption onto defection rich surfaces[23]. These distinct storage pathways are closely associated with specific features of the microstructure of hard carbons. Hence, Adaptive sodium storage capabilities of hard carbons are reliant on the precise definition of three engineering aspects: interlayer spacing, pore architecture, and defect concentration.

Interlayer spacing is one of the most critical parameters that dictate how much sodium ions can be intercalated in the hard carbon anodes. Unlike graphite, which features a well-ordered layered structure, hard carbons are characterized by a disordered, turbostratic arrangement of graphene sheets. As a result, the (002) XRD peaks are broader and less intense than one would expect from a well-defined crystal. The diffuse (002) reflection is associated with disordered carbon and helps distinguish hard carbon from soft carbon, which is more defined in its crystalline characteristics[24].

The sensitivity of sodium ion intercalation to layer spacing distance is remarkable. Only some interlayer spacings from 0.36 to 0.40 nm enable effective sodium intercalation. The barrier to ion insertion becomes a prohibitive energy barrier if below 0.36 nm. On the other hand, if the spacing is greater than 0.40 nm, the layers become loosely packed and true intercalation is replaced with low energy adsorption[25]. Those loosely stacked microdomains do, however, are where the Na^+ insertion energy barrier approaches zero look like adsorption sites and can behave similarly to activated carbon.

The hard carbons' porous architecture unlocks further enhancements in sodium storage, especially for the additional capacity attained at the high-voltage slope. Based on pore dimensions, carbon pores are subdivided into macropores (>50 nm), mesopores (2-50 nm), and micropores (<2 nm)[23]. Among them, the micropores are the most important in sodium storage because they form confined nanospaces which are ideal for ion filling and possible cluster formation[18d].

Several synthesis approaches can be applied to modify the pore structure of hard carbons. Hard templating techniques, like those employing silica nanoparticles, permit the creation of well-defined porous frameworks[26]. The electrospinning[27] and pyrolysis[28] also offer scalable approaches to producing porous carbon with hierarchical structures. Regardless, each method requires strict control of precursor composition, heating rate, and atmosphere to yield desired pore morphology.

It is important to highlight that while pores can enhance capacity, too much porosity can negatively influence the initial Coulombic efficiency due to the surface area accelerating electrolyte decomposition and solid electrolyte interphase (SEI) formation. Thus, a practical range of pore volume and specific surface area is required.

Finally, defect sites have a notable effect toward sodium adsorption, especially assisting in the capacity seen in the sloping voltage region. Usually, these defects exist at the boundary of the disordered graphitic domains or in the amorphous regions. They serve as high-energy sodium ion adsorption sites. While pure graphene suffers from ion-induce capacitance due to defects[29], hard carbons exhibit what is termed "pseudo-adsorption," a hybrid between electrostatic adsorption and intercalation[24].

Chapter3: Literature review: Synthesis Strategies for Hard Carbon

3.1 Polymer-Derived Hard Carbon

As a kind of macromolecular materials, polymers which are formed from repeating units (monomers) have greater chemical and structural tunability. This strategic molecular ability makes them ideal precursors for high-performance hard carbons, especially in the context of anodes for SIBs. Based on thermal responses, polymers can be roughly divided into thermoplastics and thermosets[30]. The former includes polyethylene and polyvinyl chloride, which are linear or branched structured pyrogenic plastics characterized through weak intermolecular bonds, allowing them to be softened and reshaped multiple times upon heating. Thermosetting polymers, for example, epoxy and phenolic resins, differ as these 3D cross-linked polymers do not change when heat and pressure are applied. They become permanently set and possess a cured state. Due to this, thermosets have improved thermal stability and rigidity.

The essential distinctions between these two kinds of polymers have a direct impact on the resulting hard carbon morphology and carbonization behavior. Under melt-alignment conditions, turbostratic domain formation is easier to fulfill in thermoplastics while they carbonize. Thermoplastic flexible chain structures make it easier to foster mesopore development through phase separation during the carbonization process[31]. Thermosets tend to form highly cross-linked, defect-rich amorphous carbons where excess topological defects sodium ions can latch onto at defect regions, which improves its capacity in the sloped section of the discharge profile[32].

Polymer-derived carbons have several advantages. To begin with, the reproducibility and consistency of carbon performance from batch to batch, which is critical for commercial scalability, is guaranteed because of the well-defined and uniform molecular structures of synthetic polymers. Furthermore, many synthetic polymers have heteroatoms like nitrogen, sulfur, oxygen, or phosphorus, which can be incorporated or redistributed during pyrolysis and therefore modified to change electronic conductivity, surface polarity, or active site density. Finally, the polymer chemistry allows modification on molecular scales and thus permits a tailored design of the frameworks of carbon precursors that will determine the pore structure, interlayer spacing, and defect density.

3.1.1 Phenolic resins

Phenolic resins have one of the highest carbon yield percentages (50-60 wt%), and they are the most thermosetting polymers used for hard carbon production. They are easy to

chemically modify, and are characterized with an aromatic rich backbone. They are synthesized from condensation reaction between phenol and formaldehyde, and are classified into resole and novolac types based on the pH of the synthesis environment and the ratios of the reactants[33]. These resins undergo curing followed by pyrolysis which transforms them into carbon structures with rigid, cross-linked networks, and tunable microstructures. Crucial parameters such as heating rate, pyrolysis temperature, and the atmospheres enable control of crosslinking and carbonization which directly influence pore morphology and electrochemical characteristics of the hard carbon produced[32].

Effective ways to improve hard carbons derived from phenolic resins have been reported recently. As an example, Fan et al controlled pyrolysis temperature considerably increases graphitization and to some extent, increases the dimensions of the nanopores which leads to an increase in both plateau capacity as well as total reversible capacity(Figure 3a)[34]. Lin and coworkers also used steric hindrance(Figure 3b) to create closed pores which is vital for Na^+ storage and obtained a specific capacity of 340.3 $mAh \cdot g^{-1}$[35]. As a concern regarding toxicity and sustainability, Beda et al. synthesized Phenolic resins from green raw materials like phloroglucinol and glyoxylic acid(Figure 3c), resulting in hard carbons with low environmental impact that still maintained stable long-term cycling behaviors[36].

3.1.2 Waste plastics

Simultaneously, increasing understanding of plastic waste pollution has sparked interest in converting waste plastics to value-added carbon materials. Plastics like polyethylene terephthalate (PET) and polycarbonate (PC) are particularly favorable for hard carbon synthesis due to the presence of ester or carbonate functional groups in their structure. Their high oxygen content restrains carbon atom rearrangement during pyrolysis, aiding the formation of turbostratic microstructures with greater interlayer spacing. For example, Chen et al. produced hard carbons from PET and PC with a coulombic efficiency (ICE) over 84%(Figure 3d)[37]. Furthermore, PET-derived carbons can be nitrogen doped and obtained with connected mesoporous networks through the 2D self-template method with nitrogen rich compounds like guanine(Figure 3e)[38]. Such structures offer not only efficient pathways for Na^+ transport but also a great number of adsorption sites resulting in higher reversible capacities of 452 $mAh \cdot g^{-1}$ as shown by Zhang and coworkers.

3.1.3 Other synthetic polymers

Apart from upcycling, synthetic polymer chemistry allows for the direct synthesis of carbon precursors with specific desired attributes and functions. Template-assisted polymerization is one such approach. In this process, soft templates such as Pluronic F-127 are used to polymerize monomers e.g., aniline and pyrrole, leading to the generation of uniform polymer spheres[39]. Carbonization of these results in hollow carbon spheres with precisely defined shell thickness and porosity which is optimal for fast sodium ion diffusion and mechanical strength (Figure 3f). Additionally, Ma et al. demonstrated that hyper-crosslinked polymers synthesized from naphthalene and tetraphenylporphyrin-zinc complexes could be carbonized into hard carbons that are robust and have good rate capability and cycling performance(Figure 3g)[40]. Their capacity (e.g. 170 $mAh \cdot g^{-1}$ at 2 $A \cdot g^{-1}$) is moderate, but the tunable structure and mechanical strength makes them attractive for high power use.

To summarize, polymer-derived hard carbons are an exceptionally versatile and tunable class of anode materials for sodium-ion batteries. They exhibit the full advantage of molecular design at the nanoscale, high carbon yield, potential heteroatom doping, and desirable features such as strain engineering in layered materials and hierarchical porosity. Regardless of their origin from commercial polymers, designed resins, or even recycled plastics, these materials provide an economically friendly and scalable way to tailor sodium microstructures for improved sodium storage performance. With the ongoing refinement of carbonization techniques and synthetic approaches, hard polymers are expected to have a growing impact towards the development of the next generation energy storage systems.

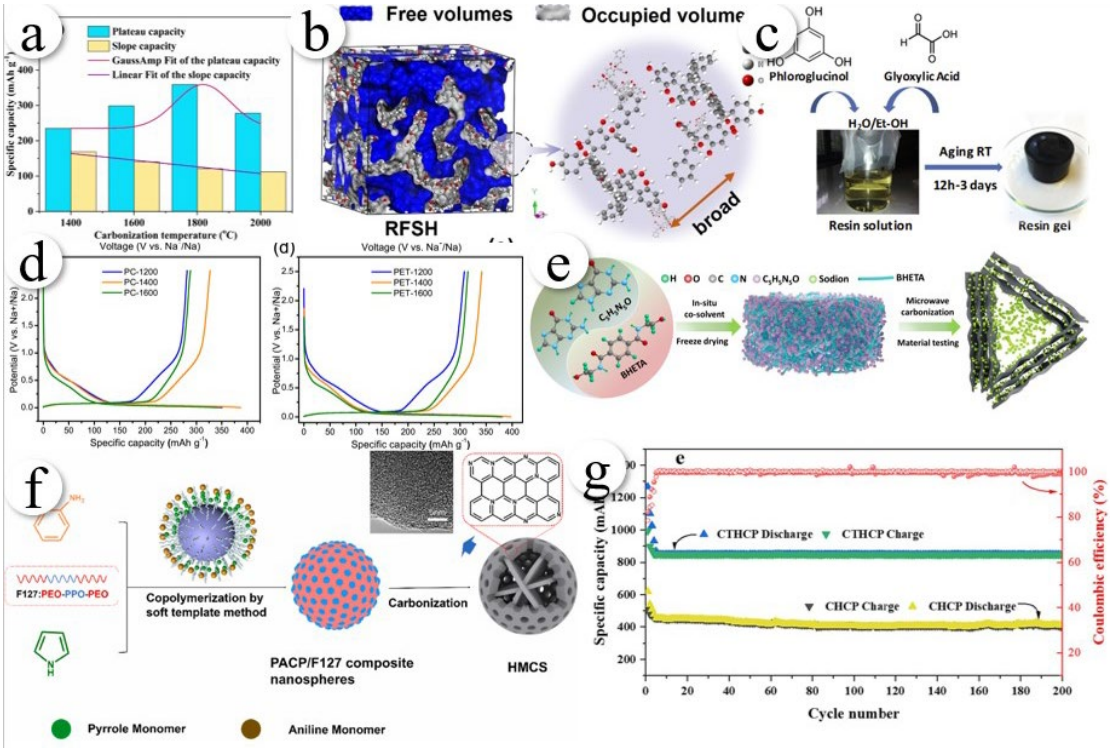


Figure 3. (a) Reversible specific capacities contributed by the plateau and slope regions of epoxy phenol novolac resin hard carbons. Reproduced with permission[34]. (b) Computational simulation model of free volumes in phenolic resin precursor. Reproduced with permission[35]. (c) Synthesis route of resin gel. Reproduced with permission[36]. (d) Charge/discharge curves of PC-hard carbon and PET-hard carbon at different carbonization temperatures. Reproduced with permission[37]. (e) Schematic illustration of nitrogen-doped hard carbon synthesis procedure. Reproduced with permission[38]. (f) Illustration of the information of hollow multicavity carbon spheres. Reproduced with permission[39]. (g) Cycling performance of hyper cross-linked polymers-based hard carbon at 0.5 A g^{-1}. Reproduced with permission[40].

3.2 Biomass-Derived Hard Carbon

Recently, considerable notice has been given to the use of biomass for the synthesis of hard carbon materials owing to their environmental friendliness and easy availability. Biomass's unique attributes as a renewable and carbon-rich resource makes it appealing for large scale and eco-friendly production of hard carbon anodes, marking it as a likely candidate for commercialization of sodium-ion batteries (SIBs).

Biomass is the collective term for nearly all organic matter from various life such as flora and fauna, microorganisms, residues from farming, forestry waste, and even byproducts from industries[41]. Many materials considered biomass are rich in carbon and possess natural cross-linked bonds C–O–C or C–C, which are thermally

decomposed under inert atmosphere through pyrolysis to yield disordered carbon scaffolds, suitable for Na^+ storage. Besides, biomass is also known to contain heteroatoms such as nitrogen, phosphorous, sulfur, along trace metals, that are encapsulated into the carbon matrix during pyrolysis, improving its electrochemical properties[42]. In particular, nitrogen doping has significantly improved the electronic structure of hard carbon and enhanced sodium adsorption. These changes accelerate the formation of nanodomain graphitic structures and nanoscopic pores through carbon lattice distortion induced by heteroatoms[43].

The precursor type combined with specific synthesis conditions greatly determine the microstructures and composition of hard carbons derived from biomass. For the sake of clarity, they are usually sub-divided into three main classes: cellulose-derived, lignin-derived, and other biomass-derived.

3.2.1 Cellulose-based precursors

Cellulose is a natural polymer that constitutes the plant cell walls and offers great utility as a renewable source for hard carbon. It is composed of repeating subunits of glucose units linked via β-1,4-glycosidic bonds in a linear fashion and organized hierarchically[44]. It can be extracted via enzymatic or acid hydrolysis as well as mechanically. These different methods result in three main products: cellulose nanocrystals and nanofibers, as well as bacterial cellulose[45].

Microcrystalline cellulose is entirely crystalline, while cellulose nanofibers contain both crystalline and amorphous regions. These structural variations influence the morphology and electrochemical performance of the resulting hard carbon. For instance, carbons derived from microcrystalline cellulose are known to form porous structures that are effective for sodium transport(Figure 4a), thereby improving transport kinetics and capacity[46].

Also, the carboxyl and hydroxyl groups are important surface functional groups. These groups lead to active sodium adsorption as well as pseudocapacitive behavior in the sloping part of the graph. Wang et al. added carboxyl groups to hard carbon materials via dry ice-assisted ball milling, obtained hard carbon materials have excellent cycling stability at high current densities(Figure 4b)[47]. In addition, pre oxidation treatments, or other modifications aimed at introducing oxygen-containing species prior to pyrolysis, were shown to improve closed pore structures and lead to better accommodation of sodium ions[48]. In this regard, hard carbons obtained from the waste cellulose separators by pre-oxidation followed by pyrolysis demonstrated considerable interlayer spacing (Figure 4c)while exhibiting excellent electrochemical

performance[49].

3.2.2 Lignin-based precursors

Lignin is a biopolymer which is obtained as a waste product from the pulp and paper industry, thus it is the second most available biopolymer. It is different from cellulose because it does not possess a particular chemical structure instead it is made up of a three-dimensional, amorphous network that consists phenolic components such as p-hydroxyphenyl, guaiacyl, and syringyl monomers[50].

Depending on the synthesis route, lignin-derived carbon can be tailored into spheres[51] or 3D porous skeletons[52]. For example, the emulsion-solvent evaporation approach has been used to synthesize carbon microspheres that exhibit fast Na^+ diffusivity and rate performance (Figure 4d)[51]. Furthermore, Flash Joule Heating (FJH) is a rapid alternative to traditional pyrolysis (Figure 4e). Luo and colleagues showed that carbon skeletons derived from lignin underwent FJH resulting in improved sodiophilicity due to the SEI structure as well as oxygen functional groups[52].

The carbonyl groups formed from the pre-oxidation of lignin precursors not only increase the interlayer spacing but also promote sodium intercalation. Lin et al. showed that the rate capability of pre-oxidized lignin-derived carbons was remarkably enhanced[53]. Additionally, oxygen doping performed via spray-drying(Figure 4f)[54] and sulfonation, such as in sodium lignosulfonate (a byproduct from the paper industry), promotes the formation of disordered structures and mesopores providing enhanced porosity along with waste reuse[55].

3.2.3 Other biomass sources

In addition to cellulose and lignin, many other natural biomass sources have been studied like nut shells[56], woody residues[57], fruit peels[58], and plant fibers[59]. These precursors have unique structures and distinct chemical characteristics that impact the carbonization process and the resulting material's electrochemical performance.

For example, the pre-oxidation technique, coupled with the intrinsic structure of olive shells, oxygenated the porous regions which assists towards the creation of disordered carbon domains[56]. The peels of fruits rich in lignocellulosic polymers like (cellulose, hemicellulose, and pectin) gave rise to hard carbons containing nanovoids and graphitic domains which translates to an enhanced capacity retention and rate performance[58]. Concerning the bark of kapok trees, Zhang et al. noted that the aggregate morphology of the bark stemmed from interconnecting fibers providing volumetric elasticity. In their work, they utilized aluminum-ion coordination that prevented structural collapse

during pyrolysis, resulting in the formation of hard carbons with 70% capacity retention under rate tests(Figure 4g)[59].

Other innovations encompass Cao et al., who created hard porous carbons with bamboo powder, yielding hierarchically porous hard carbons with an impressive ICE of 81.7%(Figure 4h)[60]. While ICE poses a challenge for biomass-derived carbons, it has been shown that reduced heating rates during carbonization leads to lower surface area and defect density, therefore decreasing SEI formation. One example is the camphor wood hard carbon, which was derived and synthesized at a heating rate of 0.25°C/min, achieving an initial charge capacity of 324.6 mAh/g at an ICE of 82.4%(Figure 4i)[57].

The hard carbons derived from biomass are a novel and economically approachable class of anode materials for sodium-ion batteries, displaying ample structural diversity along with intrinsic heteroatom doping. Depending on the biomass precursor, which includes plant-derived polymers like cellulose or lignin, distinctive microstructures with tailored interlayer spacing, hierarchical porosity, and catalytically active defect sites can be attained. Pre-oxidation, heteroatom doping, and controlled pyrolysis are some methods that enable tuning of electrochemical properties such as capacity, rate capability, and initial Coulombic efficiency. Improvements in biomass valorization and processing techniques present a feasible pathway for overcoming hurdles like low ICE and structural variability toward more robust and more widely available sodium-ion storage materials.

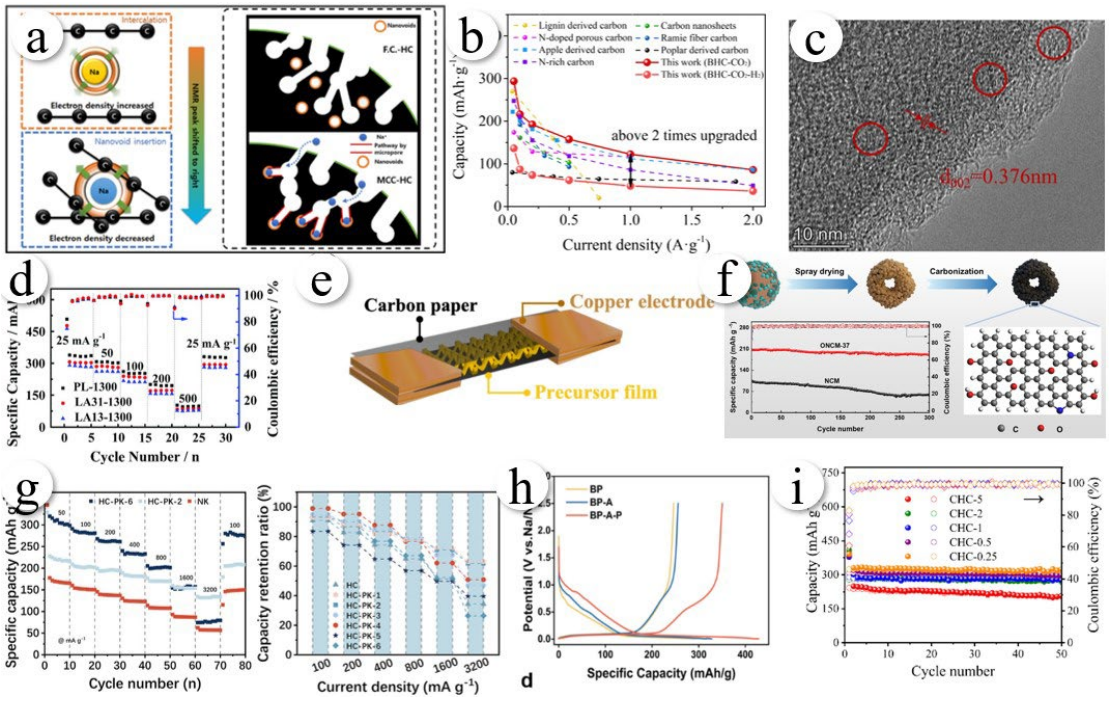


Figure 4. (a) Schematic illustration of the sodium-ion insertion mechanism into nanovoids through micropores based on NMR analysis. Reproduced with permission[46]. (b) Rate performances of carbon anodes at various current densities. Reproduced with permission[47]. (c) HRTEM image of sample from cellulose separator. Reproduced with permission[49]. (d) Rate performance of samples from 25 to 500 mA g^{-1}. Reproduced with permission[51]. (e) Schematic illustration of flash joule heating method. Reproduced with permission[52]. (f) Schematic synthesis route of oxygen-doped carbon microspheres (ONCM) and their cycling performance. Reproduced with permission[54]. (g) Rate performance and capacity retention of hard carbon materials under different current densities. Reproduced with permission[59]. (h) Charge and discharge curves (first cycle) for bamboo-based hard carbons (BP). Reproduced with permission[60]. (i) Cycling performance at 20 mAh g^{-1} for CHC prepared in different heating rates. Reproduced with permission[57].

3.3 Alternative Carbon Sources and Composites

Alongside polymer-based and biomass materials, other carbon sources are researched for manufacturing hard-carbon anodes for sodium-ion batteries. Petroleum pitch and coal tar pitch are particularly attractive owing to high carbon content and low ash content as well as excellent graphitizability[61]. Controlled pyrolysis of pitch within inert atmospheres results in the formation of hard carbons with tailored microstructures and preferable interlayer spacing. In addition, the use of templates has made it possible to produce two-dimensional porous hard carbons with defined morphology and high surface area that enhances ionic and charge transport accessibility[62]. At the same time, newly developed hard carbon-based composites, which integrate hard carbon with phosphides[63] or transition metal nitrides[64] or sulfides[65], have advanced the multifunctionality by improving the electric conductivity, structural stability and rate performance. These new approaches expand the scope of hypothetic precursors and make it easier to design advanced anodes for sodium-ion batteries.

3.3.1 Pitch-based hard carbon

Within the alternative carbon sources, materials derived from pitch, which is a by-product from petroleum and coal, is gaining interest due to its low cost and plentiful supply[66]. Unlike other sources, pitch is constant throughout the year and does not depend on seasonal supply variations. Furthermore, pitch is composed of polycyclic aromatic hydrocarbons along with many other complex hetero-atomic derivatives. Based on the origin of production, one can classify pitch into either petroleum pitch or coal tar pitch; both have unique chemical compositions as well as distinct carbonization behaviors.

Long-chain hydrocarbons are present in higher quantities in petroleum pitch. Because of this, its hydrogen content is generally around 10%, which leads to greater amounts of volatile compounds during pyrolysis[67]. This enables smoother decomposition at lower temperatures, allowing for the formation of porous carbon due to the escape of these volatile compounds. Due to its abundance of aromatic structures, coal tar pitch contains hydrogen at levels around 5%, leading to denser structures of carbon but lower pore volumes[68]. Another difference to consider is petroleum pitch contains heteroatoms[69]. This results in an in-situ heteroatom doping during carbonization which assists the pitch hard-carbons to be used as sodium battery anodes due to their better sodium-ion adsorption and charge transfer.

Once viewed as a precursor for soft carbon due to its low oxygen content, coal tar pitch can be transformed into hard carbon with chemical activation methods. One of the most popular methods, KOH activation, facilitates the creation of oxygen functional groups, allowing for the conversion of pitch to a hard carbon form. Zhao et al. produced porous hard carbon from coal tar pitch using KOH activation, and the material attained remarkably over 85% capacity retention over 415 cycles(Figure 5a)[70].

Oxygen-containing functional groups are known to greatly impact the carbonization process. These groups are capable of preventing excessive graphitization at elevated temperatures, which allows disorder regions to remain that enhance sodium ion adsorption due to increased defect density and surface activity (Figure 5b). Li and coworkers showed that hard carbon derived from petroleum pitch contained high amounts of these functional groups, enabling a reversible capacity of 333.7 $mAh \cdot g^{-1}$, underscoring the efficacy of the hard carbon as a high-capacity anode[71].

In addition, pitch fractions have considerable influence on the final carbon morphology and its electrochemical properties. For example, Zhang et al. studied the pitch fraction that is insoluble in tetrahydrofuran and noticed that it had a very high concentration of polar oxygen functionalities, which aided the development of a three-dimensional cross-linked carbon network[72]. This peculiar structure synergistically enhanced the sodium storage capability (Figure 5c) due to the combined effect of porosity, chemical activity, and increased structural resistance to solid electrolyte interphase (SEI) formation.

3.3.2 Templated synthesis of porous hard carbon

Carbon based two-dimensional (2D) nanostructures with heteroatom dopants, nitrogen in particular, are very promising for the storage of energy owing to vast surface area, improved electron transport, and a large number of active sites. However, the

conventional approaches to the synthesis of such structures are usually complicated by multistep techniques and specific apparatus, which greatly reduce their scale-up potential.

To tackle these issues, Liu and coworkers developed a one-step metal-organic coordination approach to fabricate a 2D nitrogen-doped carbon framework. The nanosheets obtained after carbonization showed remarkable structural uniformity and electronic conductivity. Importantly, the material achieved a specific capacity of 194 $mAh \cdot g^{-1}$ at an extremely high current density of 10 $A \cdot g^{-1}$(Figure 5d), showcasing endurance and stability[62]. This work demonstrates the promise of template-assisted methods in morphology control and heteroatom incorporation for the design of high-capacity SIB anodes.

3.3.3 Hybrid carbon materials

The strategy of compositing hard carbon with other materials has proven to be effective in overcoming the inherent low electrical conductivity or low sodium storage capacity problems. With the addition of synergistic elements, these hybrid structures can enhance ion or electron transport, mechanical strength, and electrode kinetics.

Shao et al. have reported the synthesis of manganese–zinc phosphides embedded in nitrogen-doped carbon matrices via phosphorization of metal-organic frameworks (MOFs)(Figure 5e)[63]. These materials provided improved charge transfer and ion diffusion, which in turn enhanced the electrochemical performance of the materials. These transition metal phosphides are known for their suitable redox potentials and economic value.

The other class of additives that has equally impressive electrical conductivity are transition metal nitrides due to their high theoretical capacities. Cheng et al developed a hard carbon composite with vanadium nitride particles which served as high capacity active sites while the hard carbon buffered sodium ions and provided structural support[64]. The composite showed a much greater capacity compared to the pristine hard carbon, demonstrating enhanced performance (Figure 5f).

Among metal sulfides, Fe_7S_8 is particularly remarkable for its high potential in sodium storage. A novel composite material reported recently consists of Fe_7S_8 microspheres embedded in N-doped hard carbon(Figure 5g), showing better cycling stability and capacity retention than many previously studied anode materials[65]. The hybrid structure helped mitigate volume expansion alongside enhancing the conversion for sodium.

Thus, these alternative sources of carbon like pitch, template-derived 2D structures, and

hard carbon-based composites showcase new pathways towards enhancing sodium storage performance. Through designed pore architectures, heteroatom doping, and the addition of functional materials, these approaches all enhance the traditional hard carbons to enable lower weight, higher capacity, faster, and volumetric scalable anode materials for sodium-ion batteries.

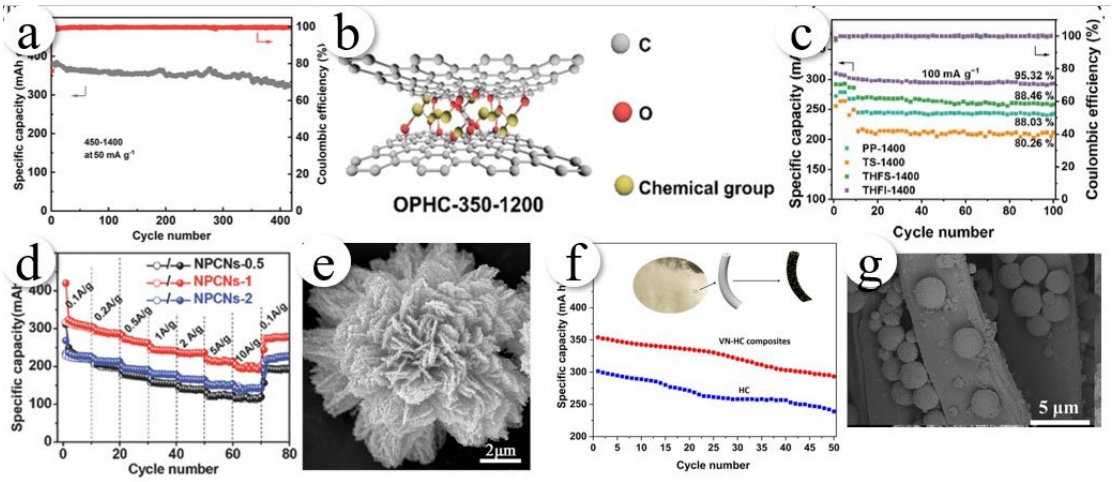


Figure 5. (a) Cycling performance of KOH‐added pitch-derived hard carbon. Reproduced with permission[70]. (b) Modeling of organic groups in carbon layers. Reproduced with permission[71]. (c) Cycling performance of different pitch fractions-derived hard carbons. Reproduced with permission[72]. (d) Rate performance of the N-rich porous carbon nanosheets. Reproduced with permission[62]. (e) SEM image of flower-like MnP-ZnP_2 composites. Reproduced with permission[63]. (f) Cycling performance of hard carbon and vanadium nitride/hard carbon composites. Reproduced with permission[64]. (g) SEM image of Fe_7S_8/N-doped carbonized silk textile. Reproduced with permission[65].

Table 1 summarizes classification and properties of hard carbon anodes mentioned in previous section. This table highlight precursor, carbonization condition, electrolyte system, and cycling performance.

Table 1. Summary of Classification and Properties of Hard Carbon Anodes for SIBs.

Classification	Precursor	Annealing condition	Electrolyte	Specific capacity (mAh/g)	ICE %	Cycle number	Ref.
Polymer	Epoxy phenol novolac resin	1800 ° C for 1 h, Ar atmosphere	1 M $NaPF_6$ in DME	389.2 at 500 mA/g	84.6	1000	[34]

Polymer	Phenolic resin	1400 ° C for 1 h, Ar atmosphere	1 M $NaPF_6$ in diglyme	217.9 at 2 C	88.5	1000	[35]
Polymer	Phloroglucinol and glyoxylic acid monohydrate	1300 °C Ar atmosphere	1 M $NaPF_6$ in EC/DMC (1/1, v/v)	250 at 0.1 C	71.6	40	[36]
Polymer	Waste PC and PET	1400 ° C for 2 h, Ar atmosphere	1 M $NaPF_6$ in EC/DMC (1/1, v/v)	342 at 20 mA/g	86.1	50	[37]
Polymer	PET	800 °C by microwave Ar atmosphere	1 M $NaPF_6$ in DME	257 at 500 mA/g	83	2000	[38]
Polymer	Naphthalene, DMB and TPP-Zn	910 °C for 10 min, Ar atmosphere	1 M $NaPF_6$ in EC/PC (1/1, v/v)	170 at 2A/g	47.46	500	[40]
Biomass	Lignin	800/1600 ◦C by Flash Joule heating	1 M $NaPF_6$ in diglyme	0.75 mAh/cm^2 at 1 mA/cm^2	99.8	450	[52]
Biomass	Commercially available alkali Lignin	1350 ° C for 2 h, Ar atmosphere	1 M $NaPF_6$ in diglyme	288.7 at 200 mA/g	81.4	250	[53]
Biomass	3-aminophenol formaldehyde resin	1100 ° C for 2 h, Ar atmosphere	1 M $NaClO_4$ in EC/DEC (1/1, v/v)	184 at 100 mA/g	81	300	[54]
Biomass	Sodium lignosulfonate	1400 ° C for 2 h, Ar atmosphere	1 M $NaClO_4$ in PC with 5% FEC	332.24 at 50 mA/g	56.45	200	[55]

Biomass	Olive shells	1300 ° C for 2 h, Ar atmosphere	1 M $NaClO_4$ in EC/DEC (1/1, v/v)	222 at 0.3 A/g	77	500	[56]
Biomass	Lagerstroemia speciosa	1300 ° C for 2 h, Ar atmosphere	1 M $NaClO_4$ in EC/PC (1/1, v/v)	240 at 30 mA/g	70.7	100	[58]
Biomass	Kapok fiber	1200 ◦C for 2 h, N_2 atmosphere	1 M $NaPF_6$ in diethylene glycol dimethyl ether	110 at 5000 mA/g	76.05	250	[59]
Biomass	Bamboo powder	1300 ◦C for 3 h	1 M $NaPF_6$ in EC/DMC (1/1, v/v)	338 at 0.1 C	81.7	100	[60]
Biomass	Camphor wood residues	1300 ° C for 2 h, Ar atmosphere	1 M $NaClO_4$ in EC/DMC (1/1, v/v)	319.5 at 20 mA/g	82.8	50	[57]
Alternative Carbon Sources and Composites	Coal tar pitch	1400 ° C for 6 h, Ar atmosphere	1 M $NaClO_4$ in EC/DEC (1/1, v/v)	323 at 50 mA/g	84	415	[70]
Alternative Carbon Sources and Composites	Petroleum pitch	1200 ° C for 6 h, Ar atmosphere	1 M $NaClO_4$ in EC/DEC (1/1, v/v)	121.3 at 1 A/g	-	500	[71]
Alternative Carbon Sources and Composites	Pitch	1400 ° C for 2 h, Ar atmosphere	1 M $NaPF_6$ in diglyme	205.3 at 1 A/g	90.96	500	[72]
Alternative Carbon Sources and	Zinc nitrate and HMT	800 °C for 2 h, Ar	1 M $NaSO_3CF_3$ in diglyme	170 at 1 A/g	74.82	1000	[62]

Composites		atmosphere				
Alternative Carbon Sources and Composites	H_3BTC, $Mn(NO_3)_2{\cdot}4H_2O$, $Zn(NO_3)_2{\cdot}6H_2O$ and PVP K30	600 °C for 2 h, Ar atmosphere	1 M $NaSO_3CF_3$ in diethylene glycol dimethyl ether	403.3 at 2 A/g	65.35	1000	[63]
Alternative Carbon Sources and Composites	Hexane and $VOCl_3$	1400 ◦C for 2 h, N_2 atmosphere	1 M $NaClO_4$ in EC/DEC (1/1, v/v)	294 at 50 mA/g	74	50	[64]
Alternative Carbon Sources and Composites	$FeSO_4.7H_2O$, urea and silk fabric	1500 ° C for 3 h, N_2 atmosphere	1 M $NaClO_4$ in EC/DEC with 5%FEC (1/1, v/v)	0.39 mAh/cm^2 at 5 mA/cm^2	55.5	600	[65]

Chapter4: Literature review: Structure-Performance Correlation on Hard Carbon

4.1 Interlayer Spacing Control

As stated in the earlier discussions, sodium storage in the hard carbon anodes occurs through three main processes: intercalation into graphitic nanodomains, pore filling, and surface adsorption at defect sites. Of these, interlayer sodium ion intercalation within turbostratically graphene sheets contributes significantly to the low-voltage plateau capacity, which is critical from a high energy density perspective in sodium-ion batteries (SIBs). Graphitic nanodomains, produced from disordered or curved graphene layers, create interlayer spaces that can, under certain conditions, become thermodynamically advantageous for sodium insertion.

Multiple sources have so far confirmed that interlayer spacings between 0.33 and 0.41 nm can host sodium ions[73], with a more preferred range of between 0.37 and 0.38 nm. Within this range, misaligned or turbostratic layers of graphene perform some intercalation behavior similar to that seen with lithium-ion intercalation into graphite, although with greater spacing due to the larger radius of Na^+ ion[18a]. While sodium storage mechanisms in the low-voltage plateau region are still subject to debate, evidence suggests that a moderate increase in interlayer distance significantly improves sodium accessibility, diffusion barriers, and the total reversible capacity[74]. Therefore, the precise control and rational design of interlayer spacing fundamentally define strategies to optimize hard carbons in SIBs.

The chemical composition and crystallinity of the precursor carbon exhibit the greatest influence over the derived interlayer structure of the carbon product[75]. Precursor biomasses, for example, wood residues, contain a natural mixture of cellulose, hemicellulose, and lignin, which makes it difficult to obtain defined structure-property relations[76]. These natural constituents of the biomass exhibit such diverse ways of thermally decomposing that they yield different carbonization pathways and inconsistent microstructural features.

To resolve this complexity, researchers tend to explore simpler molecular precursors first. In this respect, Alvin et al. studied carbonized cellulose and they discovered that less crystalline cellulose is more capable of developing disordered graphitic nanodomains[77]. During pyrolysis, less crystallized cellulose undergoes greater rearrangement, increasing the proportion of turbostratic regions favorable for sodium intercalation(Figure 6a). On the other hand, highly crystalline cellulose tends to

preserve its rigid backbone structure during pyrolysis, which invites ordered graphitization and limits interlayer expansion.

To control the interlayer distance more precisely, Du and others used chemical crosslinking to replace the hydrogen bonds within cellulose with covalent bonds, thus increasing the distance between the polymer chains before carbonization[78]. This approach produced graphitic nanodomains with increased interlayer distance which enhanced plateau capacity (Figure 6b). In the same way, other attempts on the design of interpenetrating polymer networks have been proven useful in the suppression of graphitization. Zhang and his colleagues prepared co-precursors by blending lignin and phenolic resin[79]. The resulting crosslinked structure suppressed long-range graphitization and produced hard carbons with increased turbostratic disorder and enhanced sodium storage capacity.

Particularly, pyrolysis temperature plays a central role in how the interlayer structure of hard carbon is formed as a result of the carbonization process. With the increase in pyrolysis temperature, the material undergoes dehydrogenation as well as rearrangement of carbon atoms which increases the degree of graphitization and narrow the interlayer spacing. Hou and others studied this phenomenon by synthesizing hard carbons from biomass at different temperatures[80]. With the rise in pyrolysis temperature, there was a consistent decrease in interlayer spacing. While excessive graphitization might improve conductivity, it reduces sodium intercalation sites. Thus, optimal treatment must provide a balance between extended interlayer spacing and ordered structures. Achieving an ICE of 80% proves temperature control as a method for high-performance industrial scalable anodes (Figure 6c).

Doping heteroatoms into carbon materials offers opportunities to modify the interlayer spacing of hard carbon. For such modifications, boron (B), phosphorus (P), sulfur (S), and nitrogen (N) are often added either through precursor design or later via post-synthesis modification. Such atoms are able to create distortions and lattice strain locally and thus increase the spacing between the layers while being able to add new electrochemically active sites.

Phosphorus and sulfur atoms with larger atomic radii can sterically expand the planar graphene structure[81]. P-doped hard carbons show shorter coherence lengths in the a–b plane of the graphene sheets, which suggests greater curvature and more turbostratic disorder. This curvature also reduces the van der Waals interactions between the layers, making it easier for sodium to intercalate.

Different forms of nitrogen, such as pyridinic-N, pyrrolic-N, and graphitic-N, are well known for their electrochemical advantages and have garnered greater attention due to

their bonding configurations[82]. Pyridinic and pyrrolic nitrogen species increase sodium adsorption and pyrrolic nitrogen expands the interlayer distance, energetically reduce the barrier for ion insertion[83]. Zhao et al. synthesized N-doped carbon nanosheets from a mixture of sodium carboxymethyl cellulose and graphitic carbon nitride[84]. The product widened interlayer spacings (Figure 6d), which allowed for the rapid accommodation of sodium ions and buffered volumetric changes during sodiation resulting in enhanced long-term stability.

Co-doping techniques offer a more prominent enhancement to this effect. Co-doped hard carbon microspheres were synthesized with boron and phosphorus by Chen et al[85]. In this scenario, n-type dopants such as B contribute electrons while p-type dopants like P develop regions rich in holes, thus achieving balanced charge transport. The modified hard carbon anode showed greater interlayer spacing and a capacity of 289.4 $mAh \cdot g^{-1}$ after 1000 cycles (Figure 6e), demonstrating the combustion benefits of dual-element doping.

As Wu et al. showed, it is also possible to dope in situ with heteroatom rich biomasses – in this case, the coconut endocarp, which contains high concentrations of potassium got potassium naturally[86]. During pyrolysis, some K+ ions were trapped within the carbon structure, functioning as interlayer expansion agents, which increased interlayer spacing and improved the sodium intercalation behavior of the derived carbon(Figure 6f).

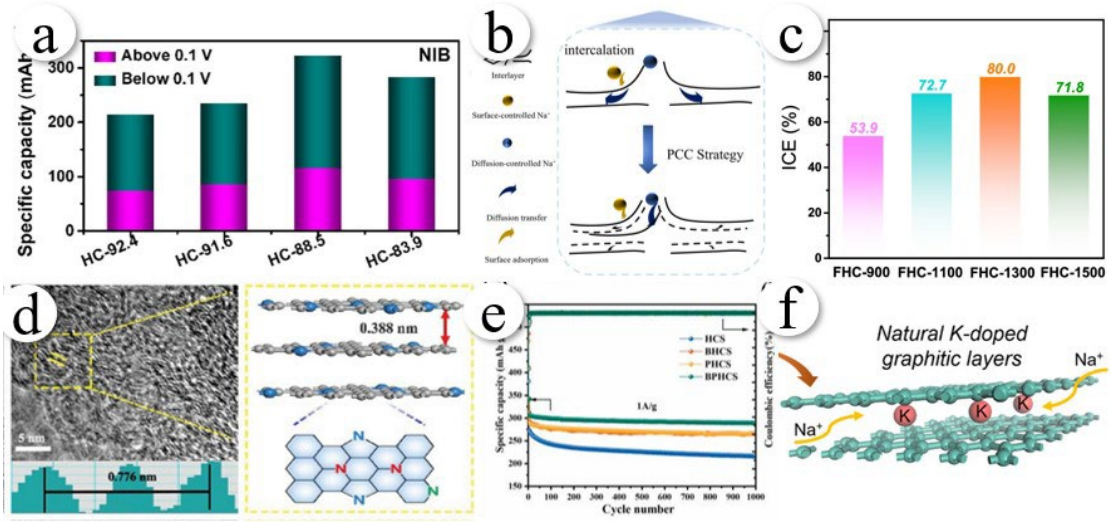


Figure 6. (a) The sloping and plateau regions capacities of hard carbons from celluloses with different crystallinities. Reproduced with permission[77]. (b) Schematic illustration of the sodiation process in hard carbon and hard carbons from crosslinked precursors. Reproduced with permission[78]. (c) ICE comparison of hard carbons from different pyrolysis temperatures. Reproduced with permission[80]. (d) HRTEM image for hard carbon. Reproduced with permission[84]. (e) Cycling performance of phenolic resin-based hard carbons. Reproduced with permission[85]. (f) Schematic illustration of K-doped hard carbon. Reproduced with permission[86].

4.2 Pore Structure Engineering

Hard carbon is a non-graphitic carbonaceous substance composed of sp^2-hybridized graphene layers and sporadically located sp^3-hybridized regions[87]. These disordered and curved graphene sheets are held together in a loose, turbostratic layered framework through weak van der Waals forces[24]. The pyrolysis of organic precursors involves a series of complex transformations, such as aromatization, polycondensation, and the growth of carbon layers, which not only determines the level of structural order but also the evolution of pore architecture[88].

Carbonization occurs in stages. For example, in the first stage which lasts up until 500 °C, more volatile species like H_2O, CO, CO_2, NH_3 release from the precursor as heteroatoms such as O and N are removed. The gaseous byproducts create spaces within the carbon matrix and, stepwise, a porous structure forms[24]. These pores can be subclassed into two major types: closed pores, which are isolated in nested graphitic domains and thus, impossible to access by gas-phase probes, and open pores which are accessible to external molecules and can be detected via nitrogen adsorption-desorption measurements[89].

Open pores act as a reservoir to store sodium via surface adsorption. However, they also promote excessive solid electrolyte interphase (SEI) formation due to increased surface area exposure[90]. Excessive SEI Formation may result in low initial Coulombic efficiency (ICE) and weak cycling stability in the system. On the other hand, closed pores are thought to accommodate sodium clusters that are quasi-metallic which is widely believed to be the reason for the low voltage plateau region in the charge-discharge curve. The exact mechanism for sodium storage in this region is not settled, but simulations indicate that prior sodium adsorption during the sloping region is necessary to fill closed pores with quasi-metallic sodium. Thus, the need to design hard carbon with appropriate ratios of open and closed pores in order to improve capacity and reversibility is paramount.

In addition, the role of size of closed pores is equally crucial. Researches show that pore

radius of 0.7-1.4 nm is optimal for stabilizing small sodium clusters and minimizes dendritic growth[89]. If the pore size exceeds this value, there is an increased tendency for accumulation of metallic sodium which increases the chances of sodium plating, thus reducing cycling reversibility. Hence, hard carbon design focuses on control of abundance and size of closed pores.

A range of synthetic strategies like template-assisted synthesis, chemical vapor deposition (CVD), precursor molecular design, and controlled carbonization have been developed to form closed pore structures in hard carbon.

Metal salts like ZnO and MgO serve as pore forming agents and can act as sacrificial templates during pyrolysis. These nanoparticles react with the carbon matrix at elevated temperatures to carve out and create porous structures. By controlling the distribution and size of the nanoparticles, one can fine-tune the final porous structure[91]. To illustrate this, kamiyama et al. modified magnesium gluconate to serve as MgO precursor[91]. Upon carbonization with glucose, hard carbon was obtained that has high reversible capacity of 478 $mAh \cdot g^{-1}$ along with remarkable cycling stability. In comparison to traditional template methods that leave behind metal oxides to require an acid washing removal step, more sophisticated one-step methods have been developed. Qiu and her coworkers proposed a pyrolysis technique with ZnO where etched temperatures of 1100 °C result in the formation of open pores[11b]. At higher temperatures, open pores undergo partial pore shrinkage along with Zn evaporation which results in the formation of closed pores (Figure 7a). This process eliminates the need for any post treatment or purification.

CVD represents a versatile method for transforming open pores into closed ones through the deposition of carbonaceous materials into the voids[90]. The co-pyrolysis of polystyrene waste with microporous activated carbon from walnut shells was done by Li et al(Figure 7b)[92]. During this process, polystyrene decomposed into aromatic fragments which permeated and thus, sealed the open pores. The small angle x-ray scattering (SAXS) confirmed closed pores were formed with a radius of 1.30 nm. Likewise, methane (CH_4) was utilized as a CVD precursor by Deng et al[93]. Along with introducing Fe catalysts which lowered the activation barrier for CH_4 decomposition. This method provided closed pores of an optimum radius 0.90 nm which increased the stability of sodium clusters and enhanced ionic conductivity. The hard carbon produced showed a reversible capacity of 457 $mAh \cdot g^{-1}$ and ICE of 90.6%, which surpass most conventional hard carbons (Figure 7c).

Phenolic resins and other polymers are often employed as hard carbon precursors because of their adjustable structure. The covalently linked 3D networks of polymers

result in some internal space which can be utilized to form closed pores[94]. Guo et al. changed the properties of phenolic resins by modifying the side groups of aldehydes so that the degree of crosslinking and the rigidity of the backbone could be controlled[94]. Upon carbonization, these features were found to translate to hard carbon with a generous amount of closed pores and a reversible capacity of 324.7 mAh·g^{-1} featuring a plateau contribution of 243.2 mAh·g^{-1}(Figure 7d). In a similar manner, Lin et al. added aromatic side groups within and between polymer chains to increase free volume while also increase steric hindrance, thus limiting excessive graphitization[35]. This form of carbon showed 86.4% capacity retention after 1000 cycles, demonstrating the closed-pore framework stability (Figure 7f).

Altering the conditions of carbonization is one way to easily control the pores. Li and colleagues used almond shells and performed a two-step pyrolysis procedure[95]. In the first step, they used a longer hold time in combination with a slower heating rate to aid in gas release and micropore development. During the second stage of high temperature, many micropores that had partially collapsed closed within the carbon matrix. The hard carbon produced provided a remarkable ICE of 87.2% which indicates the effectiveness of strategies involving temperature-controlled pore transformation methods (Figure 7e).

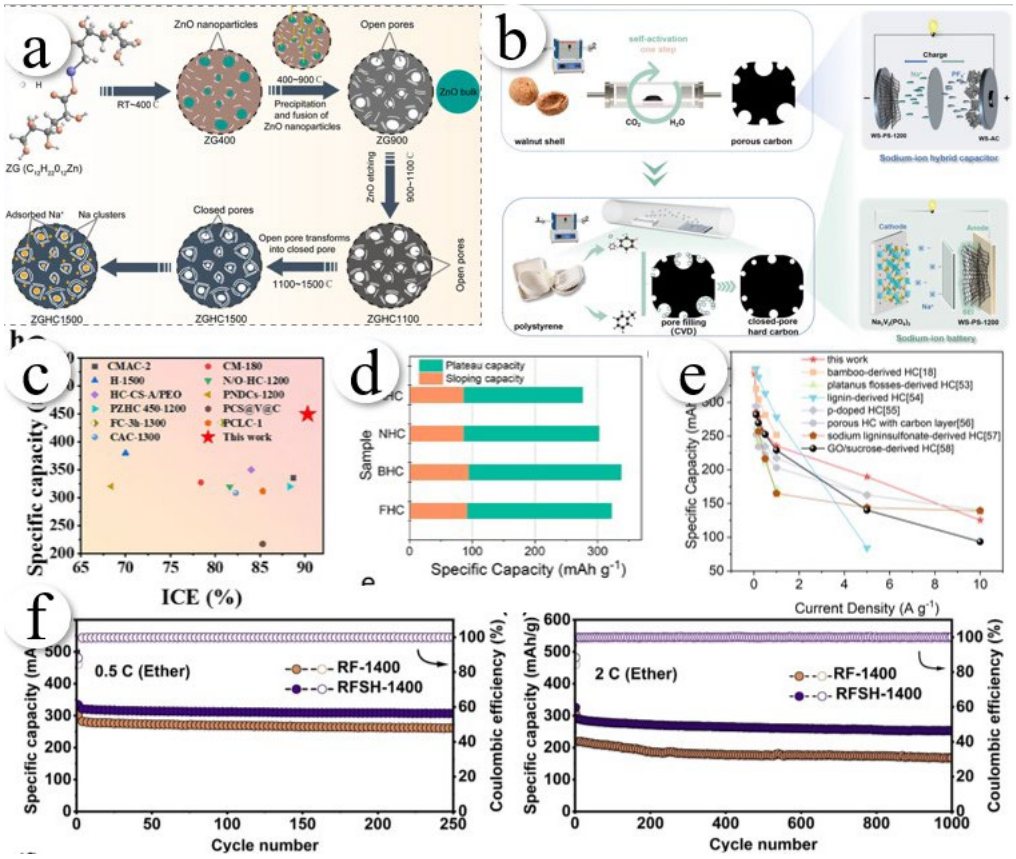


Figure 7. (a) Schematic diagram of the closed-pore formation mechanism in the pyrolysis process. Reproduced with permission[11b]. (b) Schematic diagram of the preparation of CVD hard carbon. Reproduced with permission[92]. (c) The comparison of reversible specific capacity and ICE of CVD hard carbon with previous reported hard carbon anodes. Reproduced with permission[93]. (d) Capacity contributions from the plateau and slope regions. Reproduced with permission[94]. (e) Comparison of rate capability between A-2.25-6-T and recently reported hard carbon anode. Reproduced with permission[95]. (f) Cycling performance of RFSH-1400 and RF-1400 in ether-based electrolyte. Reproduced with permission[35].

4.3 Defects and Functional Groups

As mentioned earlier, the microstructure of hard carbon is disordered, consisting of defect-rich randomly stacked graphene layers with coexisting turbostratic domains[96]. These defects—both intrinsic and extrinsic—are known to directly affect the behavior of sodium capacitance during the discharge and charge cycles, particularly in the high-voltage slope region.

Intrinsic defects include edges, carbon vacancies, as well as non-hexagonal rings created due to lattice distortion within the carbon framework[97]. On the other hand, extrinsic defects are usually introduced by heteroatom N, S, P, or B doping, which changes the electronic and bonding framework of neighboring carbon atoms[98]. Both kinds of disorder characteristics are important for the hard carbon electrochemical behavior owing to their ability to induce high energy adsorption centers, alter the charge density distribution, and create ion transport pathways.

Hard carbon's intrinsic defects, which stem from its amorphous precursors, are intimately associated with sodium-ion interactions. Sodium ions can be stored at edge defects as well as at basal plane vacancy sites[19]. The sodium ions suffixed at these locations interact more freely with the electronic environment compared to other regions. DFT calculations have shown a positive correlation between an increased density of defects and the capacity of Na+ ion uptake[97]. Local charge transport and adsorption activity is improved with modifications of the local electronic structure due to the presence of Stone-Wales defects and carbon vacancies[99].

As an illustration, Stone-Wales defects can promote metal-to-metal interactions to form quasi-sodium metallic clusters in closed pore spaces[100]. In the same way, carbon vacancies, which are formed through removal of an atom, lead to structures with unsaturated C-dangling bonds that strongly bind with sodium ions[96]. On the other hand, excessive binding energy can produce defects that act as ion traps, hindering desorption, which in turn makes the structure less reversible[101]. A well-thought-out combination of defect types, densities, and patterns is necessary to maximize capacity while

maintaining cycling stability.

The use of heteroatoms enriches extrinsic defects that intensify the interaction with sodium ion. Elements like nitrogen and phosphorus not only act as dopants, but also serve as active sites for adsorption due to their unpaired electrons that disturb surrounding carbon lattices, creating localized, discrete defects that promote pseudocapacitance[102].

Using a polyacrylamide hydrogel template, Wang et al. introduced N and P dopants into carbon precursors homogeneously[102]. Carbonization resulted in evenly distributed defect networks that strengthened Na^+ adsorption and enhanced structural stability during cycling (Figure 8a). These heteroatoms participated in pseudocapacitive storage through Faradaic reactions, enhancing reversible pseudocapacitive storage.

The nature and configuration of heteroatoms will define their influence. For nitrogen doping, pyridinic-N and pyrrolic-N are favorable and represent efficient active sites for adsorption while also promoting interlayer expansion. To this end, Yang et al. designed N/S co-doped hard carbon using methylene-bridged precursors through carbonization[103]. The decomposition of methylene bridges provided abundant intrinsic defects and the corresponding material had a reversible capacity of 238 $mAh \cdot g^{-1}$ at under 1 V, which captures significant low-voltage slope-region improvement (Figure 8b).

Yuan and coworkers developed a thermal etching method based on the Co and Ti salt catalysts to obtain planar intrinsic defects, which include carbon vacancies and non-hexagonal rings, on hard carbon derived from collagen fibers[104]. The presence of these defect structures greatly enhanced the kinetic reversibility of sodium ion transport, maintaining stable slope capacity even with elevated current densities (Figure 8c).

Further advances were put forward by Wang et al. They employed corn stalk flour as the carbon source and thiourea as the donor of heteroatoms[105]. During low-temperature pyrolysis, heteroatoms from thiourea were incorporated into the carbon matrix. With rising temperatures, these heteroatoms would vaporize, leaving behind structural voids that increased interlayer spacing. DFT calculations showed that the sodium ion diffusion barrier was lowered and interlayer adsorption was facilitated by such defects. The refined hard carbon exhibited remarkable capacity of 284.5 $mAh \cdot g^{-1}$ with ICE of 85.9%, thus confirming the synergistic effects of interlayer modification and defect creation (Figure 8d).

In addition to lattice defects, the presence of surface functional groups particularly of the type –OH, –C=O, –COOH, and –C–O–C– substantially modifies the electrochemical behavior. These groups contribute to greater surface hydrophilicity,

better wettability of the electrolyte, and take part in redox reactions, particularly in the sloping potential region[106]. Carbonyl groups, for example, can act as sodium ion adsorption redox centers, thus supporting the capacitive part of the total capacity[107]. Furthermore, surface functionalities can also affect the composition and stability of the solid electrolyte interphase (SEI) directly. Inhomogeneous SEI layers of non-uniform thickness and poor stability are often a result of uncontrolled decomposition stemming from traditional ester-based electrolytes[108]. Conversely, ether-based electrolytes are known to form layered SEI structures composed of inorganic materials in the inner layer that facilitate Na^+ diffusion.

With these ideas, Liu and colleagues modified the structure of hard carbon by putting oxygen functional groups with the aim of simulating ether-derived SEIs within an ester electrolyte[108]. By selective carbonyl functionalization, they drove the preferential decomposition of certain salt species which aided in achieving a more uniform inorganic-rich SEI. As a consequence, this approach produced a hard carbon anode that exhibited a reversible capacity of 379.6 $mAh \cdot g^{-1}$ with an ultra-high ICE of 93.2% (Figure 8d).

The combination of structural defects and surface functional groups has a synergistic effect on sodium storage. Wang and coworkers showed this by modifying the carbonization temperature which regulated both the defect concentration and the amount of oxygen functional groups[109]. The material that they optimized showed an improved surface wettability and better Na^+ diffusion, having a specific capacity of 270.2 $mAh \cdot g^{-1}$ with ICE of 90.2% (Figure 8e).

To conclude, the sodium storage capacity of hard carbon is the result of the interplay of the exact microstructural features of the material. Suitable spacing between interlayers enhances the ease of intercalation of Na^+ ions, ideal pore geometry contributes to a balance between active surface area and mechanical stability, and designed defect sites and functional groups improve the adsorption of ions and SEI layer formation. Balancing all these structural features establishes the design principles which will enable the development of advanced hard carbon anodes for sodium-ion batteries.

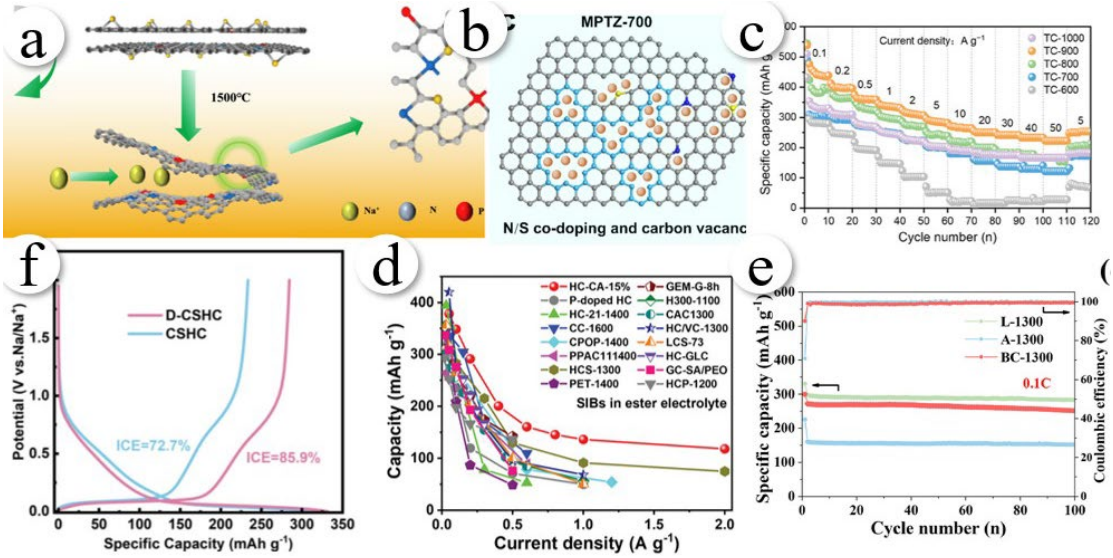


Figure 8. (a) Schematic diagram of the optimization mechanism of NP-CNS-T. Reproduced with permission[102]. (b) Schematic diagram of sodium ions absorption/desorption mechanisms in MPTZ-700. Reproduced with permission[103]. (c) Rate performance of all samples from 0.1 to 50 A g^{-1}. Reproduced with permission[104]. (d) The initial charge – discharge curves of D-CSHC and CSHC. Reproduced with permission[105]. (e) Rate performance of the HC-CA-15% anode with reported hard carbon anodes. Reproduced with permission[108]. (f) Cycling performance of BC-1300, L-1300, and A-1300 at 0.1 C. Reproduced with permission[109].

Table 2 summarizes optimization strategies and properties of hard carbon anodes mentioned in previous section. This table highlight precursor, carbonization condition, electrolyte system, and cycling performance.

Table 2. Summary of Optimization Strategies and Properties of Hard Carbon Anodes for SIBs.

Strategy	Precursor	Annealing condition	Electrolyte	Specific capacity (mAh/g)	ICE %	Cycle number	Ref.
Interlayer Spacing Control	Microcrystalline cellulose powder	1300 ◦C for 6 h, N_2 atmosphere	1 M $NaClO_4$ in PC/EC/DMC (9/9/2, v/v/v)	225.7 at 0.3 A/g	57.9	700	[77]
Interlayer	Microcrystallin	1350 ° C	1 M $NaPF_6$ in	262.2 at	-	150	[78]

Spacing Control	e cellulose	for 24 h, Ar atmosphere	EC/DMC/EMC (1/1/1, v/v/v)	0.5C			
Interlayer Spacing Control	Phenolic resin and lignin	1400 ° C for 2 h, Ar atmosphere	1 M $NaPF_6$ in EC/DMC (1/1, v/v)	330 at 0.1C	88	150	[79]
Interlayer Spacing Control	Platanus flosses	1300 ° C for 2 h, Ar atmosphere	1 M $NaPF_6$ in diglyme	177.7 at 0.5 A/g	80	1000	[80]
Interlayer Spacing Control	Sodium carboxymethyl cellulose	1050 ° C for 2 h, Ar atmosphere	1 M $NaPF_6$ in DME	233.3 at 0.5 A/g	79.52	2000	[84]
Interlayer Spacing Control	Phenolic resin	1300 ° C for 2 h	1 M $NaPF_6$ in DME	174 at 5 A/g	-	5000	[85]
Interlayer Spacing Control	Coconut endocarp	1100 ° C for 2 h, Ar atmosphere	1 M $NaClO_4$ in PC with 5% FEC	288.7 at 50 mA/g	69.2	200	[86]
Pore Structure Engineering	Glucose	1500 ° C for 2 h, Ar atmosphere	1 M $NaPF_6$ in EC/DEC (1/1, v/v)	478 at 25 mA/g	88	35	[91]
Pore Structure Engineering	Zinc gluconate	1500 ° C for 2 h, Ar atmosphere	1 M $NaClO_4$ in EC/DEC (1/1, v/v)	481.5 at 0.05 A/g	72.1	170	[11b]
Pore Structure Engineering	Walnut shells	1000 ° C for 2 h, Ar atmosphere	1 M $NaPF_6$ in EC/DEC (1/1, v/v)	385 at 50 mA/g	88	300	[92]
Pore	Commercial	900 °C	1 M $NaPF_6$ in	387.9 at	90.6	100	[93]

Structure Engineering	porous carbon	Ar atmosphere	EC/DMC (1/1, v/v)	0.05 A/g			
Pore Structure Engineering	Phenolic resin	1500 °C Ar atmosphere	1 M $NaPF_6$ in EC/DEC (1/1, v/v)	192.2 at 0.05 A/g	75.4	150	[94]
Pore Structure Engineering	Phenolic resin	1400 ° C for 1 h, Ar atmosphere	1 M $NaPF_6$ in diglyme	217.9 at 2 C	88.5	1000	[35]
Pore Structure Engineering	Almond shell	1300 ° C for 1 h, Ar atmosphere	1 M $NaPF_6$ in DME	282.5 at 0.3 A/g	87.19	400	[95]
Defects and Functional Groups	Polyacrylamide hydrogel and carboxymethyl cellulose	1500 ° C for 1 h, N_2 atmosphere	1 M $NaPF_6$ in DME	142.7 at 100 mA/g	63.5	300	[102]
Defects and Functional Groups	Phenothiazine	700 °C for 2 h	1 M $NaPF_6$ in diethylene glycol dimethyl ether	221 at 1 A/g	-	2000	[103]
Defects and Functional Groups	Collagen fibers	900 °C for 4 h, Inert atmosphere	1 M $NaPF_6$ in diglyme	241.7 at 10 A/g	90	12000	[104]
Defects and Functional Groups	Corn stalk flour	1400 ° C for 2 h,	1.5 M $NaPF_6$ in EC/DEC/EMC (1/2/2, v/v/v)	247.8 at 0.15 A/g	85.9	500	[105]
Defects and Functional Groups	Xyloses	1200 ° C for 3 h, Ar atmosphere	1 M $NaPF_6$ in EC/DEC	67.6 at 5 A/g	93.2	10000	[108]
Defects and Functional Groups	Coal	1300 ° C for 2 h, Ar	1 M $NaPF_6$ in diethylene glycol	235.6 at 1 C	89	500	[109]

	atmospher e	dimethyl ether

4.4 Future Perspectives

While sodium-ion batteries (SIBs) are emerging as alternatives to lithium-ion systems, the development of readily available hard carbon anodes that are cost efficient and have optimal performance remains a core issue. Despite the understanding of sodium storage mechanisms and the optimization of carbon structures having advanced greatly, there are still several crucial steps that need to be undertaken in order to fully utilize the potential of hard carbon materials. These steps include exploration of new precursors, advanced precise control over microstructures and interface engineering, which can form the basis for the most recent innovations in sodium-ion battery technology.

The exploration of novel carbon precursors, particularly those sourced from sustainable and economically viable biomass or waste materials, stands out as one of the most urgent problems. Harnessing renewable biomass as well as recycled polymers not only serves environmental objectives, but also provides holistic compositional diversity for tailoring structural features. Nonetheless, these natural precursors are often plagued with batch variability and structural ambiguity, making reproducibility and controllability a challenge. Thus, future research should aim for molecularly designed precursors featuring precisely defined functional architectures. For instance, controlled heteroatom sites or crosslinking are programmable within synthetic polymers and these modifications can endow carbon frameworks with tunable interlayer spacing, pore geometry, or defect density[40]. From another angle, waste valorization—the transformation of industrial and agricultural byproducts into value-added carbon materials—captures the dual-benefit of environmental activism and energy storage device technology. Such materials can be enriched with functional groups or metal ions, allowing in situ doping or templating effects during carbonization to form hard carbon with superior electrochemical performance.

Apart from precursor design, the meticulous control of the hard carbon microstructure remains one of the primary strategies to control material characteristics and electrochemical behavior. While traditional thermal treatments achieved a basic level of control over the extent of graphitization and porosity, there is need for more exacting refinement. Some advanced processing methods including templated carbonization, chemical vapor deposition (CVD) and confined-space synthesis offer the possibility to engineer carbon domains with suitable interlayer spacing, pore radius, and distribution of heteroatoms. More importantly, in situ and operando structural characterization such

as in situ XRD, Raman spectroscopy, and transmission electron microscopy (TEM) offer strategies to observe the real-time evolution of carbon structure during sodium insertion/extraction, helping clarify the role and dynamics of storage sites such as closed pores and defect-rich regions[110]. There is also the combination of machine learning and data-driven methodologies, which is equally fascinating[111]. Studying and analyzing synthesis-structure-performance datasets, enables algorithms to predict optimal synthesis conditions or recommend unexplored regions of multi-parameter spaces. This collaboration between machine and experiment will greatly enhance the accelerated development of the next generation hard carbons.

Simultaneously, interface design has become a crucial consideration for the enduring stability and rate capability of hard carbon anodes. The nature of hard carbons shows that they have a high surface area as well as a rich concentration of defects. When they are used in combination with conventional ester-based electrolytes, they tend to form unstable or inhomogeneous solid electrolyte interphase (SEI) layers[112]. This results in low initial coulombic efficiency (ICE) and capacity fade through numerous cycles. In future work, focus must be directed to changing surface chemistry to regulate electrolyte–electrode interactions. Certain approaches, including surface functionalization with carbonyl-rich groups, thin-film coatings, and even pre-sodiation treatments have been beneficial in guiding SEI formation to enhance compatibility[108, 113]. Additionally, designing novel electrolytes (e.g., ether-based or fluorinated) or changing their formulations could stabilize SEI composition and enhance ionic transport[114]. At the same time, development of solid-state electrolytes opens new avenues for interface stability[115]. The combination of hard carbon with solid inorganic or polymer electrolytes not only mitigates the risks of flammability and leakage but also diminishes the risk of parasitic reactions. Thus, these combinations may result in cleaner, thinner SEI layers.

As for the future, the combination of approaches from molecular precursor design to structure-informed synthesis and interfacial tailoring will be necessary to fulfill the practical needs of commercial SIB. Specifically, reproducibility, cost containment, and scalability can be achieved but only with thorough investigations that connect raw material selection, process design, and full-cell performance[116]. Moreover, for real-world applicability, the integration of hard carbon anodes into full-cell configurations with suitable cathode materials (e.g. Prussian blue analogs, layered oxides) will need to be tested under realistic conditions, which include extreme temperature ranges and high areal loadings[117].

To summarize, the efficient optimization of the next generation of hard carbon anodes requires an integration of materials chemistry, nanostructure design, electrochemical engineering, and thorough interdisciplinary collaboration. This will enable the design of the next generation of hard carbon materials for sodium ion energy storage systems, making them more efficient to manufacture and easier to integrate seamlessly into multi-scale structures for enhanced performance without compromising sustainability.

Chapter5: Regulating Interlayer Spacing and Defects on Nitrogen-Doped Hard Carbon Anodes from Waste Plastic for Sodium-Ion Batteries

5.1 Introduction

As earlier chapters have explained, modern society still leans heavily on coal, petrol, and other fossil fuels for energy production, particularly in electrical generation and transportation. Burning these carbon-rich fuels sends out a steady stream of smoke, gases, and tiny particles that harm the air we breathe and the planet's climate. For example, light-duty vehicles are said to contribute around 10 percent of the total global CO_2 emissions[118]. Such disturbingly high figures have greatly accelerated the global shift towards electric vehicles (EVs) and an increased reliance on the use of renewable energy technologies, such as wind and solar energy. Nevertheless, due to their sporadic and unpredictable nature, there is a demand for the development of advanced and highly effective electrical energy storage systems (ESS) to guarantee consistent energy provision.

Among existing ESS technologies, lithium-ion batteries (LIBs) are universally acknowledged for their high efficiency, versatility, and scalability, rendering them optimal for portable electronics and large-scale storage applications. However, as we discussed before, worrying factors related to the scarcity and geographically uneven distribution of critical LIB components, particularly cobalt and lithium, raise concerns regarding the long-term sustainability of LIB based systems[119]. Given the explosive growth in demand for EVs industry and grid-scale storage, the currently available lithium reserves might fall short of meeting the global needs.

In response, we have seen a lot of effort trying to develop new alternative sustainable ESSs. Sodium-ion batteries (SIBs), once overshadowed by LIBs, have recently regained attention as an appealing alternative because sodium is much cheaper, more accessible, and chemically behaves very similar to lithium. Initial research on SIBs dates back to the late 1970s and early 1980s, but it is only recently that their practical potential has been seriously reconsidered[120]. Aside from the sodium's advantages of low-cost and abundance, SIBs are also economically attractive because aluminum foil can be used to replace copper as current collectors for anodes, thus decreasing the overall cost of the system[121]. Structurally similar to LIBs, a typical SIB contains a cathode and anode separated by a sodium-conducting electrolyte, thus forming a

complete cell[122].

Shifting from lithium-ion batteries to sodium-ion ones sounds simple in theory, yet it remains a tough engineering problem. For instance, graphite, the go-to anode in today's LIBs, is cheap and cycles impressively. Yet its layered structure refuses to accept larger Na^+ ions[123]. Because of that size mismatch, researchers have turned to a wide collection of carbon forms for SIB anodes, including graphene, carbon nanotubes, soft carbon, and hard carbon[124].

Understanding how each of these carbon variants microscale features affect battery performance is vital. Graphene shines with excellent conductivity, while carbon nanotubes form speedy one-dimensional channels for sodium ions. Soft carbon, which can transform into graphite with elevated temperature, has some limited structural disorder[7]. In comparison, hard carbon (HC) keeps highly disordered structure after treatment at high temperatures (>3000 °C), which significantly facilitating sodium storage[8]. HC has specific capacities close to 300 $mAh \cdot g^{-1}$, which enables its use in SIBs as one of the most economically attractive anode materials, because both performance and cost targets are achieved[125].

The increasing focus on waste plastics and associated environmentally friendly solutions has sparked innovation aimed at turning waste plastics into value-added carbon materials. Plastics that are not biodegradable pose a serious environmental challenge due to their ability to break down into microplastics that absorb toxic chemicals and enter the human food chain biochemically[30]. Functional carbonaceous materials such as graphene, carbon nanotubes, carbon dots, and hard carbon can be produced through chemical recycling pathways which involves depolymerization of these materials into valuable precursors or direct conversion of such structures[126]. Polyethylene terephthalate (PET), which is abundant in beverage bottles, has been proved to be a carbon precursor among many other waste plastics.

The microstructural features of a hard carbon material strongly influence its sodium storage properties. Specifically, nitrogen-doped hard carbon materials have increased interest, especially because of their improved properties during electrochemical processes and low cost. As an instance, Zhu et al. produced nitrogen-doped carbon nanofibers from polyacrylonitrile, which exhibited a remarkable reversible capacity of 150 $mAh \cdot g^{-1}$ with a current density of 1000 $mA \cdot g^{-1}$[127]. In addition, Song and co-workers synthesized three-dimensional N/O co-doped hard carbons which had enlarged interlayer distance and remarkable long-term cycling stability of 69.8% capacity retention after 15,000 cycles[128]. More recently, Zhang et al. utilized a 2D self-templating technique to synthesis nitrogen-doped hard carbon from waste PET,

generating mesoporous structures containing interconnected channels. The carbons showed excellent reversible capacity of 452 $mAh \cdot g^{-1}$, which was due to increased ion transport pathways and abundant adsorption sites[38].

Considering these developments, the creation of nitrogen-doped hard carbon materials from waste plastics, namely PET, offers a dual solution towards sodium storage and ecological concerns. It is possible to design sophisticated anode materials for future sodium-ion batteries by utilizing the performance tunability of waste carbon and the defect-engineering potential of heteroatom doping. In this case, we proposed the synthesis of nitrogen-doped hard carbon from waste PET using a straightforward chemical transformation approach. The derived materials are systematically analyzed for their structures, morphologies, and electrochemical properties, paying special attention to sodium storage mechanism and the effect of nitrogen doping and its relationship with sodium storage capacity.

5.2 Experimental Section

5.2.1 Materials and Chemicals

Graphite was purchased at Alfa Aesar (USA), and multi walled carbon nanotubes (MWCNTs) were supplied by Cheap Tubes Inc. (Grafton, USA), these two chemicals were used without any purification. Used water bottles (Real Canadian Brand) were collected and cleaned as the source of polyethylene terephthalate (PET). Potassium hydroxide (KOH) (ACS reagent grade, ≥97%), hydrochloric acid (HCl) (ACS reagent grade, 37%), urea (ACS reagent grade, ≤0.001% (Heavy Metals by ICP-OES, metals basis), 99.0-100.5%, solid), nitric acid (HNO_3) (ACS reagent, 70%), sulfuric acid (H_2SO_4) (ACS reagent, 95.0-98.0%), phosphoric acid (H_3PO_4) (ACS reagent, ≥85 wt. % in H_2O), hydrogen peroxide (H_2O_2) (30 wt. % in H_2O, ACS reagent), ethanol (anhydrous, ≥99%), dimethyl carbonate(anhydrous, ≥99%), ethylene carbonate (98%) and sodium perchlorate (≥99.9% trace metals basis) were all purchased from Sigma-Aldrich (Canada).

5.2.2 Synthesis of Reduced Graphene Oxide (rGO)

rGO was synthesized by an improved method[129] alongside with thermal reduction. For GO production, 3.0 g graphite, 360 mL concentrated H_2SO_4 and 40 mL H_3PO_4 (9:1 volume ratio) was put in an erlenmeyer flask in an ice bath. Then 18.0 g KMnO4 was added slowly in the mixture. The reaction was stirred and heated to 45 °C for 16 h. Water and H_2O_2 were added into the cooled down resultant to stop the reaction. The mixed liquid was centrifuged by hydrochloric acid, ethanol and water. After washing,

GO samples were freeze-dried to remove water content. The thermal reduction was conducted by heating GO samples at 950 °C under Ar atmosphere.

5.2.3 Synthesis of Multi Walled Carbon Nanotubes (MWCNTs-COOH)

Typically, 24 mL HNO_3, 72 mL H_2SO_4 and 0.75 g MWCNTs were heated at 105 ℃ for 6 hours in a round-bottom flask. The resultant was washed by centrifugation to remove remaining acid. The final product was obtained after freeze-drying.

5.2.4 Synthesis of Hard Carbon (HC)

The hard carbon was prepared through method reported earlier[130]. Briefly, smashed used poly (ethylene terephthalate) (PET) bottles pieces were frozen by liquid nitrogen, then ground and sieved to reduce their sizes. 1:1 mass ratio of KOH and ground PET were mixed in water. By heating at 80 ◦C overnight, the water was completely boiled off. The KOH coated PET was annealed at 800 ◦C under nitrogen atmosphere. Carbonized sample was washed with 1 M HCl for 1 h, then were washed by centrifugation. After drying overnight at 80 ◦C, the final hard carbon was obtained.

5.2.5 Synthesis of Nitrogen-doped Hard Carbons (NHC)

The nitrogen-doped hard carbon (NHC) was synthesized using method in literature[82]. Urea and hard carbon were mixed with a mass ratio 1:3. These mixtures were initially heated at 400 °C for 2 h under an Ar atmosphere. Then, they were calcinated at 700, 800, 900 °C for 3 h. Calcinated products were washed with HCL solution, ethanol, and water. After drying at 80 °C for 24 h in a vacuum oven, the nitrogen-doped hard carbons were obtained, denoted as NHC-T, where T is the carbonization temperature (700, 800, and 900°C).

5.2.6 Material Characterization

Morphology of samples and elemental mapping were examined by a field-emission scanning electron microscopy (SEM) with energy-dispersive X-ray spectroscopy (EDS) capability (UltraPlus, Zeiss, Switzerland). HR-TEM (LIBRA 200 MC, Zeiss, Switzerland) was employed to visualize nanostructure of hard carbons. X-ray diffraction (XRD) measurements were conducted via a XRD machine (Miniflex 600, Rigaku, Japan) using Cu Kα radiation (λ = 1.5406 nm). X-ray photoelectron spectroscopy (XPS) was conducted through a PHI 5000 VersaProbe III. Raman spectra were collected using a WITec alpha300R confocal Raman microscope (532 nm laser).

5.2.7 Electrode Fabrication and Electrochemical Testing

Electrode Fabrication

A half-cell setup (two-electrode configuration) assembled in CR2032 coin cell was employed for electrochemical performance tests[131]. Polished sodium metal plate was cut into 13 mm disks as both reference and counter electrodes. The preparation of working electrode using active material, acetylene black and polyvinylidene fluoride (PVDF) at a weight ratio of 70: 10: 20 dissolved in appropriate amount of N-methyl-2-pyrrolidone (NMP). The viscous slurry was cast onto a piece of copper foil and dried in a vacuum oven for 12 h at 70 ℃. 1M $NaClO_4$ in a mixture of ethylene carbonate (EC) and dimethyl carbonate (DMC) (volume ratio: 1:1) was utilized as electrolyte. Glass fiber from Whatman (GF/D) was used as the separator. All coin Cells were assembled in argon-filled glove box (Mbraun, USA) where oxygen and water content are less than 0.5 ppm.

Electrochemical Testing

The galvanostatic charge-discharge tests were conducted by a Land CT2001A battery test system (Land, Wuhan, China) between 0.01 and 2 V. Cyclic voltammetry (CV) curves, electrochemical impedance spectra (EIS) were carried out on the electrochemical station (VSP-300, BioLogic, France).

5.3 Results and Discussion

5.3.1 Morphological and Structural Characterization

A precise insight at the fine microstructure of the carbon samples came from scanning electron microscopy (SEM), as displayed in Figure 9a through Figure 9c. In Figure 9a, the reduced graphene oxide (rGO) appears as a loose stack of paper-thin, wrinkled sheets that spread out in rough, lamellar swaths a few micrometers wide. That crinkled, accordion-like shape is promising because it has a large surface area and facilitates ion transport during electrochemical reactions. Switch to the picture in Figure 9b and an entirely different scene unfolds: a tangled, three-dimensional web of carbon nanotubes (MWCNTs-COOH) where each tube has a barely-visible nanometer width. The filaments twist and intertwine, forming a spongy skeleton that improves both electrical conductivity and electrolyte accessibility. Finally, Figure 9c tells the story of hard carbon (HC), which shows a scattering of jagged, brick-like particles locked together in a stubborn, dense mass. These irregular chunks sport rough surfaces, speckled with wispy carbon flakes likely caused during the high-temperature treatment, and that disorder boosts the number of active sites and may affect the overall electrochemical

behavior. The unique shapes and appearances of rGO, MWCNTs-COOH and HC highlight their intrinsic structural differences and play a critical role in determining their performance as electrode materials.

A high-resolution transmission electron microscopy (HRTEM) image of the nitrogen-doped hard carbon which is doped at 800 ℃ (NHC-800) appears in the left panel of Figure 9d. The micrograph betrays no long-range order one would associate with classic graphite[78]. Short carbon layers curl and stack turbostratically, indicating only partial graphitization[80]. The amorphous nature of the material is confirmed by randomly oriented carbon fringes. However, there are some localized parallel domains suggest the presence of limited short-range ordering. Fast Fourier transform (FFT) pattern, shown as the right panel in Figure 9d, lends its own confirmation. Diffuse concentric rings pop up where sharp diffraction spots normally rest, repeating that the material is amorphous or poorly crystalline[132]. That highly defect-rich and disordered microstructure may end up being a benefit, providing abundant active sites and facilitating sodium storage in electrochemical applications.

Figure 10a and Figure 10b compares NHC-800 with pristine HC using N_2 adsorption-desorption isotherms and BJH pore-size distributions Both samples show that classic type-IV loop with the H4-type hysteresis loops, a hallmark of slit-shaped micro-/mesopores originating from the turbostratic graphene stack[133]. The HC isotherm rises quickly below P/P0 0.05 and it has the larger overall adsorption capacity, which is a sign of it's porous network built by plentiful mesoporous. The pore-size curve peaks sharply below 2 nm and spreads out between 15 and 40 nm. After nitrogen introduction at 800 °C, the global isotherm is shifted downward and the hysteresis loop becomes narrower, indicating that total pore volume and specific surface area have trimmed back. In Figure 10b, the micro-pore peak of NHC-800 is attenuated, the shoulder at 3–5 nm almost disappears, and the mesopore maximum is slightly shifted toward smaller diameters. These shifts imply that N incorporation and thermal reconstruction densify the carbon walls, block some ultramicropores, yet leave a hierarchical micro/mesoporous texture that facilitates Na^+ diffusion.

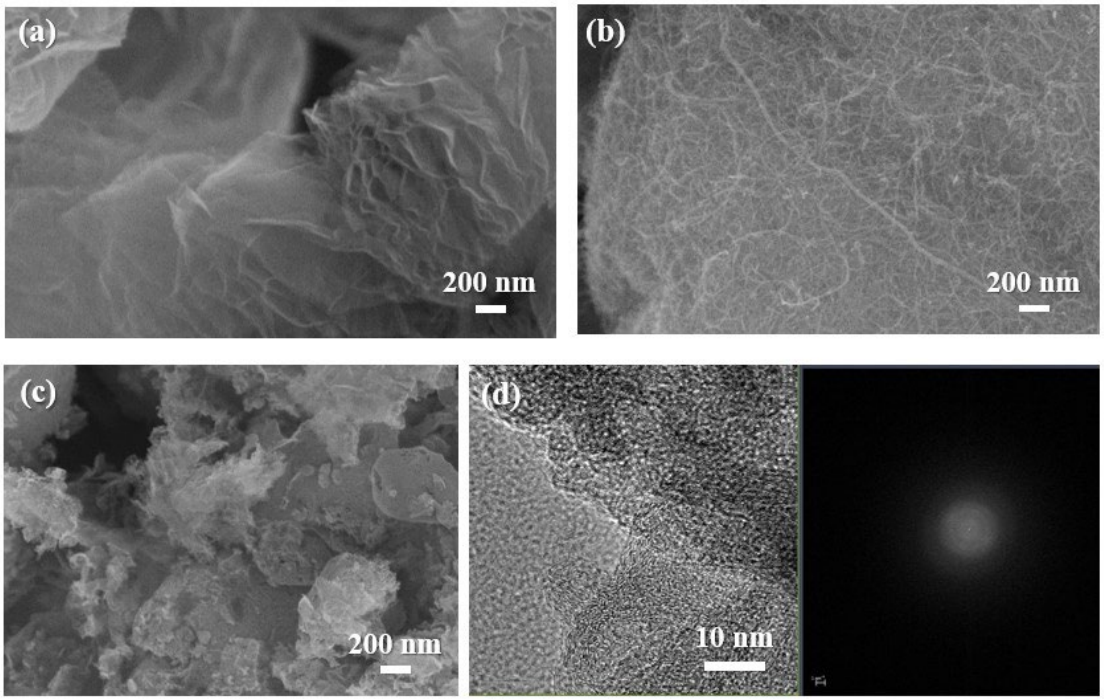


Figure 9. (a-c) SEM images of rGO, MWCNTs-COOH and HC; (d) HRTEM and FFT images of NHC-800.

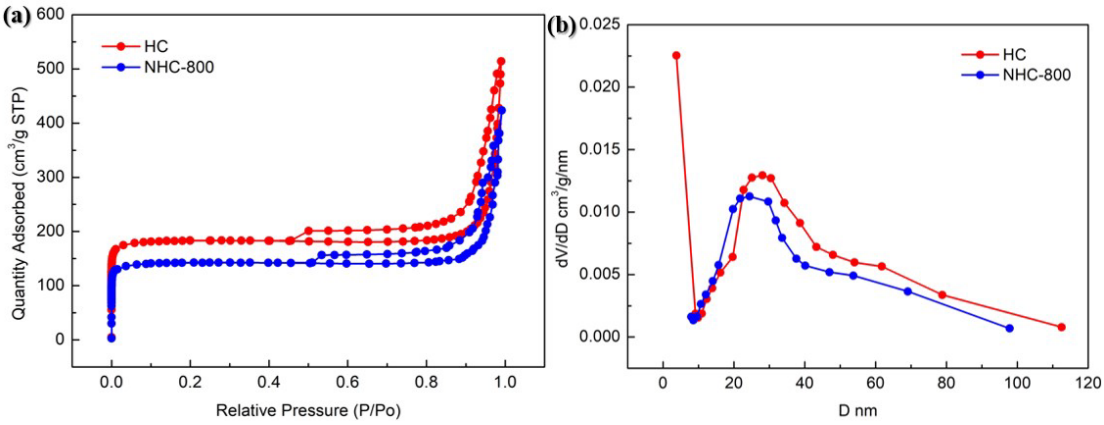


Figure 10. (a) N_2 adsorption-desorption isotherms of hard carbons; (b) Pore size distribution of hard carbons.

The evolution of carbon microstructure from pristine hard carbon (HC) to N-doped hard carbons prepared at 700, 800 and 900 °C (NHC-700, NHC-800 and NHC-900) was quantified by simultaneous Raman and X-ray diffraction (XRD) analysis (Figure 11). Figure 11a presents the Raman spectra of the four carbon materials. Each profile shows the characteristic pair of peaks near 1350 cm^{-1} and 1580 cm^{-1}, assigned to the defect-related D peak and the graphitic E_2g G peak, respectively[75]. The I_D/I_G intensity ratio, which provides a semiquantitative measure of the defect density, rises from 1.06 in

pristine hard carbon (HC) to 1.10, 1.20 and 1.18 in the NHC-700, NHC-800 and NHC-900. This clear upward trend confirms that nitrogen incorporation markedly increases the overall defect population.

Detailed structural information is needed for analyzing these samples, the broad D peak in spectrum was deconvoluted into four components by using Lorentzian equation (Figure 12). The D1 sub-peak, which is centered at 1350 cm^{-1}, originates from A_1g breathing modes of disordered graphitic domains[134]. The D2 feature (around 1620 cm^{-1}) is attributed to defect scattering in few-layer graphene regions[95]. The D3 peak (near 1500 cm^{-1}), reflects vibrational modes of short-range sp^3-hybridized carbon within the amorphous matrix[135]. Finally, the D4 peak at 1200 cm^{-1} is related to stretching vibrations of heteroatom-terminated sp^2-sp^3 edge sites[135]. Together, the evolution of these sub-peaks offers a nuanced picture of how nitrogen doping modulates the balance between graphitic order, amorphous carbon, and heteroatom-functionalized edges.

As shown in table 3, the D1 component rises progressively with treatment temperature, from 63.4 % to 71.6 %, signaling the fragmentation of graphitic domains into smaller crystallites rich in edge sites. At 700 °C, N species insert between neighboring graphitic layers, the shearing and turbostratic slip they introduce are captured by the D2 sub-peak, which is known to arise from defect-scattering in few-layer or misaligned graphene sheets. Consequently, the D2 area jumps to about 15% in NHC-700, but once the heat-treatment is raised to 800 °C and 900 °C the layers have enough mobility to realign, so the D2 share collapses to roughly 6% and then 3%. Meanwhile, many N- and O-containing fragments remain chemisorbed on the carbon surface or are trapped at sp^2–sp^3 terminations, giving a high D4 contribution (16%). Further annealing strips these weakly bound moieties: de-oxygenation and de-nitrogenation reactions progressively happen, so the D4 area falls to about 13% at 800 °C and only 8% at 900 °C. The amorphous-carbon D3 share remains 14–19 % throughout all these samples.

The Raman trends are echoed in the XRD data (Figure 11b and Figure 13). As shown in Figure 11b, two typical broad peaks appear at approximately 23° and 43.7° in all samples, which correspond to (002) and (100) diffraction peaks for non-graphitized carbon, respectively[136]. By using Bragg's Equation, the interlayer spacing of hard carbons can be estimated (Eq. (1))[137]:

$$2d \sin\theta = n\lambda \quad (1)$$

where d is the spacing between the crystal planes (interlayer spacing), θ is the angle between the incident X-ray and the crystal plane, n is the order of reflection, and λ is the wavelength of X-ray (λ=1.5406A˚ for Cu Kα radiation).

In order to further investigate the evolution of the microcrystalline phase with increasing nitrogen doping temperature, the (002) peaks were simulated using a profile-fitting process, which divided (002) peak into two carbon phases, highly disordered and pseudo-graphitic[138]. In table 4, nitrogen doping lifts the highly disordered (002) fraction from 24.17% in HC to 66.39% in NHC-700, while the pseudo-graphitic share collapses to 33.61%. Further heating gradually re-establishes graphitic order, with the pseudo-graphitic area rebounding to 39.70% at 800 °C and 55.16% at 900 °C. Despite this partial restoration, the inter-layer spacing d_{002} keeps widening, expanding from 0.399 nm in HC to 0.413 nm in NHC-900, residual nitrogen atoms therefore remain lodged between graphene layers and act as persistent spacers.

Altogether, the sample treated at 800 °C offers the most balanced architecture. Its d_{002} value of 0.408 nm eases sodium-ion intercalation, and a domain distribution of roughly 60% disordered carbon and 40% pseudo-graphite blends abundant active sites with uninterrupted electron pathways. The elevated D1 level supplies plentiful edge defects, yet a moderate D4 content preserves enough surface functionality for reversible redox. This synergy is expected to grant NHC-800 the best mix of reversible capacity, rate capability and cycling life. By comparison, NHC-700, though rich in defects, suffers from excessive disorder, whereas NHC-900, while electrically better, trades off capacity because many functional and defect sites have been annealed away.

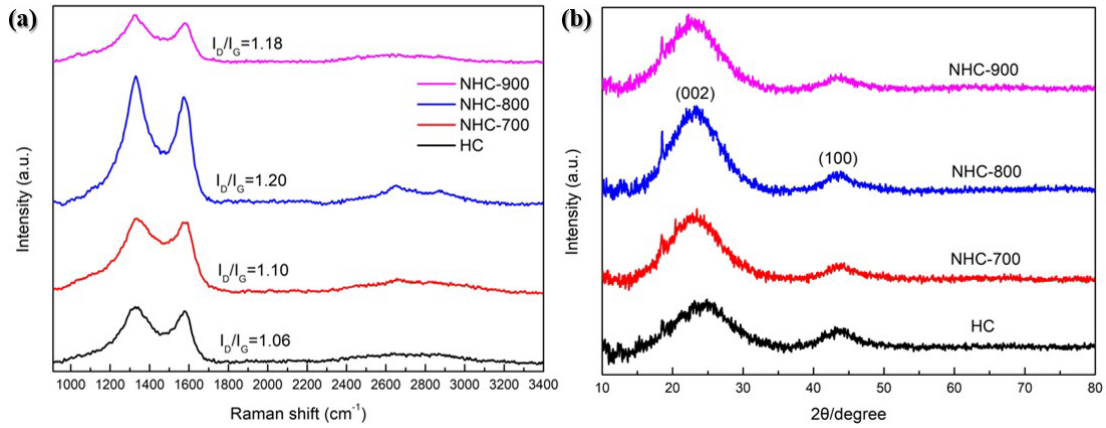


Figure 11. (a) Raman spectra of hard carbons; (b)XRD patterns of hard carbons.

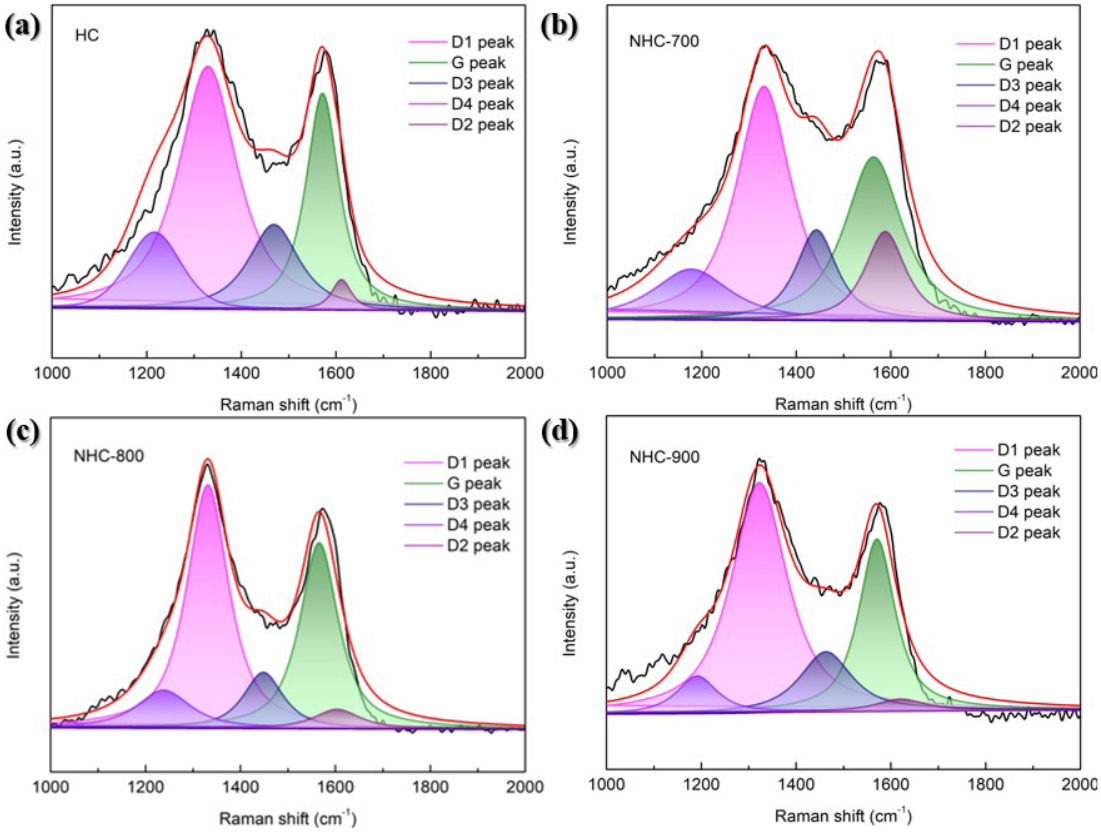


Figure 12. Raman fitting curves of hard carbons.

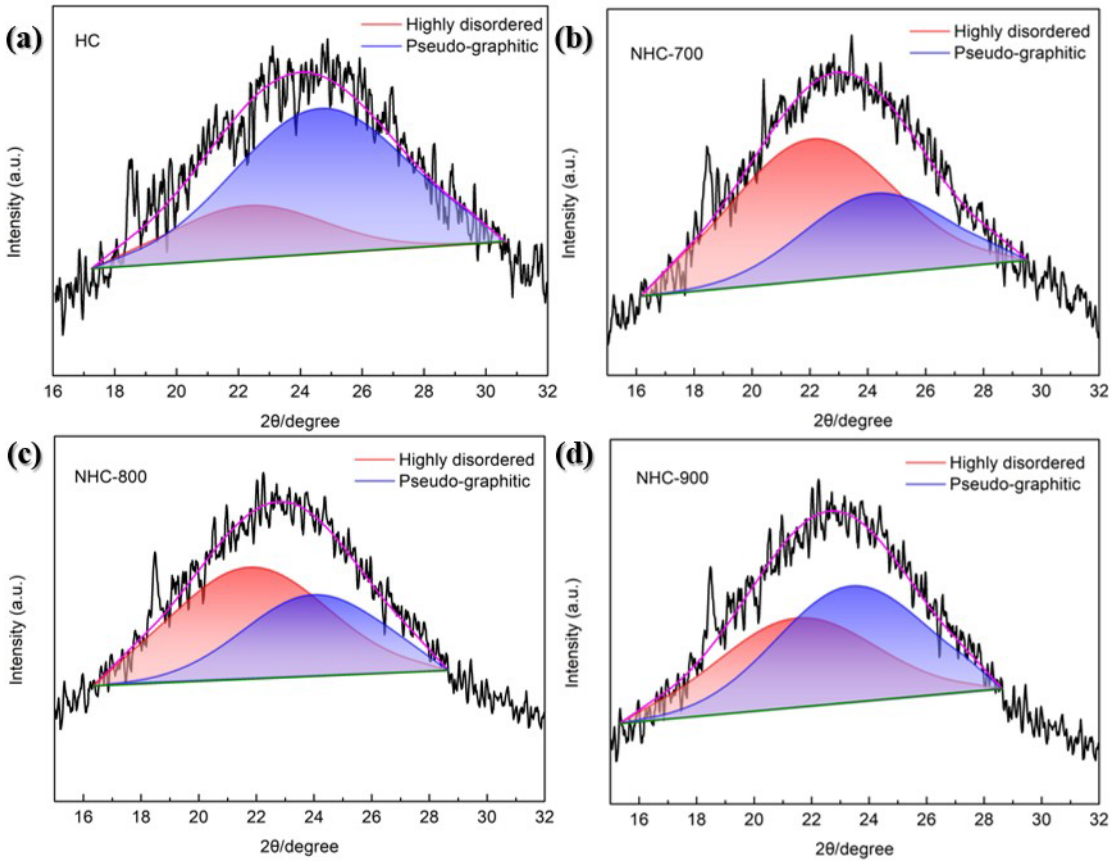


Figure 13. XRD fitting curves of hard carbons.

Table 3. Physical parameters of the hard carbon samples from Raman spectra.

Sample	D1/%	D2/%	D3/%	D4/%	I_D/I_G
HC	63.38	2.63	19.10	14.89	1.06
NHC-700	53.52	15.09	15.32	16.07	1.10
NHC-800	66.54	5.74	14.46	13.27	1.20
NHC-900	71.59	2.95	17.06	8.40	1.18

Table 4. Physical parameters of the hard carbon samples from XRD patterns.

Sample code	Highly disordered			Pseudo-graphitic		
	2θ (◦)	d002 (nm)	Area (%)	2θ (◦)	d002 (nm)	Area (%)
HC	22.28754	0.3991	24.17	24.6481	0.3611	75.83

NHC-700	22.0902	0.4022	66.39	24.23714	0.3674	33.61
NHC-800	21.76733	0.4080	60.30	23.98105	0.3711	39.70
NHC-900	21.4813	0.4135	44.84	23.37972	0.3803	55.16

5.3.2 Surface Chemistry and Defect Engineering

X-ray photoelectron spectroscopy (XPS) was used to probe the surface composition and bonding configurations of the nitrogen-doped hard carbons (NHCs). In the survey spectra (Figure 14a) the C 1s, N 1s, and O 1s envelopes are centered at 285.00, 399.07, and 532.92 eV, respectively, confirming the coexistence of the three elements on each sample[139]. Quantitative fitting gives total N contents of 4.56 at % (NHC-700), 2.78 at % (NHC-800), and 2.41 at % (NHC-900); the corresponding O levels fall from 9.49 to 7.46 at % as the pyrolysis temperature rises. This monotonic decrease is typical of high-temperature carbonization, where volatile N- and O-containing groups are progressively expelled, leaving behind a more ordered sp^2 lattice. High-resolution N 1s spectra (Figure 14b-d) can be deconvoluted into three components located at 398.43 eV (pyridinic-N), 399.29 eV (pyrrolic-N) and 400.21 eV (graphitic-N)[140]. The relative distributions extracted from peak-area normalization are summarized in Table 5. Pyridinic-N introduces localized states near the Fermi level, strengthening Na^+ adsorption via an ionic–covalent interaction and effectively enlarging the charge-storage stage[141]. Pyrrolic-N bends adjacent graphene sheets and expands interlayer spacing, which lowers the diffusion barrier for Na^+ intercalation and facilitates fast sodium kinetics[84]. Graphitic-N is beneficial for electronic conductivity, lacks Lewis-basic lone pairs and therefore contributes little to sodium binding, excessive graphitic-N can even reduce wettability and suppress electrolyte penetration[103, 142]. From 700 °C to 800 °C, the sharp jump in pyridinic-N comes mainly at the expense of pyrrolic-N and graphitic-N. Thermal rearrangement converts the less stable five-membered pyrrolic rings to six-membered pyridinic moieties, while a small fraction of graphitic-N is cleaved. Because both pyridinic and pyrrolic nitrogen reside at edge/defect sites, the total edge-N fraction climbs to a maximum of 83.9 %. This high density of electronegative lone-pair centers increases the affinity of the carbon surface for Na^+ and provides abundant adsorption sites. From 800 °C to 900 °C, further heating only marginally reduces total N content, but drives slight graphitization and reconstructs some pyrrolic-N back into the basal plane. Although graphitic-N improves electrical

conductivity, it offers few active sites for Na^+ adsorption and can partially passivate pores. The net result is a modest drop in edge-N to 82.8 %.

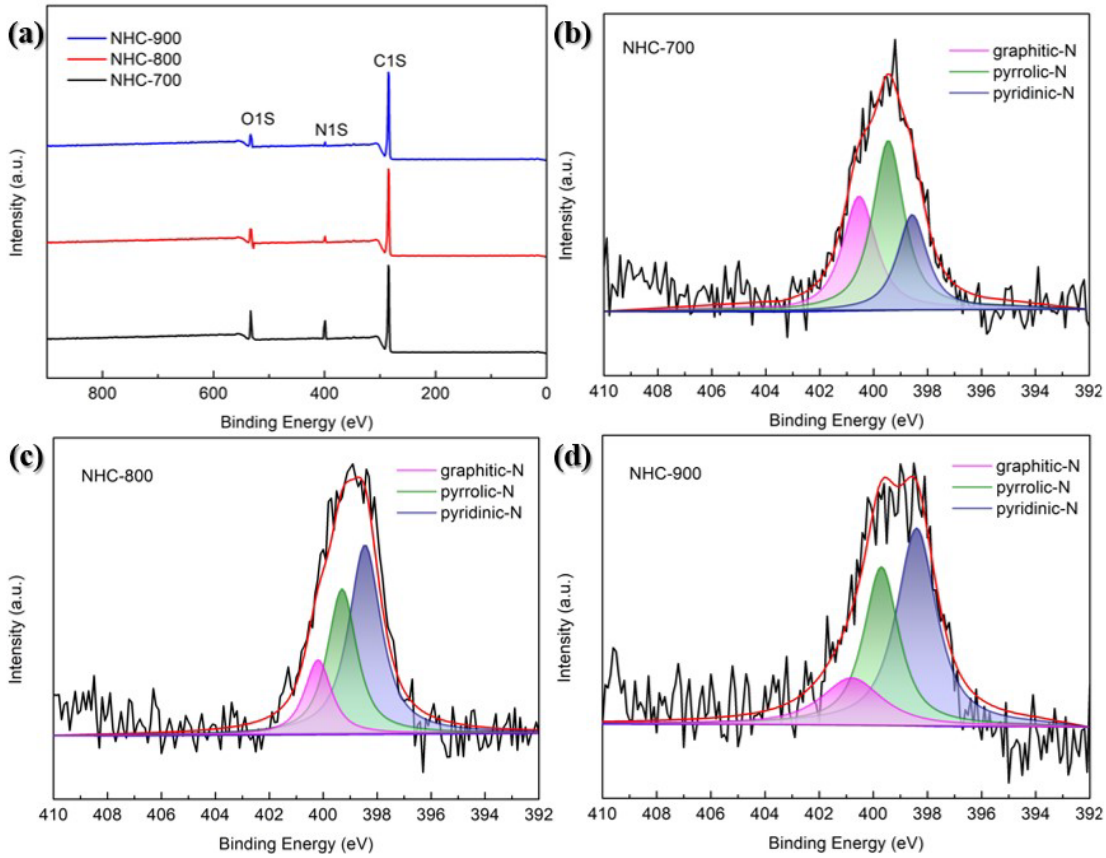


Figure 14. (a) XPS survey spectra of NHCs; (b) High-resolution N 1s spectra for NHC-700; (c) High-resolution N 1s spectra for NHC-800; (d) High-resolution N 1s spectra for NHC-900.

Table 5. Relative percentage of different nitrogen species for NHCs.

Sample code	Pyridinic N/%	Pyrrolic N/%	Graphitic N/%
NHC-700	32	44.2	23.8
NHC-800	49.7	34.2	16.1
NHC-900	48.6	34.2	17.2

5.3.3 Electrochemical Performance Comparison

Galvanostatic charge-discharge (GCD) analyses electrochemical performance of rGO, MWCNTs-COOH and HC. Figure 15a presents cycling performance curves obtained at a current density of 20mA/g. The initial specific charge capacities for rGO,

MWCNTs-COOH and HC are 110.1, 110.6 and 115.2 mAh g^{-1}, respectively. The difference appears in the subsequent cycles. After 220 cycles, HC maintains high reversible capacity of 81 mA h g-1, shows higher capacity retention (70.31%) than rGO (44.87%). The oxidized MWCNTs lose activity completely after 150 cycles. HC's outstanding performance can be attributed to its turbostratic stacking graphitic layers, the expanded interlayer spacing accommodates Na^+ reversibly while resisting mechanical stress. In rGO, progressive restacking of graphene may narrow interlayer spacing and accelerate capacity decay. For MWCNTs-COOH, the large number of edge-carboxyl groups catalyzes continuous side reactions. The rate capability of the three samples is further investigated in Figure 15b. At low current densities (10 mA/g and 15 mA/g), there is no obvious deference in specific capacity between HC and MWCNTs-COOH. However, during high-rate testing (200 mA/g), HC still delivers 53 mAh g^{-1}, whereas rGO and MWCNTs fall to 41.5 and 30.5 mAh g^{-1}, respectively.

The first charge-discharge curves for three nitrogen-doped samples are presented in Figure 15c, NHC-800 exhibits the highest initial Coulombic efficiency (ICE), outperforming both NHC-700 and NHC-900. All the curves have a sloping region, followed by a steep low-voltage plateau (<0.1 V). The nitrogen configuration plays an important role in NHCs performance. At 800 °C, the concentration of pyridinic and pyrrolic N reach maximum, they can introduce surface defects that strengthen Na-adsorption. At higher temperature (900 °C), part of these sites converts into graphitic N, reducing active-site density. At 700 °C, there are excessive surface heteroatoms and oxygenated groups on the surface, intensifying SEI formation. Meanwhile, N_2 adsorption-desorption test results show NHC-800 has a lower specific surface area than HC, indicating less fresh carbon exposes to electrolyte. Furthermore, XRD calculation demonstrates the interlayer spacing of pseudo-graphitic area in NHC-800 is 0.3711 nm, which is an optimal spacing for Na^+ intercalation. These three factors contribute to satisfactory performance. Cycling performance for NHCs and HC is displayed in Figure 15d, all NHCs surpass pristine HC, indicative of successful electronic/ionic tuning by nitrogen. NHC-800 reaches 340.4 mAh g^{-1} after 44 cycles, NHC-900 and NHC-700 settle at 203.9 and 166.2 mAh g^{-1}, still higher than HC (90.6 mAh g^{-1}), confirming that nitrogen doping contributes to sodium storage. In terms of rate capability, when the current density steps from 10 to 200 mA g^{-1}, the specific capacities of NHCs gradually decline (Figure 15e). Upon returning to 10 mA g^{-1}, the capacities nearly fully recover, indicting the mechanical integrity and elastic deformability of the disordered carbon matrix.

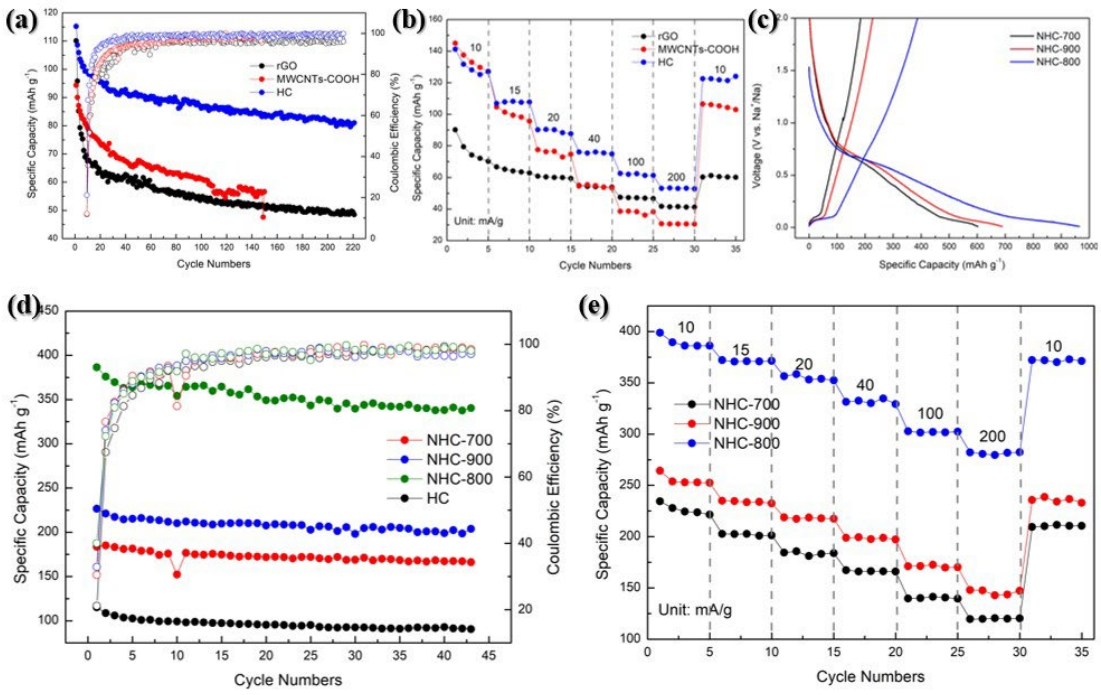


Figure 15. (a) Cycling performance of rGO, MWCNTs-COOH and HC; (b) Rate performance of rGO, MWCNTs-COOH and HC from 10 mAh g^{-1} to 200 mAh g^{-1} (c) The initial galvanostatic charge-discharge curves of NHCs; (d) Cycling performance of NHCs; (e) Rate performance of NHCs from 10 mAh g^{-1} to 200 mAh g^{-1}.

5.3.4 Kinetic and Mechanistic Insights

Cyclic voltammetry (CV) tests were conducted in the voltage range from 0 to 2.5 V at a scan rate of 0.1 mV s^{-1} to probe the electrochemical behavior of rGO, MWCNTs-COOH, HC and NHC-800. The initial three cycles CV curves of these carbon electrodes are presented in Figure 16. Several common findings emerge, yet the subtleties among rGO, MWCNTs-COOH, HC and NHC-800 offer valuable clues to their sodium-storage mechanisms and kinetics. During the initial cycle, all the electrodes exhibit an irreversible reduction peak centered at 0.42 V. The appearance of these peaks is widely assigned to the formation of the solid electrolyte interphase (SEI) layer, where electrolyte decompose on the electrode surface, and some irreversible chemical reactions. There is a wide, unobvious reduction peak appears at around 0.86 V in rGO, HC and NHC-800 samples, may cause by the reduction of residual surface functional groups. Stable interphase is established after the first sodiation step, proving by the disappearance of these irreversible peaks in following cycles. In nearly 0.01V, a sharp reduction peak appears indicating sodium storage in all the curves. For MWCNTs-COOH, HC and NHC-800, they show an oxidation peak at approximately 0.11, 0.09,

and 0.13 V, which is a clear sign of sodium release, respectively. These redox couples represent Na^+ insertion/extraction process in hard-carbon-type anodes[143]. However, no obvious oxidation peak emerges in the first three scan for rGO. The absence of a clear anodic peak in rGO suggests sluggish desodiation, explaining its modest reversible capacity. It is worth noting that the desodiation peaks of MWCNTs-COOH, HC and especially NHC-800 sharpen and intensify from the 2nd to 3rd cycle, signaling lower charge-transfer resistance and electrode activation[144]. The redox peak current reflects the extent of Faraday reaction in the voltage range where redox peaks appear. Generally speaking, Faraday reaction is a chemical reaction with electron transfer. In our case, this reaction represents desodiation/sodiation process. When the peak current increases, there are more sodium ions involved in this process[145].

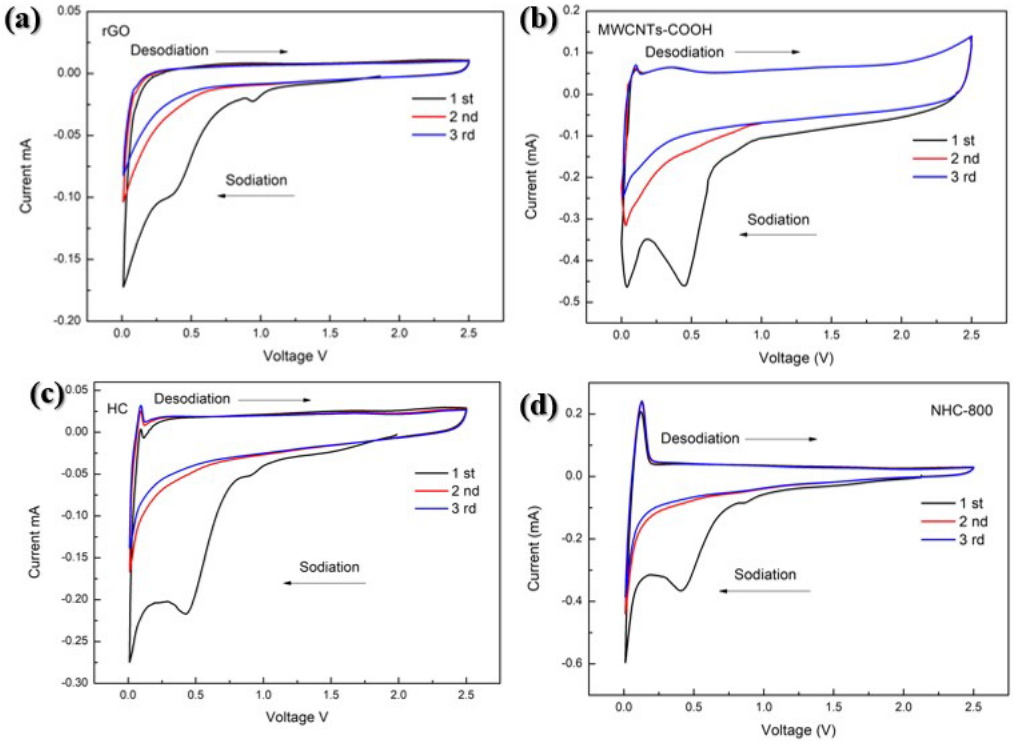


Figure 16. (a) Cyclic voltammograms of rGO; (b) MWCNTs-COOH; (c) HC; (d) NHC-800 at 0.1 mV s^{-1}.

The sodium storage kinetic of various carbon electrodes was further revealed through CV scanning from 0.1 mV s^{-1} to 1 mV s^{-1}. It is commonly known that the electrochemical reaction of sodium with carbon electrodes contains two processes: diffusion-controlled process and capacitive-controlled process. The way of the current response is generated during electrochemical reactions is different. For diffusion-

controlled process, the current is limited by the speed which sodium ions diffuse from the electrolyte into the bulk of the electrode material[146]. This slow process depends on ion mobility and material structure. In terms of capacitive-controlled process, the current comes from charge storage at or near the surface and it does not need for ion diffusion into the bulk[147]. In order to distinguish sodium storage kinetic, the following equation is employed to calculate b value[134]:

$$i = av^b \quad (2)$$

This equation provides a relation between peak current I and scan rate v, a is a constant and b value is estimated by linear-fitting. When b approach to 0.5, the entire reaction is controlled by diffusion, while b equals 1.0 means a capacitive behavior, such as sodium ions adsorption on defects, edges and functional groups.

Capacitive contribution of current is evaluated through deconvolution of current profiles using the equation as follow[148]:

$$i(V) = k_1 v + k_2 v^{1/2} \quad (3)$$

where k_1v denotes the capacitive-controlled contribution in the exact current and $k_2v^{1/2}$ reflects the diffusion-controlled contribution.

As presented in Figure 17a, d, g, all three electrodes show a pair of well-defined cathodic/anodic peaks in the CV curves, showing a typical of reversible Na^+ uptake/release. Meanwhile, with the increasing scan rates, an enhanced potential polarization is observed in all samples. rGO and MWCNTs-COOH exhibit similar results in terms of b value (slope) (Figure 17b, e), b values for these two carbon materials are around 0.5 to 0.6, which is a signal for diffusion-limited process. The situation is different for HC, b values for peak 1 and peak 2 are 0.74 and 0.62, respectively, indicating a hybrid behavior and fasted surface kinetics (Figure 17h). Figures 17c, f, i corroborate the b-value diagnosis. At the lowest scan rate (0.1 mV s^{-1}) diffusion governs in all cases because ions have ample time to penetrate the bulk.

When the scan rate rises to 1 mV s^{-1}, capacitive contribution of rGO climbs from 28 % to 55 %, while MWCNTs-COOH increases from 22.1% to 47.1%, these results show consistency with b values. Capacitive contribution of HC soars to 73 % at 1 mV s^{-1}, even at 0.1 mV s^{-1} the surface component remains 47 %, confirming the hybrid nature of hard carbon. Widely distributed nanopores and an amorphous lattice in HC provide short solid-state paths and abundant adsorption sites, explaining its high pseudocapacitance and good high-rate capacity.

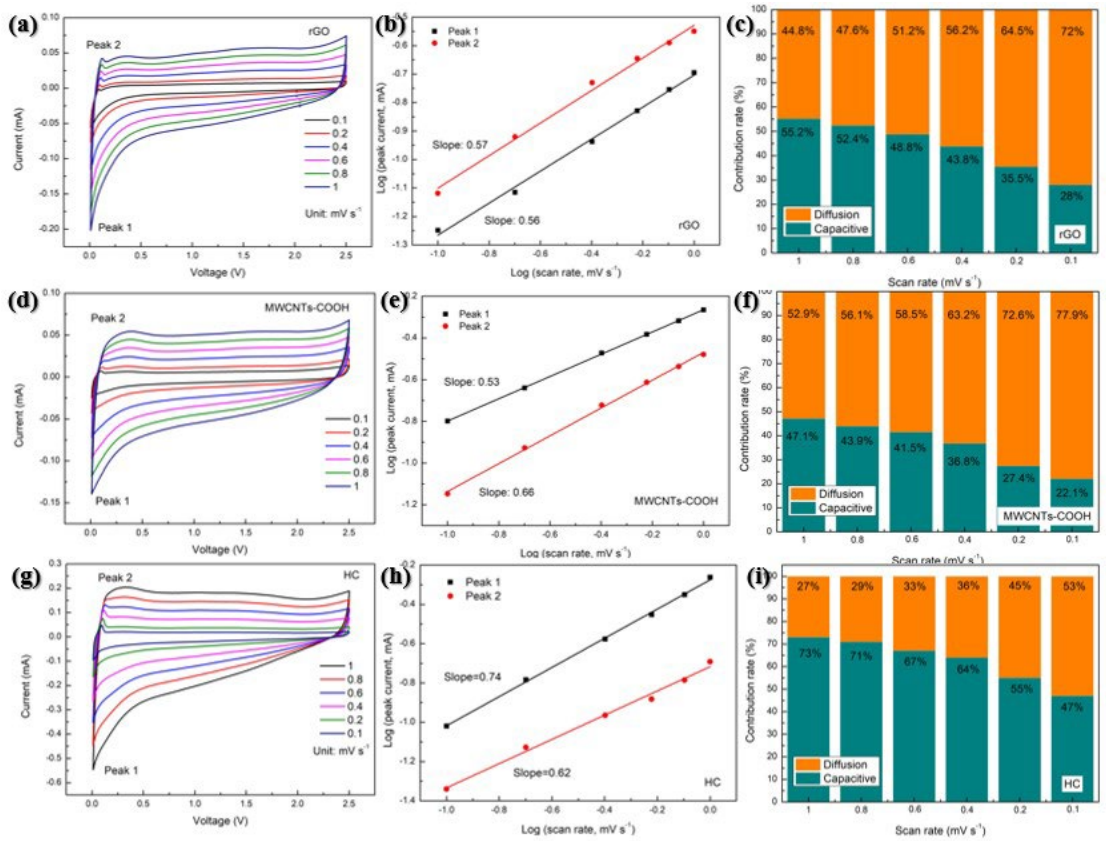
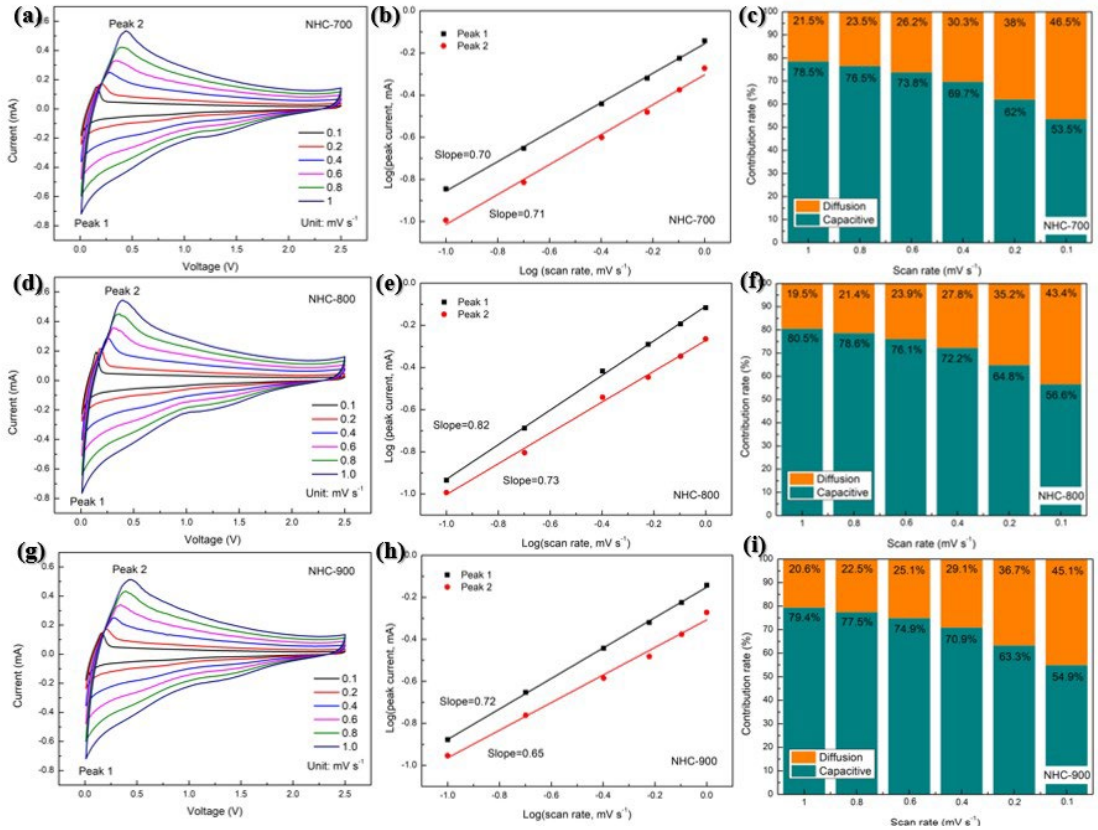


Figure 17. (a) CV curves of rGO at various scan rates from 0.1 to 1 mV s^{-1}; (b) The correlations of current scan rate (v) and peak current (i) of rGO; (c) Capacitive contributions of rGO at various scanning rates; (d) CV curves of MWCNTs-COOH at various scan rates from 0.1 to 1 mV s−1; (e) The correlations of current scan rate (v) and peak current (i) of MWCNTs-COOH; (f) Capacitive contributions of MWCNTs-COOH at various scanning rates; (g) CV curves of HC at various scan rates from 0.1 to 1 mV s−1; (h) The correlations of current scan rate (v) and peak current (i) of HC; (i) Capacitive contributions of HC at various scanning rates.

Compared with HC, all the nitrogen-doped samples exhibit the familiar pair of Na^+ insertion/extraction peaks, but the anodic current is visibly larger, which means intensive faraday reactions happen (Figure 18a, d, g). The expanded interlayer spacing of NHCs lowers the Na^+ intercalation barrier, and increased number of active sites in NHCs promotes adsorption. Nitrogen doping temperature affects sodium storage behavior to some extent, linear-fitting results of peak 1 and peak 2 in NHC-700 are 0.70 to 0.71, respectively (Figure 18b). This clear hybrid behavior is caused by high nitrogen content (4.6 at %). B values in NHC-800 are slightly higher than samples in 700℃ and 900 ℃, which are about 0.8 (Figure 18e). Capacitive-controlled process is more active in NHC-800. When temperature keeps going up to 900 ℃ (Figure 18h), b value

decreases a little, indicating high temperature removes some active sites (lower N and O contents). Figures 18c, f, i convert each CV curve into quantitative fractions. At 0.1 mV s^{-1} the process is still largely diffusion-governed, but NHC-800 already dedicates 43 % of its charge to fast surface mechanisms. When the scan rate goes up to 0.6–0.8 mV s^{-1}, NHC-800 preserves the highest capacitive contribution. At 1 mV s^{-1}, NHC-800 has the highest capacitive contribution among three samples. These figures echo the b-value trend and confirm that NHC-800 delivers the best hybrid behavior.



Figures 18. (a) CV curves of NHC-700 at various scan rates from 0.1 to 1 mV s^{-1}; (b) The correlations of current scan rate (v) and peak current (i) of NHC-700; (c) Capacitive contributions of NHC-700 at various scanning rates; (d) CV curves of NHC-800 at various scan rates from 0.1 to 1 mV s^{-1}; (e) The correlations of current scan rate (v) and peak current (i) of NHC-800; (f) Capacitive contributions of NHC-800 at various scanning rates; (g) CV curves of NHC-900 at various scan rates from 0.1 to 1 mV s^{-1}; (h) The correlations of current scan rate (v) and peak current (i) of NHC-900; (i) Capacitive contributions of NHC-900 at various scanning rates.

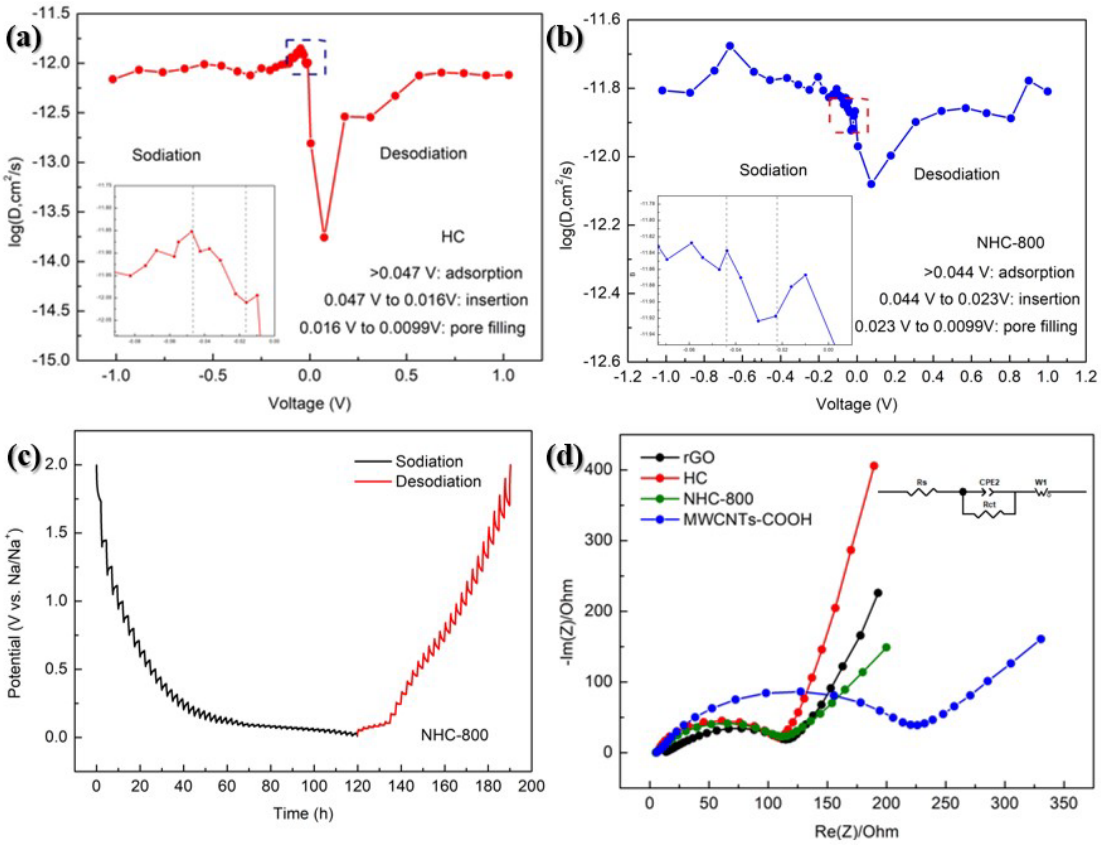
Diffusion coefficient of Na^+ is a crucial parameter to evaluate the ion diffusion and sodium storage mechanism. Galvanostatic intermittent titration (GITT) technique is a convenient tool to measure diffusion coefficient during charge-discharge process. In theory of GITT, diffusion in the solid electrode is simply assumed to be one-

dimensional and several effects are neglected, such as double-layer charging and Ohmic potential drop[149]. A pulse current is firstly applied to system during time τ as a transient process. The entire system then experiences a relaxation (no current applied) for equilibrium, where voltage is monitored. For hard carbon electrodes, 20 mA g^{-1} constant current is employed during 30 minutes pulse time, rest interval is set to 2 hours. Calculating from Fick's second law of diffusion, the following equation provide solution for diffusion coefficient of Na^+:[21c]

$$D = \frac{4}{\pi}\left(\frac{m_B V_m}{M_B S}\right)^2 \left(\frac{\Delta e_S}{\tau\left(\frac{dE_\tau}{d\sqrt{\tau}}\right)}\right)^2 \quad (4)$$

Where τ is the pulse time, m_B is the mass of electrode, M_B is the molecular weight of electrode, S is the surface area of electrode, ΔEτ is the voltage difference during pulse duration, ΔEs represents the voltage change in relaxation time.

Sodium ions diffusivities of HC and NHC-800 during the sodiation–desodiation process are presented in Figure 19a and Figure 19b. Across the entire 0–2 V window, the logarithmic Na^+ diffusion coefficient of NHC-800 is slightly higher than that of pristine HC. Enlarged interlayer spacing which reduces the migration barrier between graphitic layers and defect concentration introduced by pyridinic and pyrrolic-N synergistically improves ionic flux during both sodiation and desodiation for NCH-800. The diffusion coefficients in sodiation reaction reflect a clear three-stage sodium storage mechanism[85]. When the voltage remains above 0.047 V for HC (or 0.044 V for NHC-800), the logarithmic diffusion coefficient stays nearly constant, indicating sodium absorbs on surface active sites and defects[21a]. As the voltage drops to 0.047–0.016 V in HC or the slightly broader 0.044–0.023 V range in NHC-800, diffusion coefficient declines, caused by sodium ions overcome energy barrier of ordered graphitic layers. Wider insertion window in NHC-800 evidences its enlarged interlayer spacing. Further discharge below 0.016 V (HC) or 0.023 V (NHC-800), an increase of the Na^+ diffusion coefficient appears, sodium ions begin to occupy closed or semi-open nanopores at this stage. The macroscopic GITT pulse response is shown in Figure 19c, ΔEs and ΔEτ can be obtained from this curve. Electrochemical impedance spectroscopy (EIS) results for rGO, MWCNTs-COOH, HC and NHC-800 are displayed in Figure 19d. In the high-frequency region of spectra, there is a semicircle exists in all samples, which is caused by the charge transfer resistance (R_{ct}) while the ion diffusion impedance (Z_w) inside electrodes appears as a straight line in the low frequency region. NHC-800 exhibits the lowest charge transfer resistance, indicating fast charge transfer process.



Figures 19. (a) Diffusion coefficients of sodium ions during the sodiation and desodiation process of HC; (b) Diffusion coefficients of sodium ions during the sodiation and desodiation process of NHC-800; (c) Potential-time curve of NHC-800 for GITT test; (d) EIS of rGO, MWCNTs-COOH, HC and NHC-800.

Chapter6: Conclusion

As the demand for affordable, large-scale, sustainable energy storage speeds up, sodium-ion batteries (SIBs) are being seen more and more as a worthy substitute for lithium-ion systems. Because sodium is abundant, the raw materials are low-cost, and the battery tends to be safer, SIBs look especially appealing for stationary energy storage that help smooth out intermittent renewable energy on the grid. However, progress is held back by anode materials that do not yet deliver the capacity and cycling lifetimes engineers need.

Research has chosen hard carbon as the front-runner for SIB anodes because it is cheap, its structure can be engineered, and its precursors such as waste biomass and plastics are widely available. This thesis therefore rounds up the latest methods for synthesizing hard carbon, highlights structure-performance correlations and then zooms in on a new type, nitrogen-doped hard carbon (NHC), that we prepared from used polyethylene terephthalate (PET) bottles.

The electrochemical properties of hard carbon basically ride on three microstructural features: interlayer spacing, pore architecture, and defect chemistry. Enlarged interlayer space make it easier for sodium ions to intercalate between graphene sheets, especially in graphitic nanodomains which contribute to the low-voltage plateau capacity. A carefully designed pore network helps Na^+ adsorption, fills into closed pores and forms small clusters. Meanwhile, the introduction of intrinsic and extrinsic defects, including heteroatom doping, strengthens the material's surface reactivity and increases pseudocapacitance. When all these aspects are improved together, the resulting electrode shows enhanced capacity, rate capability, and long-term cycling stability.

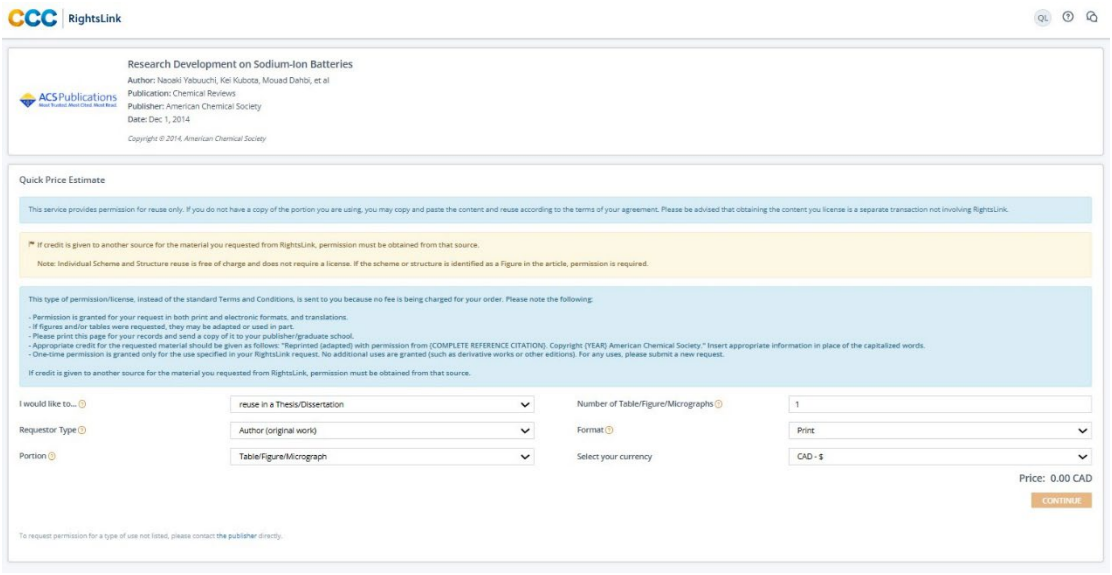
Guided by those insights, we proposed a simple, scalable route that turns discarded PET plastic into nitrogen-doped hard carbon through one-step heat treatment and element doping. In-situ nitrogen incorporation in the structure gave our NHC material expanded interlayer spacing and plenty of pyridinic and pyrrolic sites served as both redox-active sites and electronic conductance promoters. As a result, the optimized NHC-800 sample boasts a strong reversible capacity of 340.4 mAh g^{-1} when cycled at 20 mA g^{-1}, well ahead of rGO, acid-treated MWCNTs, and undoped hard carbon. GITT tests back up that picture by showing sodium storage unfolds in clear three stages: surface adsorption, interlayer insertion, and nanopore filling.

As well as advancing the performance frontier of hard carbon anodes, this study offers a sustainable path that tackles both energy needs and waste issues. By turning non-

biodegradable plastic discard into useful battery material, we promote a circular economy and create a fallback for critical-metal-intensive lithium-based systems. Moving ahead, the next steps for hard carbon anode development should combine controllable synthesis, operando characterization, and predictive modeling, so we can untangle how structure affects performance under practical conditions and speeds up their commercialization in sodium-ion batteries.

Letter of Copyright Permission

Figure 1:



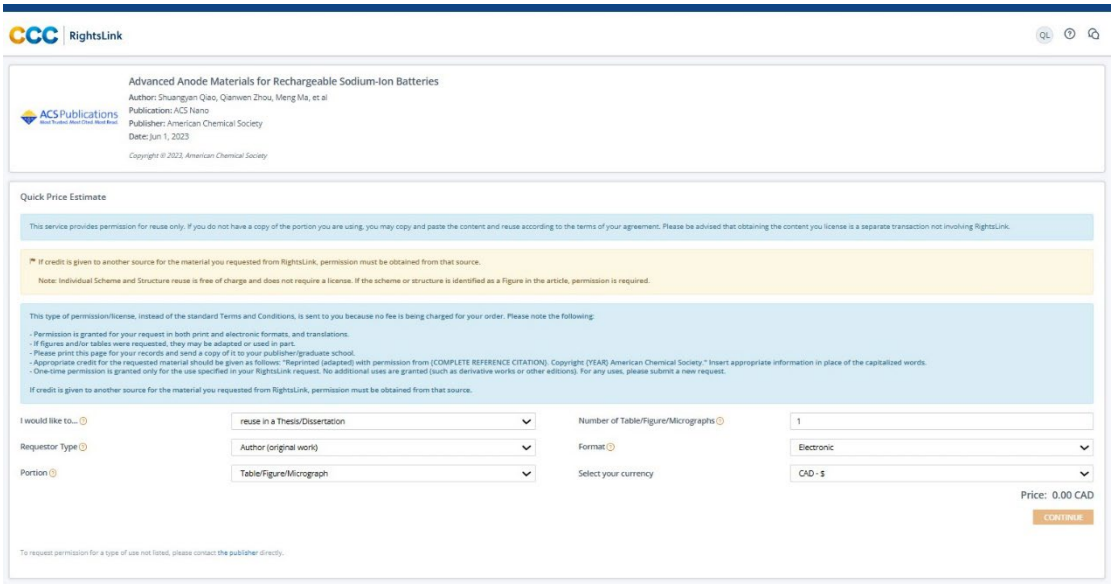


Figure 2:

CCC Marketplace

This is a License Agreement between Qiran Lu ("User") and Copyright Clearance Center, Inc. ("CCC") on behalf of the Rightsholder identified in the order details below. The license consists of the order details, the Marketplace Permissions General Terms and Conditions below, and any Rightsholder Terms and Conditions which are included below.

All payments must be made in full to CCC in accordance with the Marketplace Permissions General Terms and Conditions below.

Order Date	10-Jul-2025	Type of Use	Republish in a thesis/dissertation
Order License ID	1629402-1	Publisher	IOP Publishing
ISSN	1945-7111	Portion	Chart/graph/table/figure

LICENSED CONTENT

Publication Title	Journal of the Electrochemical Society	Country	United States of America
Author / Editor	Electrochemical Society.	Rightsholder	IOP Publishing, Ltd
Date	01/01/1948	Publication Type	e-Journal
Language	English	URL	https://iopscience.iop.org/journal/1945-7...

REQUEST DETAILS

Portion Type	Chart/graph/table/figure	Distribution	Canada
Number of Charts / Graphs / Tables / Figures Requested	1	Translation	Original language of publication
Format (select all that apply)	Electronic	Copies for the Disabled?	No
Who Will Republish the Content?	Academic institution	Minor Editing Privileges?	No
Duration of Use	Current edition and up to 5 years	Incidental Promotional Use?	No
Lifetime Unit Quantity	Up to 499	Currency	CAD
Rights Requested	Main product		

NEW WORK DETAILS

Title	Regulating Interlayer Spacing and Defects on Nitrogen-Doped Hard Carbon Anodes from Waste Plastic for Sodium-Ion Batteries	Institution Name	University of Waterloo
		Expected Presentation Date	2025-08-31
Instructor Name	Aiping Yu		

ADDITIONAL DETAILS

Order Reference Number	N/A	The Requesting Person / Organization to Appear on the License	Qiran Lu

REQUESTED CONTENT DETAILS

Title, Description or Numeric Reference of the Portion(s)	Figure 2. "House of cards" model for sodium/lithium filled hard carbon.	Title of the Article / Chapter the Portion Is From	High Capacity Anode Materials for Rechargeable Sodium-Ion Batteries
Editor of Portion(s)	D. A. Stevens and J. R. Dahn	Author of Portion(s)	Electrochemical Society.
Volume / Edition	147	Issue, if Republishing an Article From a Serial	N/A
Page or Page Range of Portion	1272	Publication Date of Portion	2000-01-01



Manipulating Adsorption–Insertion Mechanisms in Nanostructured Carbon Materials for High‐Efficiency Sodium Ion Storage

Author: Shen Qiu, Lifen Xiao, Maria L. Sushko, et al

Publication: Advanced Energy Materials

Publisher: John Wiley and Sons

Date: May 12, 2017

© 2017 WILEY - VCH Verlag GmbH & Co. KGaA, Weinheim

Order Completed

Thank you for your order.

This Agreement between Qiran Lu ("You") and John Wiley and Sons ("John Wiley and Sons") consists of your license details and the terms and conditions provided by John Wiley and Sons and Copyright Clearance Center.

Your confirmation email will contain your order number for future reference.

License Number	6065440840289
License date	Jul 10, 2025

Printable Details

Licensed Content

Licensed Content Publisher	John Wiley and Sons
Licensed Content Publication	Advanced Energy Materials
Licensed Content Title	Manipulating Adsorption–Insertion Mechanisms in Nanostructured Carbon Materials for High‐Efficiency Sodium Ion Storage
Licensed Content Author	Shen Qiu, Lifen Xiao, Maria L. Sushko, et al
Licensed Content Date	May 12, 2017
Licensed Content Volume	7
Licensed Content Issue	17
Licensed Content Pages	11

Order Details

Type of use	Dissertation/Thesis
Requestor type	University/Academic
Format	Electronic
Portion	Figure/table
Number of figures/tables	1
Will you be translating?	No

About Your Work

Title of new work	Regulating Interlayer Spacing and Defects on Nitrogen-Doped Hard Carbon Anodes from Waste Plastic for Sodium-Ion Batteries
Institution name	University of Waterloo
Expected presentation date	Aug 2025

Additional Data

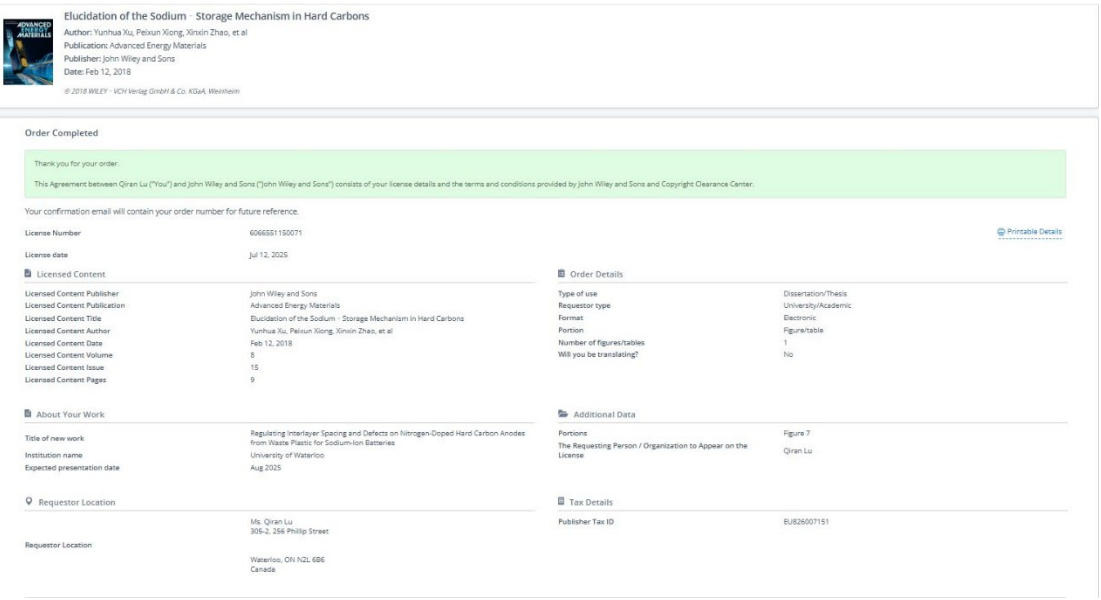
Portions	Scheme 1. Schematic illustration of the mechanisms for Na-ion storage in hard carbon: a) "intercalation–adsorption" mechanism; b) "adsorption– intercalation" mechanism.
The Requesting Person / Organization to Appear on the License	Qiran Lu

Requestor Location

Requestor Location	Ms. Qiran Lu 305-2, 256 Phillip Street Waterloo, ON N2L 6B6 Canada

Tax Details

Publisher Tax ID	EU826007151



Elucidation of the Sodium - Storage Mechanism in Hard Carbons

Author: Yunhua Xu, Peixun Xiong, Xinxin Zhao, et al
Publication: Advanced Energy Materials
Publisher: John Wiley and Sons
Date: Feb 12, 2018

© 2018 WILEY - VCH Verlag GmbH & Co. KGaA, Weinheim

Order Completed

Thank you for your order.

This Agreement between Qiran Lu ("You") and John Wiley and Sons ("John Wiley and Sons") consists of your license details and the terms and conditions provided by John Wiley and Sons and Copyright Clearance Center.

Your confirmation email will contain your order number for future reference.

Printable Details

License Number	6066551150071
License date	Jul 12, 2025

Licensed Content

Licensed Content Publisher	John Wiley and Sons
Licensed Content Publication	Advanced Energy Materials
Licensed Content Title	Elucidation of the Sodium - Storage Mechanism in Hard Carbons
Licensed Content Author	Yunhua Xu, Peixun Xiong, Xinxin Zhao, et al
Licensed Content Date	Feb 12, 2018
Licensed Content Volume	8
Licensed Content Issue	15
Licensed Content Pages	9

Order Details

Type of use	Dissertation/Thesis
Requestor type	University/Academic
Format	Electronic
Portion	Figure/table
Number of figures/tables	1
Will you be translating?	No

About Your Work

Title of new work	Regulating Interlayer Spacing and Defects on Nitrogen-Doped Hard Carbon Anodes from Waste Plastic for Sodium-Ion Batteries
Institution name	University of Waterloo
Expected presentation date	Aug 2025

Additional Data

Portions	Figure 7
The Requesting Person / Organization to Appear on the License	Qiran Lu

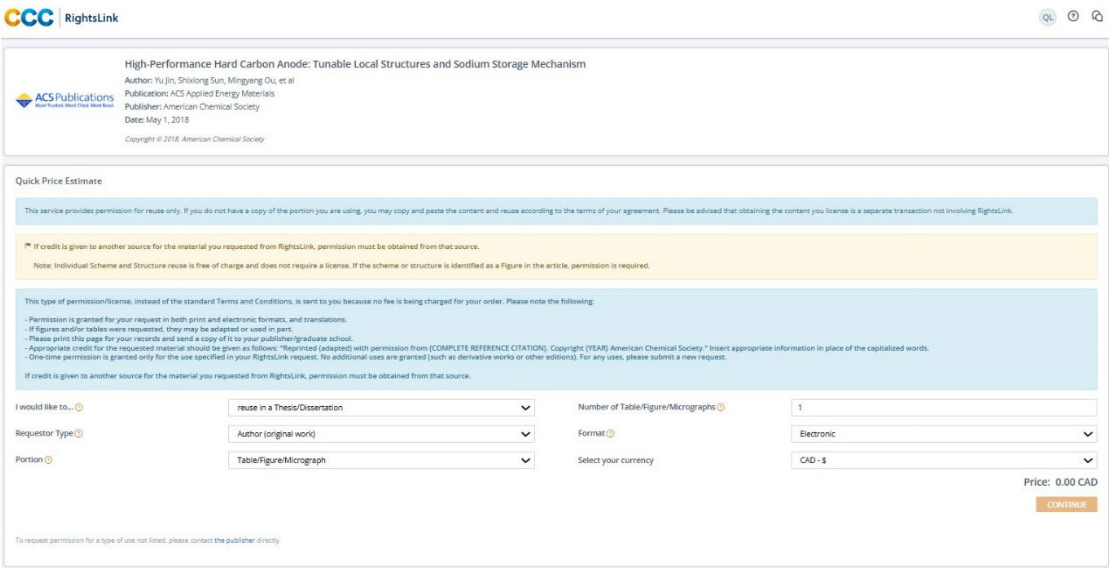
Requestor Location

Ms. Qiran Lu
305-2, 256 Phillip Street

Waterloo, ON N2L 6B6
Canada

Tax Details

Publisher Tax ID	EU826007151



CCC | RightsLink

High-Performance Hard Carbon Anode: Tunable Local Structures and Sodium Storage Mechanism

Author: Yu Jin, Shixiong Sun, Mingyang Ou, et al
Publication: ACS Applied Energy Materials
Publisher: American Chemical Society
Date: May 1, 2018

Copyright © 2018, American Chemical Society

Quick Price Estimate

This service provides permission for reuse only. If you do not have a copy of the portion you are using, you may copy and paste the content and reuse according to the terms of your agreement. Please be advised that obtaining the content you license is a separate transaction not involving RightsLink.

If credit is given to another source for the material you requested from RightsLink, permission must be obtained from that source.

Note: Individual Scheme and Structure reuse is free of charge and does not require a license. If the scheme or structure is identified as a Figure in the article, permission is required.

This type of permission/license, instead of the standard Terms and Conditions, is sent to you because no fee is being charged for your order. Please note the following:

- Permission is granted for your request in both print and electronic formats, and translations.
- If figures and/or tables were requested, they may be adapted or used in part.
- Please print this page for your records and send a copy of it to your publisher/graduate school.
- Appropriate credit for the requested material should be given as follows: "Reprinted (adapted) with permission from (COMPLETE REFERENCE CITATION). Copyright (YEAR) American Chemical Society." Insert appropriate information in place of the capitalized words.
- One-time permission is granted only for the use specified in your RightsLink request. No additional uses are granted (such as derivative works or other editions). For any uses, please submit a new request.

If credit is given to another source for the material you requested from RightsLink, permission must be obtained from that source.

I would like to...	reuse in a Thesis/Dissertation	Number of Table/Figure/Micrographs	1
Requestor Type	Author (original work)	Format	Electronic
Portion	Table/Figure/Micrograph	Select your currency	CAD - $

Price: 0.00 CAD

CONTINUE

To request permission for a type of use not listed, please contact the publisher directly.

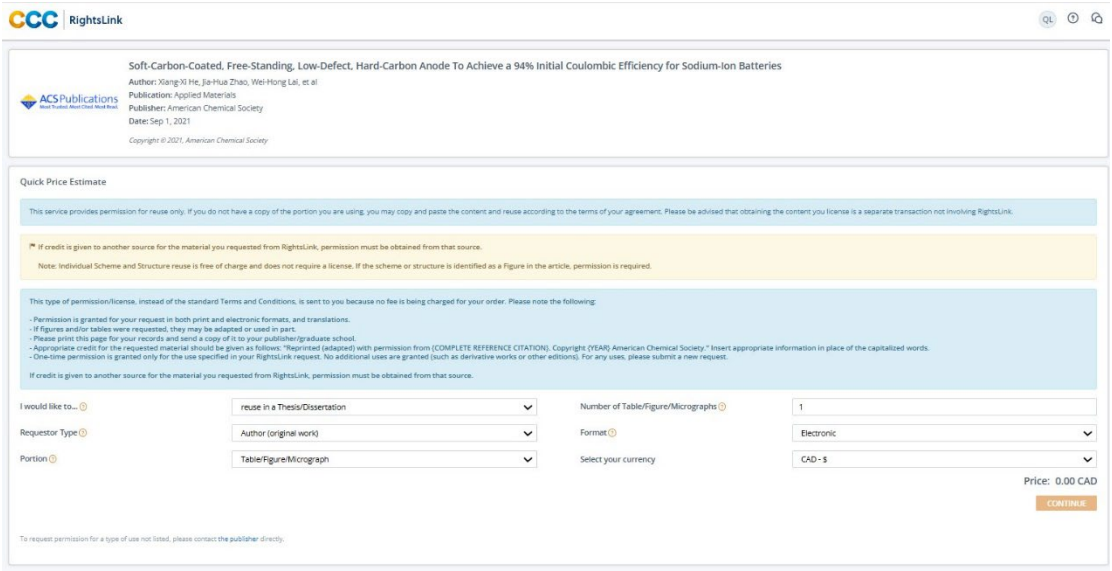
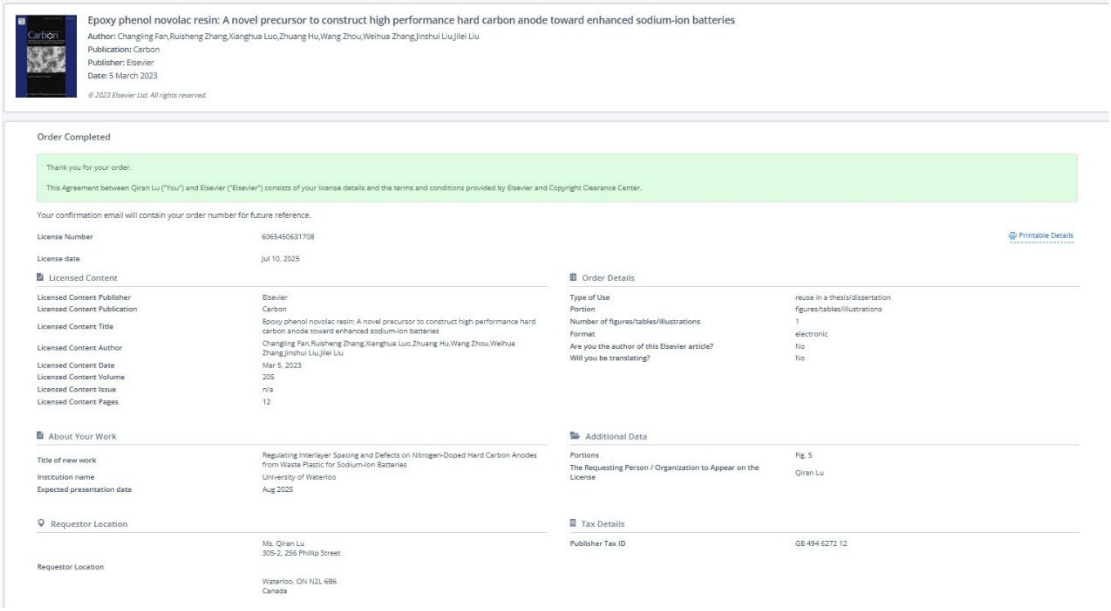

RightsLink
Soft-Carbon-Coated, Free-Standing, Low-Defect, Hard-Carbon Anode To Achieve a 94% Initial Coulombic Efficiency for Sodium-Ion Batteries
Author: Xiang-Xi He, Jia-Hua Zhao, Wei-Hong Lai, et al
Publication: Applied Materials
Publisher: American Chemical Society
Date: Sep 1, 2021
Copyright © 2021, American Chemical Society
Quick Price Estimate
This service provides permission for reuse only. If you do not have a copy of the portion you are using, you may copy and paste the content and reuse according to the terms of your agreement. Please be advised that obtaining the content you license is a separate transaction not involving RightsLink.
If credit is given to another source for the material you requested from RightsLink, permission must be obtained from that source.
Note: Individual Scheme and Structure reuse is free of charge and does not require a license. If the scheme or structure is identified as a Figure in the article, permission is required.
This type of permission/license, instead of the standard Terms and Conditions, is sent to you because no fee is being charged for your order. Please note the following:
- Permission is granted for your request in both print and electronic formats, and translations.
- If figures and/or tables were requested, they may be adapted or used in part.
- Please print this page for your records and send a copy of it to your publisher/graduate school.
- Appropriate credit for the requested material should be given as follows: "Reprinted (adapted) with permission from (COMPLETE REFERENCE CITATION). Copyright (YEAR) American Chemical Society." Insert appropriate information in place of the capitalized words.
- One-time permission is granted only for the use specified in your RightsLink request. No additional uses are granted (such as derivative works or other editions). For any uses, please submit a new request.
If credit is given to another source for the material you requested from RightsLink, permission must be obtained from that source.
I would like to... reuse in a Thesis/Dissertation
Number of Table/Figure/Micrographs 1
Requestor Type Author (original work)
Format Electronic
Portion Table/Figure/Micrograph
Select your currency CAD - $
Price: 0.00 CAD
CONTINUE
To request permission for a type of use not listed, please contact the publisher directly.

Figure 3:


Epoxy phenol novolac resin: A novel precursor to construct high performance hard carbon anode toward enhanced sodium-ion batteries
Author: Changling Fan,Ruisheng Zhang,Xianghua Luo,Zhuang Hu,Wang Zhou,Weihua Zhang,Jinshui Liu,Jilei Liu
Publication: Carbon
Publisher: Elsevier
Date: 5 March 2023
© 2023 Elsevier Ltd. All rights reserved.
Order Completed
Thank you for your order.
This Agreement between Qiran Lu ("You") and Elsevier ("Elsevier") consists of your license details and the terms and conditions provided by Elsevier and Copyright Clearance Center.
Your confirmation email will contain your order number for future reference.
License Number 6065450631708
License date Jul 10, 2025
Printable Details
Licensed Content
Licensed Content Publisher Elsevier
Licensed Content Publication Carbon
Licensed Content Title Epoxy phenol novolac resin: A novel precursor to construct high performance hard carbon anode toward enhanced sodium-ion batteries
Licensed Content Author Changling Fan,Ruisheng Zhang,Xianghua Luo,Zhuang Hu,Wang Zhou,Weihua Zhang,Jinshui Liu,Jilei Liu
Licensed Content Date Mar 5, 2023
Licensed Content Volume 205
Licensed Content Issue n/a
Licensed Content Pages 12
Order Details
Type of Use reuse in a thesis/dissertation
Portion figures/tables/illustrations
Number of figures/tables/illustrations 1
Format electronic
Are you the author of this Elsevier article? No
Will you be translating? No
About Your Work
Title of new work Regulating Interlayer Spacing and Defects on Nitrogen-Doped Hard Carbon Anodes from Waste Plastic for Sodium-ion Batteries
Institution name University of Waterloo
Expected presentation date Aug 2025
Additional Data
Portions Fig. 5
The Requesting Person / Organization to Appear on the License Qiran Lu
Requestor Location
Requestor Location Ms. Qiran Lu
305-2, 256 Phillip Street
Waterloo, ON N2L 6B6
Canada
Tax Details
Publisher Tax ID GB 494 6272 12



Steric Hindrance Engineering to Modulate the Closed Pores Formation of Polymer‐Derived Hard Carbon for High‐Performance Sodium‐Ion Batteries

Author: Jianhao Lin, Qingfeng Zhou, Yike Liu, et al
Publication: Angewandte Chemie International Edition
Publisher: John Wiley and Sons
Date: Aug 21, 2024

© 2024 Wiley-VCH GmbH

Order Completed

Thank you for your order.

This Agreement between Qiran Lu ("You") and John Wiley and Sons ("John Wiley and Sons") consists of your license details and the terms and conditions provided by John Wiley and Sons and Copyright Clearance Center.

Your confirmation email will contain your order number for future reference.

Printable Details

License Number	6065450919298
License date	Jul 10, 2025

Licensed Content

Licensed Content Publisher	John Wiley and Sons
Licensed Content Publication	Angewandte Chemie International Edition
Licensed Content Title	Steric Hindrance Engineering to Modulate the Closed Pores Formation of Polymer‐Derived Hard Carbon for High‐Performance Sodium‐Ion Batteries
Licensed Content Author	Jianhao Lin, Qingfeng Zhou, Yike Liu, et al
Licensed Content Date	Aug 21, 2024
Licensed Content Volume	63
Licensed Content Issue	39
Licensed Content Pages	10

Order Details

Type of use	Dissertation/Thesis
Requestor type	University/Academic
Format	Electronic
Portion	Figure/table
Number of figures/tables	1
Will you be translating?	No

About Your Work

Title of new work	Regulating Interlayer Spacing and Defects on Nitrogen-Doped Hard Carbon Anodes from Waste Plastic for Sodium-Ion Batteries
Institution name	University of Waterloo
Expected presentation date	Aug 2025

Additional Data

Portions	Figure 2
The Requesting Person / Organization to Appear on the License	Qiran Lu

Requestor Location

Requestor Location	Ms. Qiran Lu 305-2, 256 Phillip Street Waterloo, ON N2L 6B6 Canada

Tax Details

Publisher Tax ID	EU826007151



Hard carbons derived from green phenolic resins for Na-ion batteries

Author: Adrian Beda,Pierre-Louis Taberna,Patrice Simon,Camélia Matei Ghimbeu
Publication: Carbon
Publisher: Elsevier
Date: November 2018

© 2018 Elsevier Ltd. All rights reserved.

Order Completed

Thank you for your order.

This Agreement between Qiran Lu ("You") and Elsevier ("Elsevier") consists of your license details and the terms and conditions provided by Elsevier and Copyright Clearance Center.

Your confirmation email will contain your order number for future reference.

Printable Details

License Number	6065451209906
License date	Jul 10, 2025

Licensed Content

Licensed Content Publisher	Elsevier
Licensed Content Publication	Carbon
Licensed Content Title	Hard carbons derived from green phenolic resins for Na-ion batteries
Licensed Content Author	Adrian Beda,Pierre-Louis Taberna,Patrice Simon,Camélia Matei Ghimbeu
Licensed Content Date	Nov 1, 2018
Licensed Content Volume	139
Licensed Content Issue	n/a
Licensed Content Pages	10

Order Details

Type of Use	reuse in a thesis/dissertation
Portion	figures/tables/illustrations
Number of figures/tables/illustrations	1
Format	electronic
Are you the author of this Elsevier article?	No
Will you be translating?	No

About Your Work

Title of new work	Regulating Interlayer Spacing and Defects on Nitrogen-Doped Hard Carbon Anodes from Waste Plastic for Sodium-Ion Batteries
Institution name	University of Waterloo
Expected presentation date	Aug 2025

Additional Data

Portions	Fig. 1
The Requesting Person / Organization to Appear on the License	Qiran Lu

Requestor Location

Requestor Location	Ms. Qiran Lu 305-2, 256 Phillip Street Waterloo, ON N2L 6B6 Canada

Tax Details

Publisher Tax ID	GB 494 6272 12



Direct conversion of ester bond-rich waste plastics into hard carbon for high-performance sodium storage

Author: Dequan Chen,Kangying Luo,Zhiwei Yang,Yanjun Zhong,Zhenguo Wu,Yang Song,Guang Chen,Gongke Wang,Benhe Zhong,Xiaodong Guo
Publication: Carbon
Publisher: Elsevier
Date: March 2021

© 2020 Elsevier Ltd. All rights reserved.

Order Completed

Thank you for your order.

This Agreement between Qiran Lu ("You") and Elsevier ("Elsevier") consists of your license details and the terms and conditions provided by Elsevier and Copyright Clearance Center.

Your confirmation email will contain your order number for future reference.

Printable Details

License Number	6065451509856
License date	Jul 10, 2025

Licensed Content

Licensed Content Publisher	Elsevier
Licensed Content Publication	Carbon
Licensed Content Title	Direct conversion of ester bond-rich waste plastics into hard carbon for high-performance sodium storage
Licensed Content Author	Dequan Chen,Kangying Luo,Zhiwei Yang,Yanjun Zhong,Zhenguo Wu,Yang Song,Guang Chen,Gongke Wang,Benhe Zhong,Xiaodong Guo
Licensed Content Date	Mar 1, 2021
Licensed Content Volume	173
Licensed Content Issue	n/a
Licensed Content Pages	9

Order Details

Type of Use	reuse in a thesis/dissertation
Portion	figures/tables/illustrations
Number of figures/tables/illustrations	1
Format	electronic
Are you the author of this Elsevier article?	No
Will you be translating?	No

About Your Work

Title of new work	Regulating Interlayer Spacing and Defects on Nitrogen-Doped Hard Carbon Anodes from Waste Plastic for Sodium-ion Batteries
Institution name	University of Waterloo
Expected presentation date	Aug 2025

Additional Data

Portions	Fig. 4
The Requesting Person / Organization to Appear on the License	Qiran Lu

Requestor Location

Requestor Location	Ms. Qiran Lu 305-2, 256 Phillip Street Waterloo, ON N2L 6B6 Canada

Tax Details

Publisher Tax ID	GB 494 6272 12



Optimizing sodium storage mechanisms and electrochemical performance of high Nitrogen-Doped hard carbon anode materials Derived from waste plastics for Sodium-ion batteries

Author: Pan Zhang,Yirui Shu,Benhe Zhong,Lin Yang,Xiaodong Guo
Publication: Chemical Engineering Journal
Publisher: Elsevier
Date: 15 October 2024

© 2024 Elsevier B.V. All rights are reserved, including those for text and data mining, AI training, and similar technologies.

Order Completed

Thank you for your order.

This Agreement between Qiran Lu ("You") and Elsevier ("Elsevier") consists of your license details and the terms and conditions provided by Elsevier and Copyright Clearance Center.

Your confirmation email will contain your order number for future reference.

Printable Details

License Number	6065460483460
License date	Jul 10, 2025

Licensed Content

Licensed Content Publisher	Elsevier
Licensed Content Publication	Chemical Engineering Journal
Licensed Content Title	Optimizing sodium storage mechanisms and electrochemical performance of high Nitrogen-Doped hard carbon anode materials Derived from waste plastics for Sodium-ion batteries
Licensed Content Author	Pan Zhang,Yirui Shu,Benhe Zhong,Lin Yang,Xiaodong Guo
Licensed Content Date	Oct 15, 2024
Licensed Content Volume	498
Licensed Content Issue	n/a
Licensed Content Pages	1

Order Details

Type of Use	reuse in a thesis/dissertation
Portion	figures/tables/illustrations
Number of figures/tables/illustrations	1
Format	electronic
Are you the author of this Elsevier article?	No
Will you be translating?	No

About Your Work

Title of new work	Regulating Interlayer Spacing and Defects on Nitrogen-Doped Hard Carbon Anodes from Waste Plastic for Sodium-ion Batteries
Institution name	University of Waterloo
Expected presentation date	Aug 2025

Additional Data

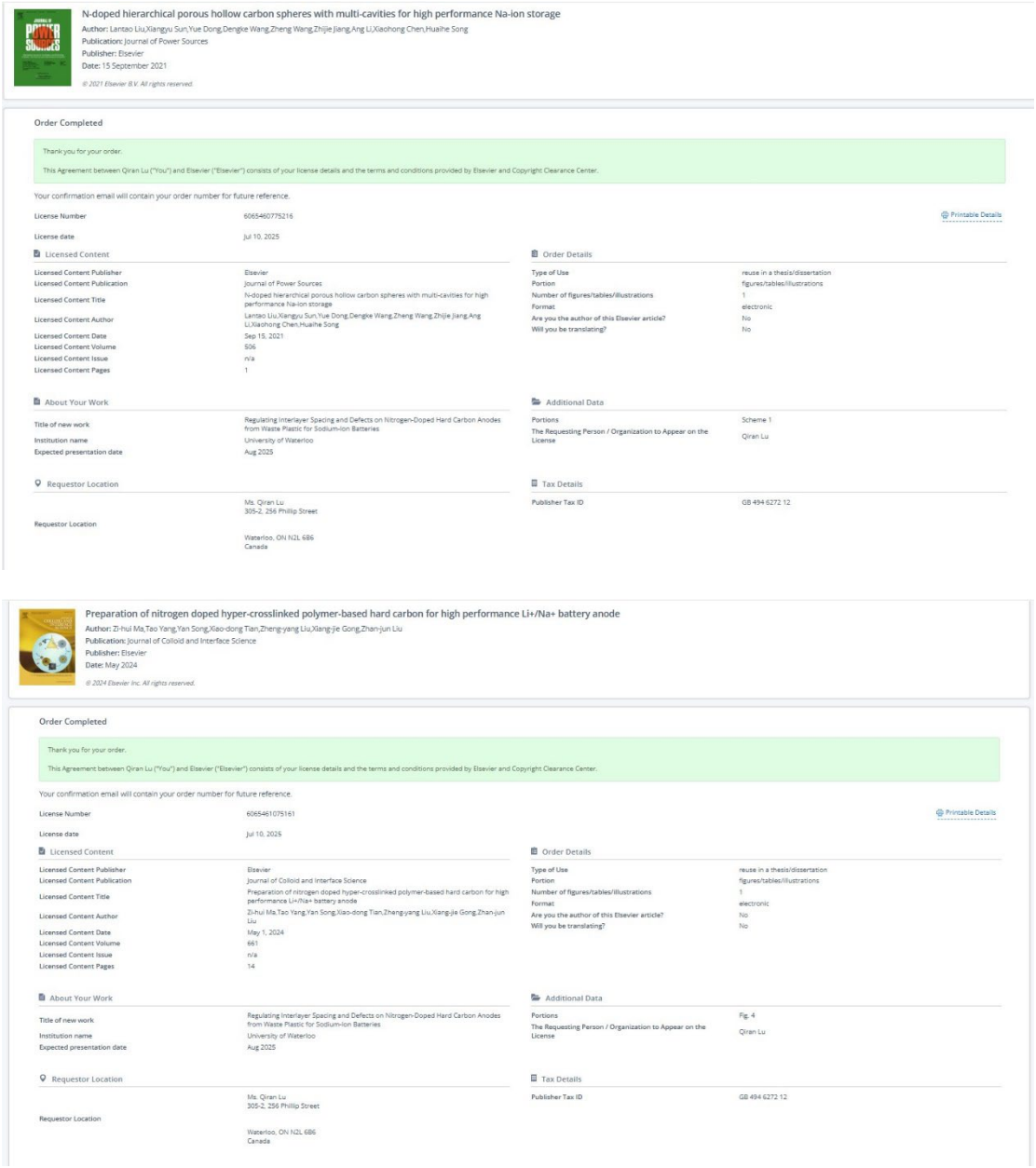
Portions	Fig. 1
The Requesting Person / Organization to Appear on the License	Qiran Lu

Requestor Location

Requestor Location	Ms. Qiran Lu 305-2, 256 Phillip Street Waterloo, ON N2L 6B6 Canada

Tax Details

Publisher Tax ID	GB 494 6272 12



N-doped hierarchical porous hollow carbon spheres with multi-cavities for high performance Na-ion storage
Author: Lantao Liu,Xiangyu Sun,Yue Dong,Dengke Wang,Zheng Wang,Zhijie Jiang,Ang Li,Xiaohong Chen,Hualhe Song
Publication: Journal of Power Sources
Publisher: Elsevier
Date: 15 September 2021
© 2021 Elsevier B.V. All rights reserved.

Order Completed

Thank you for your order.

This Agreement between Qiran Lu ("You") and Elsevier ("Elsevier") consists of your license details and the terms and conditions provided by Elsevier and Copyright Clearance Center.

Your confirmation email will contain your order number for future reference.

License Number	606546077216
License date	Jul 10, 2025

Printable Details

Licensed Content

Licensed Content Publisher	Elsevier
Licensed Content Publication	Journal of Power Sources
Licensed Content Title	N-doped hierarchical porous hollow carbon spheres with multi-cavities for high performance Na-ion storage
Licensed Content Author	Lantao Liu,Xiangyu Sun,Yue Dong,Dengke Wang,Zheng Wang,Zhijie Jiang,Ang Li,Xiaohong Chen,Hualhe Song
Licensed Content Date	Sep 15, 2021
Licensed Content Volume	506
Licensed Content Issue	n/a
Licensed Content Pages	1

Order Details

Type of Use	reuse in a thesis/dissertation
Portion	figures/tables/illustrations
Number of figures/tables/illustrations	1
Format	electronic
Are you the author of this Elsevier article?	No
Will you be translating?	No

About Your Work

Title of new work	Regulating Interlayer Spacing and Defects on Nitrogen-Doped Hard Carbon Anodes from Waste Plastic for Sodium-ion Batteries
Institution name	University of Waterloo
Expected presentation date	Aug 2025

Additional Data

Portions	Scheme 1
The Requesting Person / Organization to Appear on the License	Qiran Lu

Requestor Location

Requestor Location	Ms. Qiran Lu 305-2, 256 Phillip Street Waterloo, ON N2L 6B6 Canada

Tax Details

Publisher Tax ID	GB 494 6272 12

Preparation of nitrogen doped hyper-crosslinked polymer-based hard carbon for high performance Li+/Na+ battery anode
Author: Zi-hui Ma,Tao Yang,Yan Song,Xiao-dong Tian,Zheng-yang Liu,Xiang-jie Gong,Zhan-jun Liu
Publication: Journal of Colloid and Interface Science
Publisher: Elsevier
Date: May 2024
© 2024 Elsevier Inc. All rights reserved.

Order Completed

Thank you for your order.

This Agreement between Qiran Lu ("You") and Elsevier ("Elsevier") consists of your license details and the terms and conditions provided by Elsevier and Copyright Clearance Center.

Your confirmation email will contain your order number for future reference.

License Number	606546075161
License date	Jul 10, 2025

Printable Details

Licensed Content

Licensed Content Publisher	Elsevier
Licensed Content Publication	Journal of Colloid and Interface Science
Licensed Content Title	Preparation of nitrogen doped hyper-crosslinked polymer-based hard carbon for high performance Li+/Na+ battery anode
Licensed Content Author	Zi-hui Ma,Tao Yang,Yan Song,Xiao-dong Tian,Zheng-yang Liu,Xiang-jie Gong,Zhan-jun Liu
Licensed Content Date	May 1, 2024
Licensed Content Volume	661
Licensed Content Issue	n/a
Licensed Content Pages	14

Order Details

Type of Use	reuse in a thesis/dissertation
Portion	figures/tables/illustrations
Number of figures/tables/illustrations	1
Format	electronic
Are you the author of this Elsevier article?	No
Will you be translating?	No

About Your Work

Title of new work	Regulating Interlayer Spacing and Defects on Nitrogen-Doped Hard Carbon Anodes from Waste Plastic for Sodium-ion Batteries
Institution name	University of Waterloo
Expected presentation date	Aug 2025

Additional Data

Portions	Fig. 4
The Requesting Person / Organization to Appear on the License	Qiran Lu

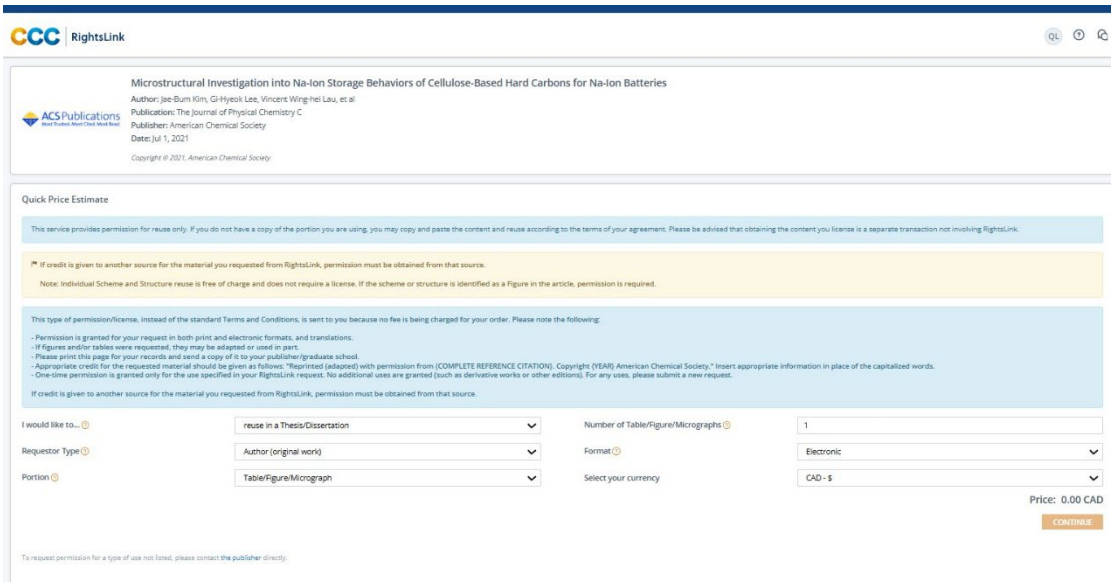
Requestor Location

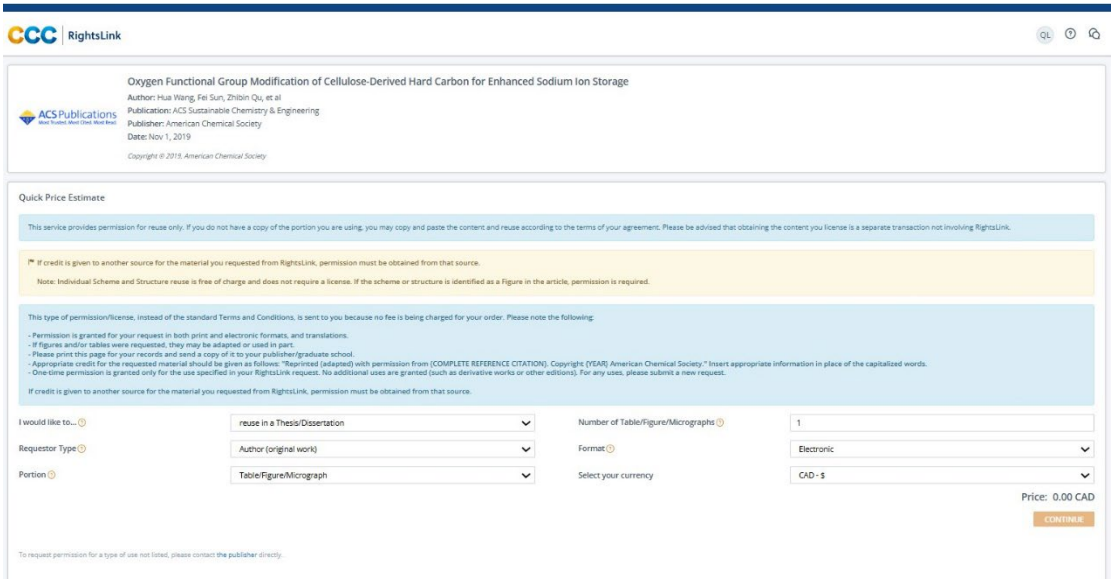
Requestor Location	Ms. Qiran Lu 305-2, 256 Phillip Street Waterloo, ON N2L 6B6 Canada

Tax Details

Publisher Tax ID	GB 494 6272 12

Figure 4:


RightsLink
Microstructural Investigation into Na-Ion Storage Behaviors of Cellulose-Based Hard Carbons for Na-Ion Batteries
Author: Jae-Bum Kim, Gi-Hyeok Lee, Vincent Wing-hei Lau, et al
Publication: The Journal of Physical Chemistry C
Publisher: American Chemical Society
Date: Jul 1, 2021
Copyright © 2021, American Chemical Society
Quick Price Estimate
This service provides permission for reuse only. If you do not have a copy of the portion you are using, you may copy and paste the content and reuse according to the terms of your agreement. Please be advised that obtaining the content you license is a separate transaction not involving RightsLink.
If credit is given to another source for the material you requested from RightsLink, permission must be obtained from that source.
Note: Individual Scheme and Structure reuse is free of charge and does not require a license. If the scheme or structure is identified as a Figure in the article, permission is required.
This type of permission/license, instead of the standard Terms and Conditions, is sent to you because no fee is being charged for your order. Please note the following:
- Permission is granted for your request in both print and electronic formats, and translations.
- If figures and/or tables were requested, they may be adapted or used in part.
- Please print this page for your records and send a copy of it to your publisher/graduate school.
- Appropriate credit for the requested material should be given as follows: "Reprinted (adapted) with permission from (COMPLETE REFERENCE CITATION). Copyright (YEAR) American Chemical Society." Insert appropriate information in place of the capitalized words.
- One-time permission is granted only for the use specified in your RightsLink request. No additional uses are granted (such as derivative works or other editions). For any uses, please submit a new request.
If credit is given to another source for the material you requested from RightsLink, permission must be obtained from that source.
I would like to... reuse in a Thesis/Dissertation
Number of Table/Figure/Micrographs 1
Requestor Type Author (original work)
Format Electronic
Portion Table/Figure/Micrograph
Select your currency CAD - $
Price: 0.00 CAD
CONTINUE
To request permission for a type of use not listed, please contact the publisher directly.


RightsLink
Oxygen Functional Group Modification of Cellulose-Derived Hard Carbon for Enhanced Sodium Ion Storage
Author: Hua Wang, Fei Sun, Zhibin Qu, et al
Publication: ACS Sustainable Chemistry & Engineering
Publisher: American Chemical Society
Date: Nov 1, 2019
Copyright © 2019, American Chemical Society
Quick Price Estimate
This service provides permission for reuse only. If you do not have a copy of the portion you are using, you may copy and paste the content and reuse according to the terms of your agreement. Please be advised that obtaining the content you license is a separate transaction not involving RightsLink.
If credit is given to another source for the material you requested from RightsLink, permission must be obtained from that source.
Note: Individual Scheme and Structure reuse is free of charge and does not require a license. If the scheme or structure is identified as a Figure in the article, permission is required.
This type of permission/license, instead of the standard Terms and Conditions, is sent to you because no fee is being charged for your order. Please note the following:
- Permission is granted for your request in both print and electronic formats, and translations.
- If figures and/or tables were requested, they may be adapted or used in part.
- Please print this page for your records and send a copy of it to your publisher/graduate school.
- Appropriate credit for the requested material should be given as follows: "Reprinted (adapted) with permission from (COMPLETE REFERENCE CITATION). Copyright (YEAR) American Chemical Society." Insert appropriate information in place of the capitalized words.
- One-time permission is granted only for the use specified in your RightsLink request. No additional uses are granted (such as derivative works or other editions). For any uses, please submit a new request.
If credit is given to another source for the material you requested from RightsLink, permission must be obtained from that source.
I would like to... reuse in a Thesis/Dissertation
Number of Table/Figure/Micrographs 1
Requestor Type Author (original work)
Format Electronic
Portion Table/Figure/Micrograph
Select your currency CAD - $
Price: 0.00 CAD
CONTINUE
To request permission for a type of use not listed, please contact the publisher directly.



Revealing the sodium storage mechanism of cellulose separator-derived hard carbon anode materials for sodium-ion batteries

Author: Xi Zhang,Rui Duan,Tiejun Zheng,Peiting Chen,Xuewen Yu,Zhijun Qiao,Dianbo Ruan
Publication: Chemical Engineering Journal
Publisher: Elsevier
Date: 15 October 2024

© 2024 Elsevier B.V. All rights reserved, including those for text and data mining, AI training, and similar technologies.

Order Completed

Thank you for your order.

This Agreement between Qiran Lu ("You") and Elsevier ("Elsevier") consists of your license details and the terms and conditions provided by Elsevier and Copyright Clearance Center.

Your confirmation email will contain your order number for future reference.

Printable Details

License Number	6065470581543
License date	Jul 10, 2025

Licensed Content

Licensed Content Publisher	Elsevier
Licensed Content Publication	Chemical Engineering Journal
Licensed Content Title	Revealing the sodium storage mechanism of cellulose separator-derived hard carbon anode materials for sodium-ion batteries
Licensed Content Author	Xi Zhang,Rui Duan,Tiejun Zheng,Peiting Chen,Xuewen Yu,Zhijun Qiao,Dianbo Ruan
Licensed Content Date	Oct 15, 2024
Licensed Content Volume	498
Licensed Content Issue	n/a
Licensed Content Pages	1

Order Details

Type of Use	reuse in a thesis/dissertation
Portion	figures/tables/illustrations
Number of figures/tables/illustrations	1
Format	electronic
Are you the author of this Elsevier article?	No
Will you be translating?	No

About Your Work

Title of new work	Regulating Interlayer Spacing and Defects on Nitrogen-Doped Hard Carbon Anodes from Waste Plastic for Sodium-Ion Batteries
Institution name	University of Waterloo
Expected presentation date	Aug 2025

Additional Data

Portions	Fig. 1
The Requesting Person / Organization to Appear on the License	Qiran Lu

Requestor Location

Requestor Location	Ms. Qiran Lu 305-2, 256 Phillip Street Waterloo, ON N2L 6B6 Canada

Tax Details

Publisher Tax ID	GB 494 6272 12



Lignin‐Derived Hard Carbon Microspheres Synthesized via Emulsion‐Solvent Evaporation as Anode for Sodium Storage

Author: Jie Zhang, Baojun Yu, Yang Zhang, et al
Publication: ENERGY TECHNOLOGY (ELECTRONIC)
Publisher: John Wiley and Sons
Date: Jan 20, 2020

© 2020 WILEY - VCH Verlag GmbH & Co. KGaA, Weinheim

Order Completed

Thank you for your order.

This Agreement between Qiran Lu ("You") and John Wiley and Sons ("John Wiley and Sons") consists of your license details and the terms and conditions provided by John Wiley and Sons and Copyright Clearance Center.

Your confirmation email will contain your order number for future reference.

Printable Details

License Number	6066180420096
License date	Jul 11, 2025

Licensed Content

Licensed Content Publisher	John Wiley and Sons
Licensed Content Publication	ENERGY TECHNOLOGY (ELECTRONIC)
Licensed Content Title	Lignin‐Derived Hard Carbon Microspheres Synthesized via Emulsion‐Solvent Evaporation as Anode for Sodium Storage
Licensed Content Author	Jie Zhang, Baojun Yu, Yang Zhang, et al
Licensed Content Date	Jan 20, 2020
Licensed Content Volume	8
Licensed Content Issue	3
Licensed Content Pages	9

Order Details

Type of use	Dissertation/Thesis
Requestor type	University/Academic
Format	Electronic
Portion	Figure/table
Number of figures/tables	1
Will you be translating?	No

About Your Work

Title of new work	Regulating Interlayer Spacing and Defects on Nitrogen-Doped Hard Carbon Anodes from Waste Plastic for Sodium-Ion Batteries
Institution name	University of Waterloo
Expected presentation date	Aug 2025

Additional Data

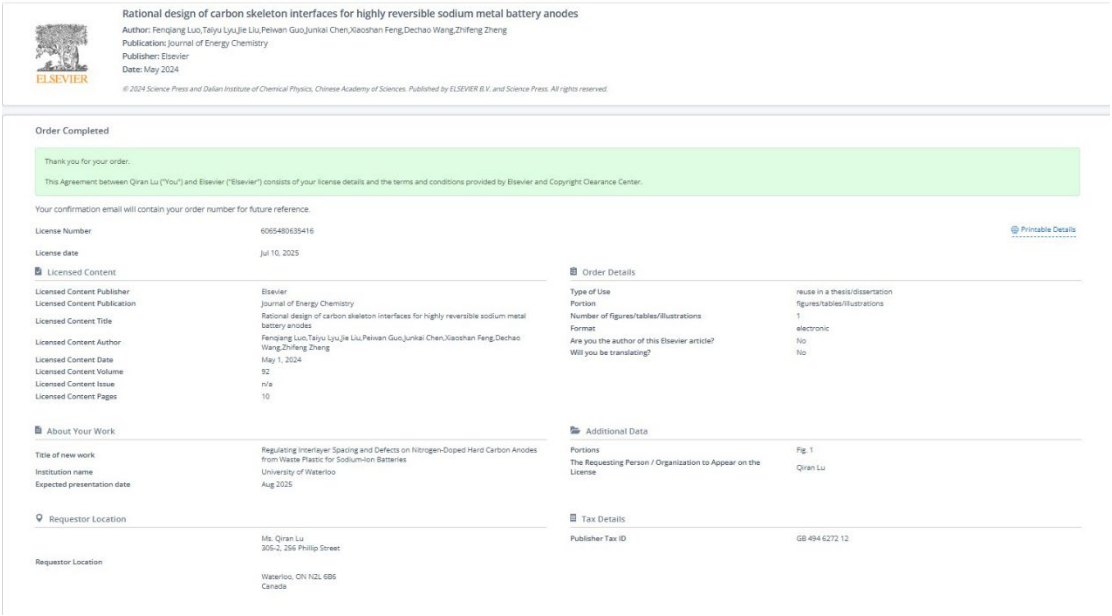
Portions	Figure 7
The Requesting Person / Organization to Appear on the License	Qiran Lu

Requestor Location

Requestor Location	Ms. Qiran Lu 305-2, 256 Phillip Street Waterloo, ON N2L 6B6 Canada

Tax Details

Publisher Tax ID	EU826007151



Rational design of carbon skeleton interfaces for highly reversible sodium metal battery anodes

Author: Fenqiang Luo,Taiyu Lyu,Jie Liu,Peiwan Guo,Junkai Chen,Xiaoshan Feng,Dechao Wang,Zhifeng Zheng
Publication: Journal of Energy Chemistry
Publisher: Elsevier
Date: May 2024

© 2024 Science Press and Dalian Institute of Chemical Physics, Chinese Academy of Sciences. Published by ELSEVIER B.V. and Science Press. All rights reserved.

Order Completed

Thank you for your order.

This Agreement between Qiran Lu ("You") and Elsevier ("Elsevier") consists of your license details and the terms and conditions provided by Elsevier and Copyright Clearance Center.

Your confirmation email will contain your order number for future reference.

License Number	6065480635416
License date	Jul 10, 2025

Printable Details

Licensed Content

Licensed Content Publisher	Elsevier
Licensed Content Publication	Journal of Energy Chemistry
Licensed Content Title	Rational design of carbon skeleton interfaces for highly reversible sodium metal battery anodes
Licensed Content Author	Fenqiang Luo,Taiyu Lyu,Jie Liu,Peiwan Guo,Junkai Chen,Xiaoshan Feng,Dechao Wang,Zhifeng Zheng
Licensed Content Date	May 1, 2024
Licensed Content Volume	92
Licensed Content Issue	n/a
Licensed Content Pages	10

Order Details

Type of Use	reuse in a thesis/dissertation
Portion	figures/tables/illustrations
Number of figures/tables/illustrations	1
Format	electronic
Are you the author of this Elsevier article?	No
Will you be translating?	No

About Your Work

Title of new work	Regulating Interlayer Spacing and Defects on Nitrogen-Doped Hard Carbon Anodes from Waste Plastic for Sodium-Ion Batteries
Institution name	University of Waterloo
Expected presentation date	Aug 2025

Additional Data

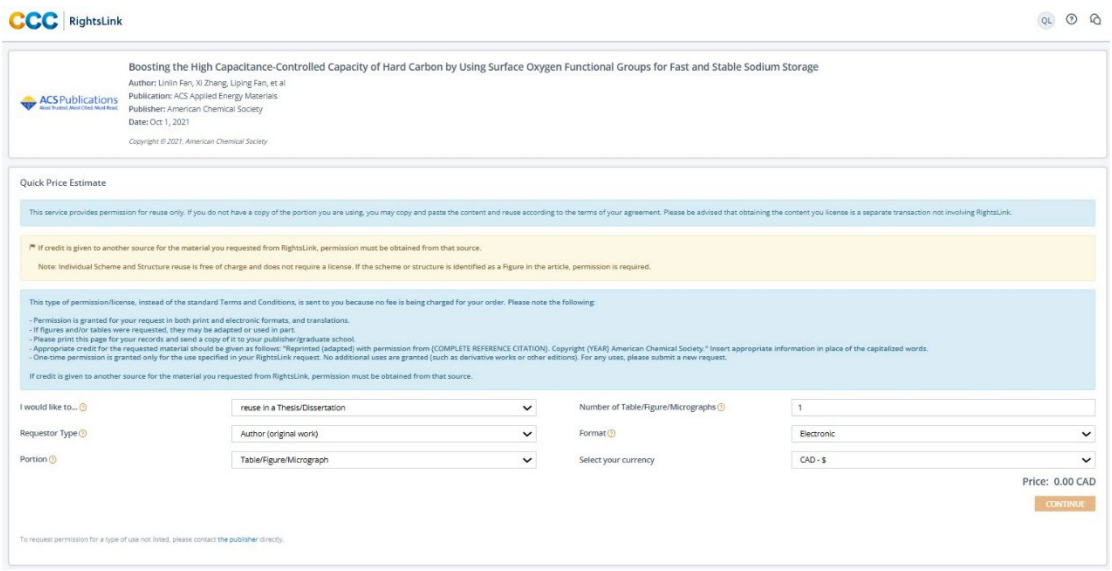
Portions	Fig. 1
The Requesting Person / Organization to Appear on the License	Qiran Lu

Requestor Location

Requestor Location	Ms. Qiran Lu 305-2, 256 Phillip Street Waterloo, ON N2L 6B6 Canada

Tax Details

Publisher Tax ID	GB 494 6272 12



RightsLink

Boosting the High Capacitance-Controlled Capacity of Hard Carbon by Using Surface Oxygen Functional Groups for Fast and Stable Sodium Storage

Author: Linlin Fan, Xi Zhang, Liping Fan, et al
Publication: ACS Applied Energy Materials
Publisher: American Chemical Society
Date: Oct 1, 2021

Copyright © 2021, American Chemical Society

Quick Price Estimate

This service provides permission for reuse only. If you do not have a copy of the portion you are using, you may copy and paste the content and reuse according to the terms of your agreement. Please be advised that obtaining the content you license is a separate transaction not involving RightsLink.

If credit is given to another source for the material you requested from RightsLink, permission must be obtained from that source.

Note: Individual Scheme and Structure reuse is free of charge and does not require a license. If the scheme or structure is identified as a Figure in the article, permission is required.

This type of permission/license, instead of the standard Terms and Conditions, is sent to you because no fee is being charged for your order. Please note the following:

- Permission is granted for your request in both print and electronic formats, and translations.
- If figures and/or tables were requested, they may be adapted or used in part.
- Please print this page for your records and send a copy of it to your publisher/graduate school.
- Appropriate credit for the requested material should be given as follows: "Reprinted (adapted) with permission from {COMPLETE REFERENCE CITATION}. Copyright {YEAR} American Chemical Society." Insert appropriate information in place of the capitalized words.
- One-time permission is granted only for the use specified in your RightsLink request. No additional uses are granted (such as derivative works or other editions). For any uses, please submit a new request.

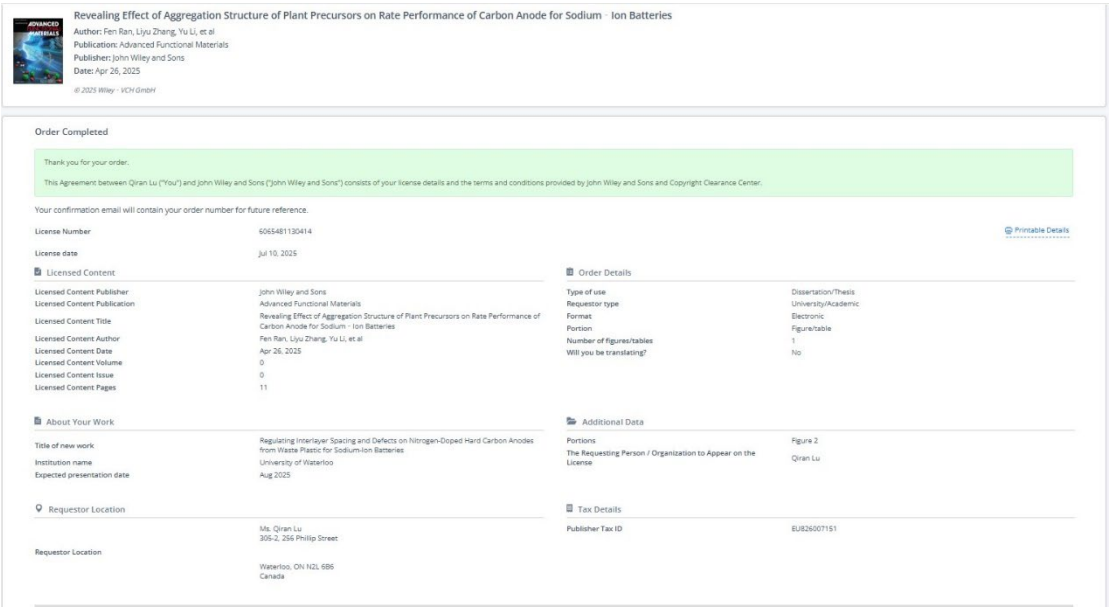
If credit is given to another source for the material you requested from RightsLink, permission must be obtained from that source.

I would like to...	reuse in a Thesis/Dissertation	Number of Table/Figure/Micrographs	1
Requestor Type	Author (original work)	Format	Electronic
Portion	Table/Figure/Micrograph	Select your currency	CAD - $

Price: 0.00 CAD

CONTINUE

To request permission for a type of use not listed, please contact the publisher directly.



Revealing Effect of Aggregation Structure of Plant Precursors on Rate Performance of Carbon Anode for Sodium - Ion Batteries

Author: Fen Ran, Liyu Zhang, Yu Li, et al
Publication: Advanced Functional Materials
Publisher: John Wiley and Sons
Date: Apr 26, 2025

© 2025 Wiley - VCH GmbH

Order Completed

Thank you for your order.

This Agreement between Qiran Lu ("You") and John Wiley and Sons ("John Wiley and Sons") consists of your license details and the terms and conditions provided by John Wiley and Sons and Copyright Clearance Center.

Your confirmation email will contain your order number for future reference.

Printable Details

License Number	6065481130414
License date	Jul 10, 2025

Licensed Content

Licensed Content Publisher	John Wiley and Sons
Licensed Content Publication	Advanced Functional Materials
Licensed Content Title	Revealing Effect of Aggregation Structure of Plant Precursors on Rate Performance of Carbon Anode for Sodium - Ion Batteries
Licensed Content Author	Fen Ran, Liyu Zhang, Yu Li, et al
Licensed Content Date	Apr 26, 2025
Licensed Content Volume	0
Licensed Content Issue	0
Licensed Content Pages	11

Order Details

Type of use	Dissertation/Thesis
Requestor type	University/Academic
Format	Electronic
Portion	Figure/table
Number of figures/tables	1
Will you be translating?	No

About Your Work

Title of new work	Regulating Interlayer Spacing and Defects on Nitrogen-Doped Hard Carbon Anodes from Waste Plastic for Sodium-Ion Batteries
Institution name	University of Waterloo
Expected presentation date	Aug 2025

Additional Data

Portions	Figure 2
The Requesting Person / Organization to Appear on the License	Qiran Lu

Requestor Location

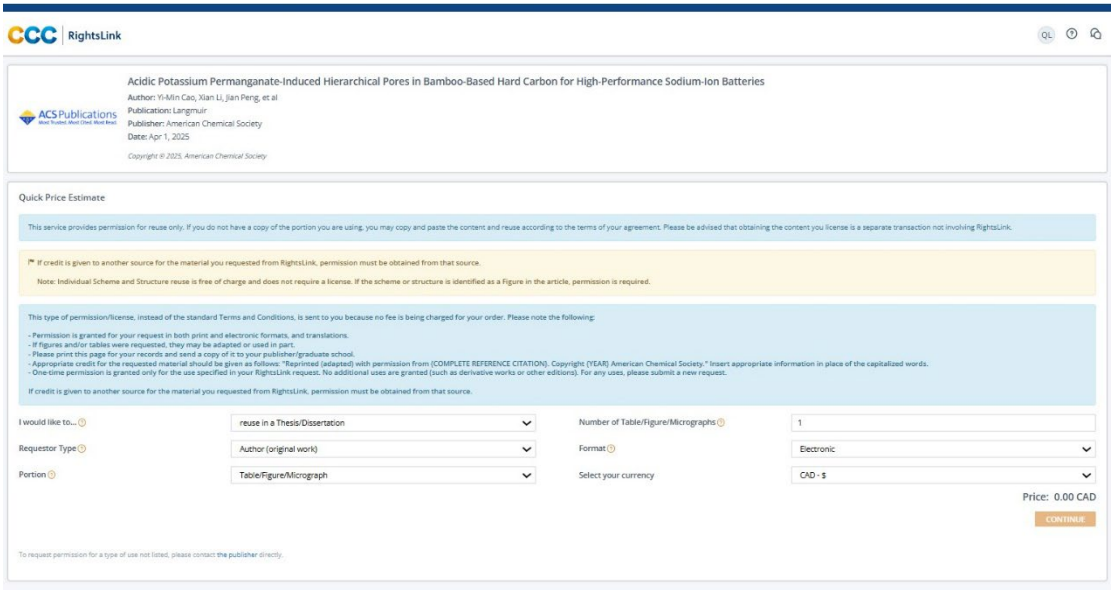
Ms. Qiran Lu
305-2, 256 Phillip Street

Requestor Location

Waterloo, ON N2L 6B6
Canada

Tax Details

Publisher Tax ID	EU826007151



CCC | RightsLink

Acidic Potassium Permanganate-Induced Hierarchical Pores in Bamboo-Based Hard Carbon for High-Performance Sodium-Ion Batteries

Author: Yi-Min Cao, Xian Li, Jian Peng, et al
Publication: Langmuir
Publisher: American Chemical Society
Date: Apr 1, 2025

Copyright © 2025, American Chemical Society

Quick Price Estimate

This service provides permission for reuse only. If you do not have a copy of the portion you are using, you may copy and paste the content and reuse according to the terms of your agreement. Please be advised that obtaining the content you license is a separate transaction not involving RightsLink.

If credit is given to another source for the material you requested from RightsLink, permission must be obtained from that source.

Note: Individual Scheme and Structure reuse is free of charge and does not require a license. If the scheme or structure is identified as a Figure in the article, permission is required.

This type of permission/license, instead of the standard Terms and Conditions, is sent to you because no fee is being charged for your order. Please note the following:

- Permission is granted for your request in both print and electronic formats, and translations.
- If figures and/or tables were requested, they may be adapted or used in part.
- Please print this page for your records and send a copy of it to your publisher/graduate school.
- Appropriate credit for the requested material should be given as follows: "Reprinted (adapted) with permission from (COMPLETE REFERENCE CITATION). Copyright (YEAR) American Chemical Society." Insert appropriate information in place of the capitalized words.
- One-time permission is granted only for the use specified in your RightsLink request. No additional uses are granted (such as derivative works or other editions). For any uses, please submit a new request.

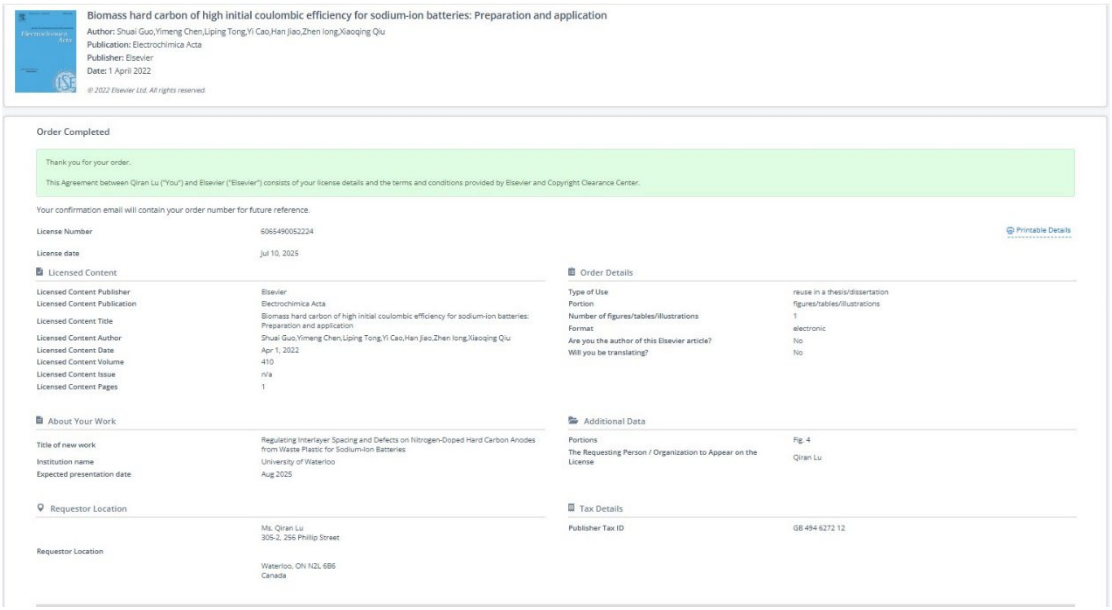
If credit is given to another source for the material you requested from RightsLink, permission must be obtained from that source.

I would like to...	reuse in a Thesis/Dissertation	Number of Table/Figure/Micrographs	1
Requestor Type	Author (original work)	Format	Electronic
Portion	Table/Figure/Micrograph	Select your currency	CAD - $

Price: 0.00 CAD

CONTINUE

To request permission for a type of use not listed, please contact the publisher directly.



Biomass hard carbon of high initial coulombic efficiency for sodium-ion batteries: Preparation and application

Author: Shuai Guo,Yimeng Chen,Liping Tong,Yi Cao,Han Jiao,Zhen long,Xiaoqing Qiu
Publication: Electrochimica Acta
Publisher: Elsevier
Date: 1 April 2022

© 2022 Elsevier Ltd. All rights reserved.

Order Completed

Thank you for your order.

This Agreement between Qiran Lu ("You") and Elsevier ("Elsevier") consists of your license details and the terms and conditions provided by Elsevier and Copyright Clearance Center.

Your confirmation email will contain your order number for future reference.

License Number	6065490052224
License date	Jul 10, 2025

Printable Details

Licensed Content

Licensed Content Publisher	Elsevier
Licensed Content Publication	Electrochimica Acta
Licensed Content Title	Biomass hard carbon of high initial coulombic efficiency for sodium-ion batteries: Preparation and application
Licensed Content Author	Shuai Guo,Yimeng Chen,Liping Tong,Yi Cao,Han Jiao,Zhen long,Xiaoqing Qiu
Licensed Content Date	Apr 1, 2022
Licensed Content Volume	410
Licensed Content Issue	n/a
Licensed Content Pages	1

Order Details

Type of Use	reuse in a thesis/dissertation
Portion	figures/tables/illustrations
Number of figures/tables/illustrations	1
Format	electronic
Are you the author of this Elsevier article?	No
Will you be translating?	No

About Your Work

Title of new work	Regulating Interlayer Spacing and Defects on Nitrogen-Doped Hard Carbon Anodes from Waste Plastic for Sodium-Ion Batteries
Institution name	University of Waterloo
Expected presentation date	Aug 2025

Additional Data

Portions	Fig. 4
The Requesting Person / Organization to Appear on the License	Qiran Lu

Requestor Location

Ms. Qiran Lu
305-2, 256 Phillip Street

Waterloo, ON N2L 6B6
Canada

Tax Details

Publisher Tax ID	GB 494 6272 12

Figure 5:

CARBON ENERGY

Open Access

RESEARCH ARTICLE | Open Access

Comprehensive insights into sodium storage in pitch-derived porous hard carbon

Tuo Zhao, Luyao Wang, Chu Zhang, Na Liu, Chuying Ouyang, Zhaoxiang Wang, Liquan Chen

First published: 23 April 2025 | https://doi.org/10.1002/cey2.649

SECTIONS PDF TOOLS SHARE

Abstract

The controversies about the mechanism of sodium storage in hard carbon (HC) hinder its rational structural design. A series of porous HC materials using coal tar pitch show a reversible capacity of 377 mAh g^{-1} and an initial Coulombic efficiency (ICE) of 87% as well as excellent cycling performance. More attention is paid to exploration of the relationships between the sodium status on various storage sites at different sodiation states and the ICE by solid-state ^{23}Na nuclear magnetic resonance spectroscopy. The adsorbed Na ions contribute the most to the irreversible capacity. The de-solvated Na ions entering the closed pores are reduced to Na atoms and aggregated to Na clusters. Also, this process contributes the most to the reversible capacity and is characteristic of a long plateau in the voltage profile. Intercalation is partially reversible; it is the main source of capacity for slope-type HCs but plays a minor role in the reversible capacity of plateau-type HCs. Therefore, increasing the content of the closed pores can improve the reversible plateau capacity and reducing the open mesopores of HC increases the ICE. These findings provide insights into the structural design and cost-efficient preparation of high-performance HC anode materials for advanced sodium-ion batteries.

1 INTRODUCTION

Hard carbon (HC) is generally regarded as the most promising anode material for sodium-ion batteries (SIBs) because of its high Na-storage capacity, low cost, and high availability.[1, 2] HC has an isotropous arrangement of defective graphene sheets and cannot be graphitized



Early View
Online Version of Record before inclusion in an issue
e649

Advertisement

WILEY
APCs are currently waived in EcoEnergy
There is no cost for making your work available to everyone
Discover more

Figures References Related Information

Metrics

Full text views: 1,106

Details

© 2024 The Authors. *Carbon Energy* published by Wenzhou University and John Wiley & Sons Australia, Ltd.

This is an open access article under the terms of the Creative Commons Attribution License, which permits use, distribution and reproduction in any medium, provided the original work is properly cited.

Check for updates



Enhancing electrochemical performance in sodium-ion batteries: Strategic modification of oxygen-containing functional groups in hard carbon

Author: Yulong Li,Yin Yang,Rundan Lin,Chen Zhang,Ting Xiao,Zhuang Ma,Qi Zhang,Xinlong Ma
Publication: Fuel
Publisher: Elsevier
Date: 1 February 2025

© 2024 Elsevier Ltd. All rights are reserved, including those for text and data mining, AI training, and similar technologies.

Order Completed

Thank you for your order.

This Agreement between Qiran Lu ("You") and Elsevier ("Elsevier") consists of your license details and the terms and conditions provided by Elsevier and Copyright Clearance Center.

Your confirmation email will contain your order number for future reference.

Printable Details

License Number	6065491134684
License date	Jul 10, 2025

Licensed Content

Licensed Content Publisher	Elsevier
Licensed Content Publication	Fuel
Licensed Content Title	Enhancing electrochemical performance in sodium-ion batteries: Strategic modification of oxygen-containing functional groups in hard carbon
Licensed Content Author	Yulong Li,Yin Yang,Rundan Lin,Chen Zhang,Ting Xiao,Zhuang Ma,Qi Zhang,Xinlong Ma
Licensed Content Date	Feb 1, 2025
Licensed Content Volume	381
Licensed Content Issue	n/a
Licensed Content Pages	1

Order Details

Type of Use	reuse in a thesis/dissertation
Portion	figures/tables/illustrations
Number of figures/tables/illustrations	1
Format	electronic
Are you the author of this Elsevier article?	No
Will you be translating?	No

About Your Work

Title of new work	Regulating Interlayer Spacing and Defects on Nitrogen-Doped Hard Carbon Anodes from Waste Plastic for Sodium-Ion Batteries
Institution name	University of Waterloo
Expected presentation date	Aug 2025

Additional Data

Portions	Fig. 4
The Requesting Person / Organization to Appear on the License	Qiran Lu

Requestor Location

Requestor Location	Ms. Qiran Lu 305-2, 256 Phillip Street Waterloo, ON N2L 6B6 Canada

Tax Details

Publisher Tax ID	GB 494 6272 12



Insight into the effect of structural differences among pitch fractions on sodium storage performance of pitch-derived hard carbons

Author: Xufeng Zhang,Zonglin Yi,Yanru Tian,Lijing Xie,Fangyuan Su,Xianxian Wei,Jingpeng Chen,Cheng-Meng Chen
Publication: Carbon
Publisher: Elsevier
Date: June 2024

© 2024 Elsevier Ltd. All rights reserved.

Order Completed

Thank you for your order.

This Agreement between Qiran Lu ("You") and Elsevier ("Elsevier") consists of your license details and the terms and conditions provided by Elsevier and Copyright Clearance Center.

Your confirmation email will contain your order number for future reference.

Printable Details

License Number	6065491368521
License date	Jul 10, 2025

Licensed Content

Licensed Content Publisher	Elsevier
Licensed Content Publication	Carbon
Licensed Content Title	Insight into the effect of structural differences among pitch fractions on sodium storage performance of pitch-derived hard carbons
Licensed Content Author	Xufeng Zhang,Zonglin Yi,Yanru Tian,Lijing Xie,Fangyuan Su,Xianxian Wei,Jingpeng Chen,Cheng-Meng Chen
Licensed Content Date	Jun 1, 2024
Licensed Content Volume	226
Licensed Content Issue	n/a
Licensed Content Pages	1

Order Details

Type of Use	reuse in a thesis/dissertation
Portion	figures/tables/illustrations
Number of figures/tables/illustrations	1
Format	electronic
Are you the author of this Elsevier article?	No
Will you be translating?	No

About Your Work

Title of new work	Regulating Interlayer Spacing and Defects on Nitrogen-Doped Hard Carbon Anodes from Waste Plastic for Sodium-Ion Batteries
Institution name	University of Waterloo
Expected presentation date	Aug 2025

Additional Data

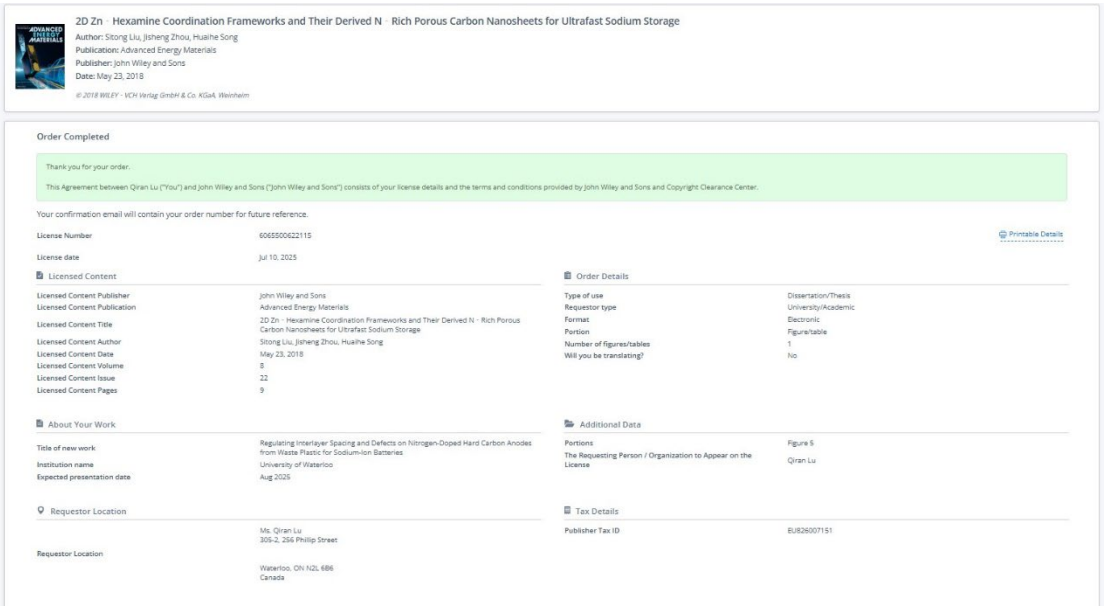
Portions	Fig. 6
The Requesting Person / Organization to Appear on the License	Qiran Lu

Requestor Location

Requestor Location	Ms. Qiran Lu 305-2, 256 Phillip Street Waterloo, ON N2L 6B6 Canada

Tax Details

Publisher Tax ID	GB 494 6272 12



2D Zn‐Hexamine Coordination Frameworks and Their Derived N‐Rich Porous Carbon Nanosheets for Ultrafast Sodium Storage

Author: Sitong Liu, Jisheng Zhou, Huaihe Song
Publication: Advanced Energy Materials
Publisher: John Wiley and Sons
Date: May 23, 2018

© 2018 WILEY - VCH Verlag GmbH & Co. KGaA, Weinheim

Order Completed

Thank you for your order.

This Agreement between Qiran Lu ("You") and John Wiley and Sons ("John Wiley and Sons") consists of your license details and the terms and conditions provided by John Wiley and Sons and Copyright Clearance Center.

Your confirmation email will contain your order number for future reference.

Printable Details

License Number	6065500622115
License date	Jul 10, 2025

Licensed Content

Licensed Content Publisher	John Wiley and Sons
Licensed Content Publication	Advanced Energy Materials
Licensed Content Title	2D Zn‐Hexamine Coordination Frameworks and Their Derived N‐Rich Porous Carbon Nanosheets for Ultrafast Sodium Storage
Licensed Content Author	Sitong Liu, Jisheng Zhou, Huaihe Song
Licensed Content Date	May 23, 2018
Licensed Content Volume	8
Licensed Content Issue	22
Licensed Content Pages	9

Order Details

Type of use	Dissertation/Thesis
Requestor type	University/Academic
Format	Electronic
Portion	Figure/table
Number of figures/tables	1
Will you be translating?	No

About Your Work

Title of new work	Regulating Interlayer Spacing and Defects on Nitrogen-Doped Hard Carbon Anodes from Waste Plastic for Sodium-Ion Batteries
Institution name	University of Waterloo
Expected presentation date	Aug 2025

Additional Data

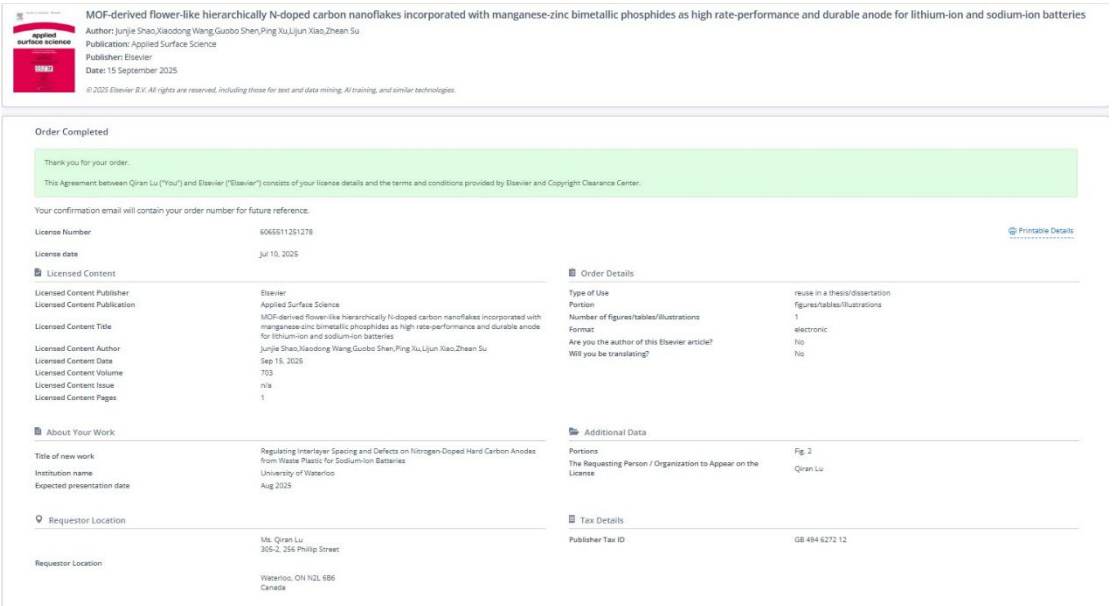
Portions	Figure 5
The Requesting Person / Organization to Appear on the License	Qiran Lu

Requestor Location

Requestor Location	Ms. Qiran Lu 305-2, 256 Phillip Street Waterloo, ON N2L 6B6 Canada

Tax Details

Publisher Tax ID	EU826007151



MOF-derived flower-like hierarchically N-doped carbon nanoflakes incorporated with manganese-zinc bimetallic phosphides as high rate-performance and durable anode for lithium-ion and sodium-ion batteries

Author: Junjie Shao,Xiaodong Wang,Guobo Shen,Ping Xu,Lijun Xiao,Zhean Su
Publication: Applied Surface Science
Publisher: Elsevier
Date: 15 September 2025

© 2025 Elsevier B.V. All rights are reserved, including those for text and data mining, AI training, and similar technologies.

Order Completed

Thank you for your order.

This Agreement between Qiran Lu ("You") and Elsevier ("Elsevier") consists of your license details and the terms and conditions provided by Elsevier and Copyright Clearance Center.

Your confirmation email will contain your order number for future reference.

Printable Details

License Number	6065511251278
License date	Jul 10, 2025

Licensed Content

Licensed Content Publisher	Elsevier
Licensed Content Publication	Applied Surface Science
Licensed Content Title	MOF-derived flower-like hierarchically N-doped carbon nanoflakes incorporated with manganese-zinc bimetallic phosphides as high rate-performance and durable anode for lithium-ion and sodium-ion batteries
Licensed Content Author	Junjie Shao,Xiaodong Wang,Guobo Shen,Ping Xu,Lijun Xiao,Zhean Su
Licensed Content Date	Sep 15, 2025
Licensed Content Volume	703
Licensed Content Issue	n/a
Licensed Content Pages	1

Order Details

Type of Use	reuse in a thesis/dissertation
Portion	figures/tables/illustrations
Number of figures/tables/illustrations	1
Format	electronic
Are you the author of this Elsevier article?	No
Will you be translating?	No

About Your Work

Title of new work	Regulating Interlayer Spacing and Defects on Nitrogen-Doped Hard Carbon Anodes from Waste Plastic for Sodium-Ion Batteries
Institution name	University of Waterloo
Expected presentation date	Aug 2025

Additional Data

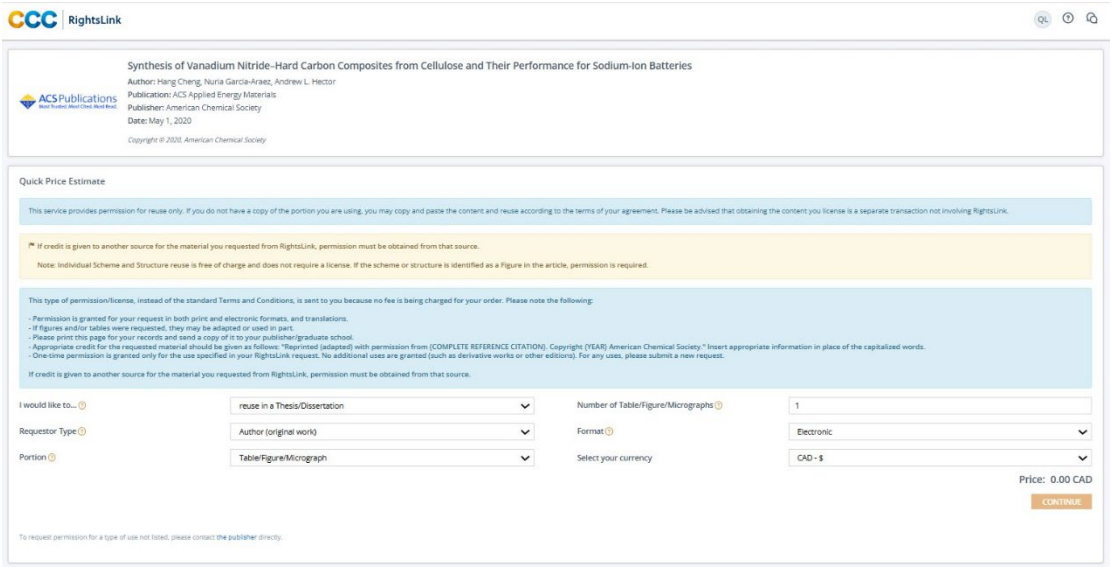
Portions	Fig. 2
The Requesting Person / Organization to Appear on the License	Qiran Lu

Requestor Location

Requestor Location	Ms. Qiran Lu 305-2, 256 Phillip Street Waterloo, ON N2L 6B6 Canada

Tax Details

Publisher Tax ID	GB 494 6272 12



This is a License Agreement between Qiran Lu ("User") and Copyright Clearance Center, Inc. ("CCC") on behalf of the Rightsholder identified in the order details below. The license consists of the order details, the Marketplace Permissions General Terms and Conditions below, and any Rightsholder Terms and Conditions which are included below.

All payments must be made in full to CCC in accordance with the Marketplace Permissions General Terms and Conditions below.

Order Date	10-Jul-2025	Type of Use	Republish in a thesis/dissertation
Order License ID	1629456-1	Publisher	Royal Society of Chemistry
ISSN	2052-1537	Portion	Image/photo/illustration

LICENSED CONTENT

Publication Title	Materials Chemistry Frontiers	Publication Type	e-Journal
Article Title	Self-supporting Fe 7 S 8 microsphere/N-doped carbonized silk textile for high-performance sodium-ion batteries †	Start Page	1747
		End Page	1757
Author / Editor	Zhongguo hua xue hui (Beijing, China), Royal Society of Chemistry (Great Britain)	Issue	11
		Volume	9
Date	01/01/2017	URL	http://www.rsc.org/journals-books-datab...
Language	English		
Country	United Kingdom of Great Britain and Northern Ireland		
Rightsholder	Royal Society of Chemistry		

REQUEST DETAILS

Portion Type	Image/photo/illustration	Distribution	Canada
Number of Images / Photos / Illustrations	1	Translation	Original language of publication
Format (select all that apply)	Electronic	Copies for the Disabled?	No
Who Will Republish the Content?	Academic institution	Minor Editing Privileges?	No
Duration of Use	Current edition and up to 5 years	Incidental Promotional Use?	No
Lifetime Unit Quantity	Up to 499	Currency	CAD
Rights Requested	Main product		

NEW WORK DETAILS

Title	Regulating Interlayer Spacing and Defects on Nitrogen-Doped Hard Carbon Anodes from Waste Plastic for Sodium-Ion Batteries	Institution Name	University of Waterloo
		Expected Presentation Date	2025-08-31
Instructor Name	Aiping Yu		

Figure 6:



Controlling intercalation sites of hard carbon for enhancing Na and K storage performance

Author: Stevanus Alvin,Christian Chandra,Jaehoon Kim
Publication: Chemical Engineering Journal
Publisher: Elsevier
Date: 1 May 2021

© 2021 Elsevier B.V. All rights reserved.

Order Completed

Thank you for your order.

This Agreement between Qiran Lu ("You") and Elsevier ("Elsevier") consists of your license details and the terms and conditions provided by Elsevier and Copyright Clearance Center.

Your confirmation email will contain your order number for future reference.

License Number	6066500399939
License date	Jul 12, 2025

Printable Details

Licensed Content

Licensed Content Publisher	Elsevier
Licensed Content Publication	Chemical Engineering Journal
Licensed Content Title	Controlling intercalation sites of hard carbon for enhancing Na and K storage performance
Licensed Content Author	Stevanus Alvin,Christian Chandra,Jaehoon Kim
Licensed Content Date	1 May 2021
Licensed Content Volume	411
Licensed Content Issue	n/a
Licensed Content Pages	1

Order Details

Type of Use	reuse in a thesis/dissertation
Portion	figures/tables/illustrations
Number of figures/tables/illustrations	1
Format	electronic
Are you the author of this Elsevier article?	No
Will you be translating?	No

About Your Work

Title of new work	Regulating Interlayer Spacing and Defects on Nitrogen-Doped Hard Carbon Anodes from Waste Plastic for Sodium-Ion Batteries
Institution name	University of Waterloo
Expected presentation date	Aug 2025

Additional Data

Portions	Fig. 3
The Requesting Person / Organization to Appear on the License	Qiran Lu

Requestor Location

Requestor Location	Ms. Qiran Lu 305-2, 256 Phillip Street Waterloo, ON N2L 6B6 Canada

Tax Details

Publisher Tax ID	GB 494 6272 12

CCC | RightsLink

Interlayer Spacing Engineering of Cellulose-Derived Hard Carbon for Enhanced Na Diffusivity and Optimized Na Storage in Anode Materials

Author: Yicheng Du, Bowen Chen, Jiao Xie, et al
Publication: Industrial & Engineering Chemistry Research
Publisher: American Chemical Society
Date: Mar 1, 2025

Copyright © 2025, American Chemical Society

Quick Price Estimate

This service provides permission for reuse only. If you do not have a copy of the portion you are using, you may copy and paste the content and reuse according to the terms of your agreement. Please be advised that obtaining the content you license is a separate transaction not involving RightsLink.

If credit is given to another source for the material you requested from RightsLink, permission must be obtained from that source.

Note: Individual Scheme and Structure reuse is free of charge and does not require a license. If the scheme or structure is identified as a Figure in the article, permission is required.

This type of permission/license, instead of the standard Terms and Conditions, is sent to you because no fee is being charged for your order. Please note the following:

- Permission is granted for your request in both print and electronic formats, and translations.
- If figures and/or tables were requested, they may be adapted or used in part.
- Please print this page for your records and send a copy of it to your publisher/graduate school.
- Appropriate credit for the requested material should be given as follows: "Reprinted (adapted) with permission from {COMPLETE REFERENCE CITATION}. Copyright {YEAR} American Chemical Society." Insert appropriate information in place of the capitalized words.
- One-time permission is granted only for the use specified in your RightsLink request. No additional uses are granted (such as derivative works or other editions). For any uses, please submit a new request.

If credit is given to another source for the material you requested from RightsLink, permission must be obtained from that source.

I would like to...	reuse in a Thesis/Dissertation	Number of Table/Figure/Micrographs	1
Requestor Type	Author (original work)	Format	Electronic
Portion	Table/Figure/Micrograph	Select your currency	CAD - $

Price: 0.00 CAD

CONTINUE

To request permission for a type of use not listed, please contact the publisher directly.

CCC | RightsLink

QL

Biomass-Derived Hard Carbon with Interlayer Spacing Optimization toward Ultrastable Na-Ion Storage

Author: Zhidong Hou, Da Lei, Mingwei Jiang, et al
Publication: Applied Materials
Publisher: American Chemical Society
Date: Jan 1, 2023

Copyright © 2023, American Chemical Society

Quick Price Estimate

This service provides permission for reuse only. If you do not have a copy of the portion you are using, you may copy and paste the content and reuse according to the terms of your agreement. Please be advised that obtaining the content you license is a separate transaction not involving RightsLink.

If credit is given to another source for the material you requested from RightsLink, permission must be obtained from that source.

Note: Individual Scheme and Structure reuse is free of charge and does not require a license. If the scheme or structure is identified as a Figure in the article, permission is required.

This type of permission/license, instead of the standard Terms and Conditions, is sent to you because no fee is being charged for your order. Please note the following:

- Permission is granted for your request in both print and electronic formats, and translations.
- If figures and/or tables were requested, they may be adapted or used in part.
- Please print this page for your records and send a copy of it to your publisher/graduate school.
- Appropriate credit for the requested material should be given as follows: "Reprinted (adapted) with permission from (COMPLETE REFERENCE CITATION). Copyright (YEAR) American Chemical Society." Insert appropriate information in place of the capitalized words.
- One-time permission is granted only for the use specified in your RightsLink request. No additional uses are granted (such as derivative works or other editions). For any uses, please submit a new request.

If credit is given to another source for the material you requested from RightsLink, permission must be obtained from that source.

I would like to...	reuse in a Thesis/Dissertation	Number of Table/Figure/Micrographs	1
Requestor Type	Author (original work)	Format	Electronic
Portion	Table/Figure/Micrograph	Select your currency	CAD - $

Price: 0.00 CAD

CONTINUE

To request permission for a type of use not listed, please contact the publisher directly.



Novel Structural Design and Adsorption/Insertion Coordinating Quasi‐Metallic Na Storage Mechanism toward High‐performance Hard Carbon Anode Derived from Carboxymethyl Cellulose

Author: Jilei Liu, Jinshui Liu, Zhixiao Liu, et al
Publication: Small
Publisher: John Wiley and Sons
Date: Jun 9, 2023

© 2023 Wiley - VCH GmbH

Order Completed

Thank you for your order.

This Agreement between Qiran Lu ("You") and John Wiley and Sons ("John Wiley and Sons") consists of your license details and the terms and conditions provided by John Wiley and Sons and Copyright Clearance Center.

Your confirmation email will contain your order number for future reference.

Printable Details

License Number	6066501330066
License date	Jul 12, 2025

Licensed Content

Licensed Content Publisher	John Wiley and Sons
Licensed Content Publication	Small
Licensed Content Title	Novel Structural Design and Adsorption/Insertion Coordinating Quasi‐Metallic Na Storage Mechanism toward High‐performance Hard Carbon Anode Derived from Carboxymethyl Cellulose
Licensed Content Author	Jilei Liu, Jinshui Liu, Zhixiao Liu, et al
Licensed Content Date	Jun 9, 2023
Licensed Content Volume	19
Licensed Content Issue	41
Licensed Content Pages	14

Order Details

Type of use	Dissertation/Thesis
Requestor type	University/Academic
Format	Electronic
Portion	Figure/table
Number of figures/tables	1
Will you be translating?	No

About Your Work

Title of new work	Regulating Interlayer Spacing and Defects on Nitrogen-Doped Hard Carbon Anodes from Waste Plastic for Sodium-Ion Batteries
Institution name	University of Waterloo
Expected presentation date	Aug 2025

Additional Data

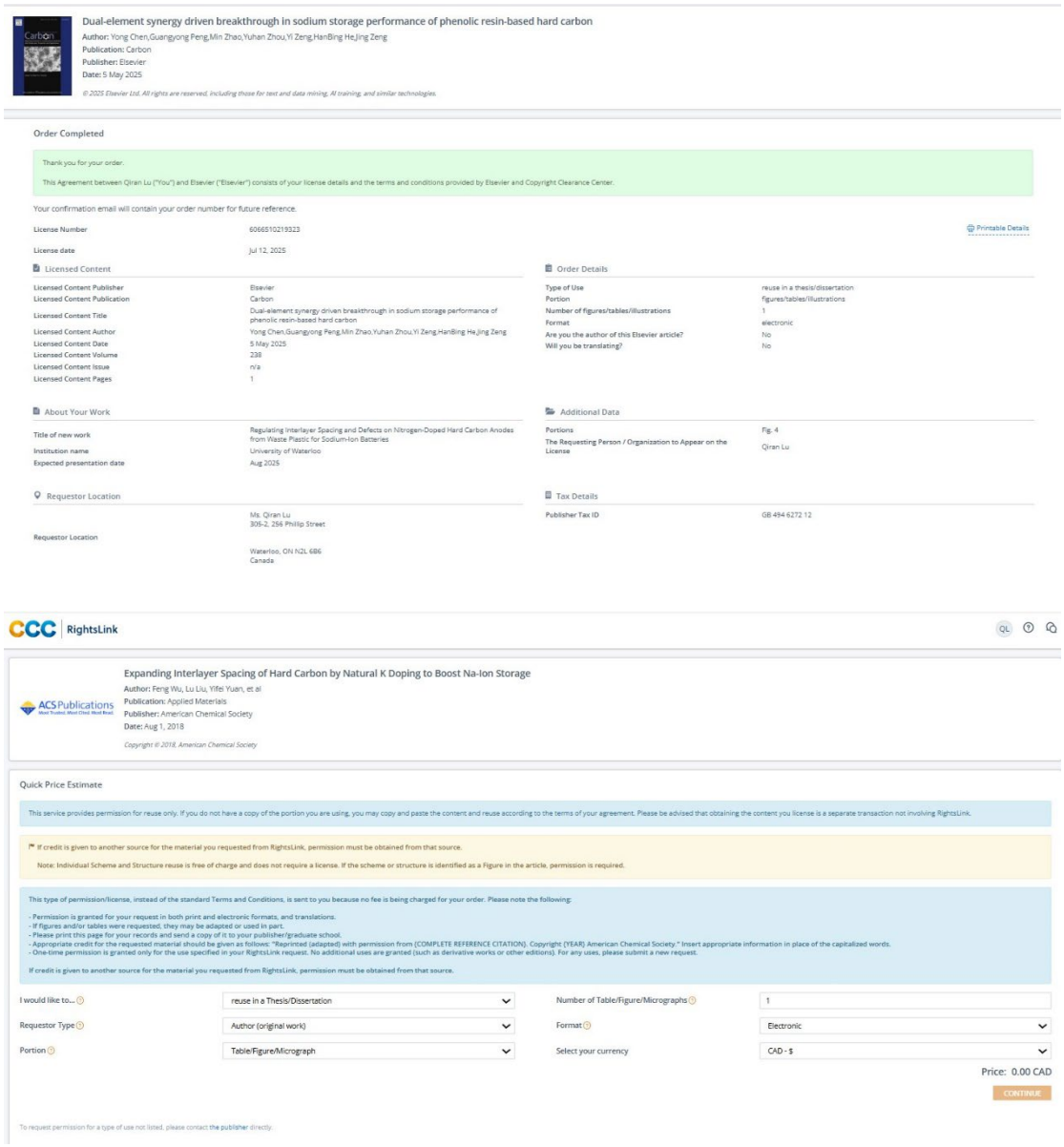
Portions	Figure 2
The Requesting Person / Organization to Appear on the License	Qiran Lu

Requestor Location

Requestor Location	Ms. Qiran Lu 305-2, 256 Phillip Street Waterloo, ON N2L 6B6 Canada

Tax Details

Publisher Tax ID	EU826007151



Dual-element synergy driven breakthrough in sodium storage performance of phenolic resin-based hard carbon

Author: Yong Chen,Guangyong Peng,Min Zhao,Yuhan Zhou,Yi Zeng,HanBing He,Jing Zeng
Publication: Carbon
Publisher: Elsevier
Date: 5 May 2025

© 2025 Elsevier Ltd. All rights are reserved, including those for text and data mining, AI training, and similar technologies.

Order Completed

Thank you for your order.

This Agreement between Qiran Lu ("You") and Elsevier ("Elsevier") consists of your license details and the terms and conditions provided by Elsevier and Copyright Clearance Center.

Your confirmation email will contain your order number for future reference.

Printable Details

License Number	6066510219323
License date	Jul 12, 2025

Licensed Content

Licensed Content Publisher	Elsevier
Licensed Content Publication	Carbon
Licensed Content Title	Dual-element synergy driven breakthrough in sodium storage performance of phenolic resin-based hard carbon
Licensed Content Author	Yong Chen,Guangyong Peng,Min Zhao,Yuhan Zhou,Yi Zeng,HanBing He,Jing Zeng
Licensed Content Date	5 May 2025
Licensed Content Volume	238
Licensed Content Issue	n/a
Licensed Content Pages	1

Order Details

Type of Use	reuse in a thesis/dissertation
Portion	figures/tables/illustrations
Number of figures/tables/illustrations	1
Format	electronic
Are you the author of this Elsevier article?	No
Will you be translating?	No

About Your Work

Title of new work	Regulating Interlayer Spacing and Defects on Nitrogen-Doped Hard Carbon Anodes from Waste Plastic for Sodium-Ion Batteries
Institution name	University of Waterloo
Expected presentation date	Aug 2025

Additional Data

Portions	Fig. 4
The Requesting Person / Organization to Appear on the License	Qiran Lu

Requestor Location

Ms. Qiran Lu
305-2, 256 Phillip Street

Waterloo, ON N2L 6B6
Canada

Tax Details

Publisher Tax ID	GB 494 6272 12

CCC RightsLink

Expanding Interlayer Spacing of Hard Carbon by Natural K Doping to Boost Na-Ion Storage

Author: Feng Wu, Lu Liu, Yifei Yuan, et al
Publication: Applied Materials
Publisher: American Chemical Society
Date: Aug 1, 2018

Copyright © 2018, American Chemical Society

Quick Price Estimate

This service provides permission for reuse only. If you do not have a copy of the portion you are using, you may copy and paste the content and reuse according to the terms of your agreement. Please be advised that obtaining the content you license is a separate transaction not involving RightsLink.

If credit is given to another source for the material you requested from RightsLink, permission must be obtained from that source.

Note: Individual Scheme and Structure reuse is free of charge and does not require a license. If the scheme or structure is identified as a Figure in the article, permission is required.

This type of permission/license, instead of the standard Terms and Conditions, is sent to you because no fee is being charged for your order. Please note the following:

- Permission is granted for your request in both print and electronic formats, and translations.
- If figures and/or tables were requested, they may be adapted or used in part.
- Please print this page for your records and send a copy of it to your publisher/graduate school.
- Appropriate credit for the requested material should be given as follows: "Reprinted (adapted) with permission from {COMPLETE REFERENCE CITATION}. Copyright {YEAR} American Chemical Society." Insert appropriate information in place of the capitalized words.
- One-time permission is granted only for the use specified in your RightsLink request. No additional uses are granted (such as derivative works or other editions). For any uses, please submit a new request.

If credit is given to another source for the material you requested from RightsLink, permission must be obtained from that source.

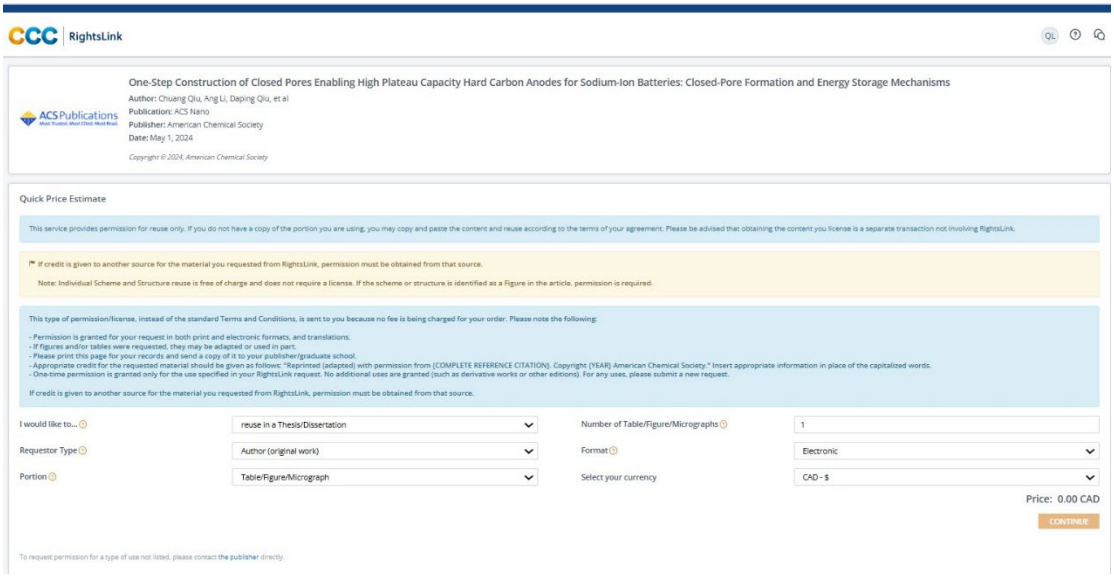
I would like to...	reuse in a Thesis/Dissertation	Number of Table/Figure/Micrographs	1
Requestor Type	Author (original work)	Format	Electronic
Portion	Table/Figure/Micrograph	Select your currency	CAD - $

Price: 0.00 CAD

CONTINUE

To request permission for a type of use not listed, please contact the publisher directly.

Figure 7:



CCC RightsLink

One-Step Construction of Closed Pores Enabling High Plateau Capacity Hard Carbon Anodes for Sodium-Ion Batteries: Closed-Pore Formation and Energy Storage Mechanisms

Author: Chuang Qiu, Ang Li, Daping Qiu, et al
Publication: ACS Nano
Publisher: American Chemical Society
Date: May 1, 2024

Copyright © 2024, American Chemical Society

Quick Price Estimate

This service provides permission for reuse only. If you do not have a copy of the portion you are using, you may copy and paste the content and reuse according to the terms of your agreement. Please be advised that obtaining the content you license is a separate transaction not involving RightsLink.

If credit is given to another source for the material you requested from RightsLink, permission must be obtained from that source.

Note: Individual Scheme and Structure reuse is free of charge and does not require a license. If the scheme or structure is identified as a Figure in the article, permission is required.

This type of permission/license, instead of the standard Terms and Conditions, is sent to you because no fee is being charged for your order. Please note the following:

- Permission is granted for your request in both print and electronic formats, and translations.
- If figures and/or tables were requested, they may be adapted or used in part.
- Please print this page for your records and send a copy of it to your publisher/graduate school.
- Appropriate credit for the requested material should be given as follows: "Reprinted (adapted) with permission from (COMPLETE REFERENCE CITATION). Copyright (YEAR) American Chemical Society." Insert appropriate information in place of the capitalized words.
- One-time permission is granted only for the use specified in your RightsLink request. No additional uses are granted (such as derivative works or other editions). For any uses, please submit a new request.

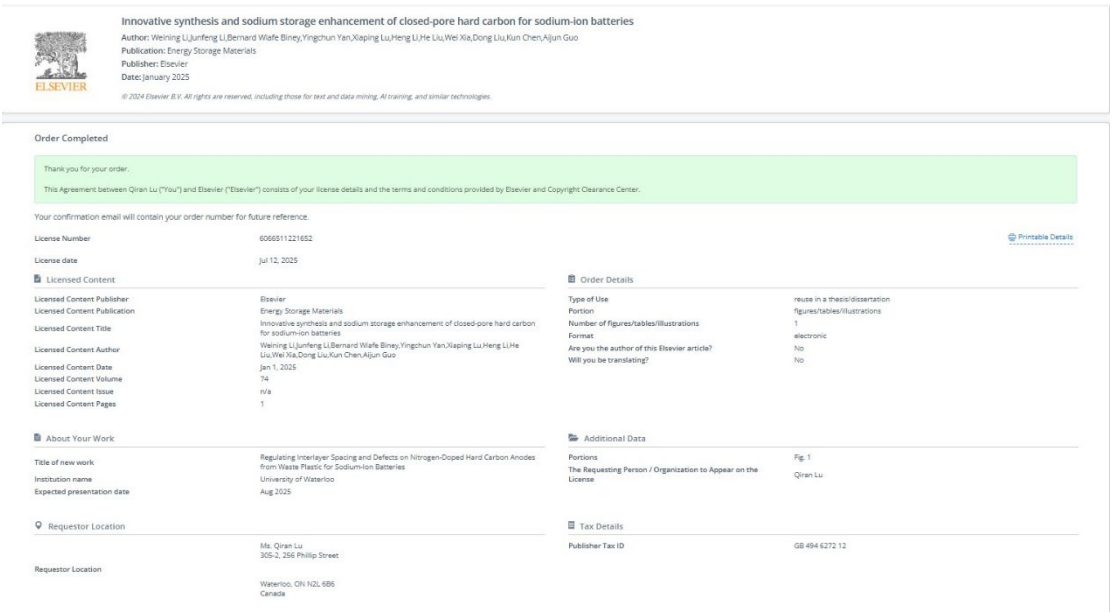
If credit is given to another source for the material you requested from RightsLink, permission must be obtained from that source.

I would like to...	reuse in a Thesis/Dissertation	Number of Table/Figure/Micrographs	1
Requestor Type	Author (original work)	Format	Electronic
Portion	Table/Figure/Micrograph	Select your currency	CAD - $

Price: 0.00 CAD

CONTINUE

To request permission for a type of use not listed, please contact the publisher directly.



Innovative synthesis and sodium storage enhancement of closed-pore hard carbon for sodium-ion batteries

Author: Weining Li,Junfeng Li,Bernard Wiafe Biney,Yingchun Yan,Xiaping Lu,Heng Li,He Liu,Wei Xia,Dong Liu,Kun Chen,Aijun Guo
Publication: Energy Storage Materials
Publisher: Elsevier
Date: January 2025

© 2024 Elsevier B.V. All rights are reserved, including those for text and data mining, AI training, and similar technologies.

Order Completed

Thank you for your order.

This Agreement between Qiran Lu ("You") and Elsevier ("Elsevier") consists of your license details and the terms and conditions provided by Elsevier and Copyright Clearance Center.

Your confirmation email will contain your order number for future reference.

Printable Details

License Number	6066511221652
License date	Jul 12, 2025

Licensed Content

Licensed Content Publisher	Elsevier
Licensed Content Publication	Energy Storage Materials
Licensed Content Title	Innovative synthesis and sodium storage enhancement of closed-pore hard carbon for sodium-ion batteries
Licensed Content Author	Weining Li,Junfeng Li,Bernard Wiafe Biney,Yingchun Yan,Xiaping Lu,Heng Li,He Liu,Wei Xia,Dong Liu,Kun Chen,Aijun Guo
Licensed Content Date	Jan 1, 2025
Licensed Content Volume	74
Licensed Content Issue	n/a
Licensed Content Pages	1

Order Details

Type of Use	reuse in a thesis/dissertation
Portion	figures/tables/illustrations
Number of figures/tables/illustrations	1
Format	electronic
Are you the author of this Elsevier article?	No
Will you be translating?	No

About Your Work

Title of new work	Regulating Interlayer Spacing and Defects on Nitrogen-Doped Hard Carbon Anodes from Waste Plastic for Sodium-Ion Batteries
Institution name	University of Waterloo
Expected presentation date	Aug 2025

Additional Data

Portions	Fig. 1
The Requesting Person / Organization to Appear on the License	Qiran Lu

Requestor Location

Requestor Location	Ms. Qiran Lu 305-2, 256 Phillip Street Waterloo, ON N2L 6B6 Canada

Tax Details

Publisher Tax ID	GB 494 6272 12



Catalyst · Assisted Chemical Vapor Deposition Engineering of Hard Carbon with Abundant Closed Pores for High · Performance Sodium · Ion Batteries

Author: Yan Yu, Hai Yang, Hongge Pan, et al
Publication: Advanced Functional Materials
Publisher: John Wiley and Sons
Date: Apr 30, 2025

© 2025 Wiley - VCH GmbH

Order Completed

Thank you for your order.

This Agreement between Qiran Lu ("You") and John Wiley and Sons ("John Wiley and Sons") consists of your license details and the terms and conditions provided by John Wiley and Sons and Copyright Clearance Center.

Your confirmation email will contain your order number for future reference.

Printable Details

License Number	6066511427623
License date	Jul 12, 2025

Licensed Content

Licensed Content Publisher	John Wiley and Sons
Licensed Content Publication	Advanced Functional Materials
Licensed Content Title	Catalyst - Assisted Chemical Vapor Deposition Engineering of Hard Carbon with Abundant Closed Pores for High - Performance Sodium - Ion Batteries
Licensed Content Author	Yan Yu, Hai Yang, Hongge Pan, et al
Licensed Content Date	Apr 30, 2025
Licensed Content Volume	0
Licensed Content Issue	0
Licensed Content Pages	11

Order Details

Type of use	Dissertation/Thesis
Requestor type	University/Academic
Format	Electronic
Portion	Figure/table
Number of figures/tables	1
Will you be translating?	No

About Your Work

Title of new work	Regulating Interlayer Spacing and Defects on Nitrogen-Doped Hard Carbon Anodes from Waste Plastic for Sodium-Ion Batteries
Institution name	University of Waterloo
Expected presentation date	Aug 2025

Additional Data

Portions	Figure 3
The Requesting Person / Organization to Appear on the License	Qiran Lu

Requestor Location

Requestor Location	Ms. Qiran Lu 305-2, 266 Phillip Street Waterloo, ON N2L 6B6 Canada

Tax Details

Publisher Tax ID	EU826007151



Spatial configuration engineering of phenolic resins to tune the closed pores of hard carbon for enhanced plateau-capacity sodium storage

Author: Liewen Guo,Chuang Qiu,Haiyan Liu,Renlu Yuan,Xiaotian Li,Xin Li,Kairan Li,Wanxiong Zhu,Mohammad Tabish,Xuewei Liu,Ang Li,Xiaohong Chen,Hualhe Song
Publication: Chemical Engineering Journal
Publisher: Elsevier
Date: 15 May 2025

© 2025 Elsevier B.V. All rights are reserved, including those for text and data mining, AI training, and similar technologies.

Order Completed

Thank you for your order.

This Agreement between Qiran Lu ("You") and Elsevier ("Elsevier") consists of your license details and the terms and conditions provided by Elsevier and Copyright Clearance Center.

Your confirmation email will contain your order number for future reference.

Printable Details

License Number	6066520176902
License date	Jul 12, 2025

Licensed Content

Licensed Content Publisher	Elsevier
Licensed Content Publication	Chemical Engineering Journal
Licensed Content Title	Spatial configuration engineering of phenolic resins to tune the closed pores of hard carbon for enhanced plateau-capacity sodium storage
Licensed Content Author	Liewen Guo,Chuang Qiu,Haiyan Liu,Renlu Yuan,Xiaotian Li,Xin Li,Kairan Li,Wanxiong Zhu,Mohammad Tabish,Xuewei Liu,Ang Li,Xiaohong Chen,Hualhe Song
Licensed Content Date	May 15, 2025
Licensed Content Volume	512
Licensed Content Issue	n/a
Licensed Content Pages	1

Order Details

Type of Use	reuse in a thesis/dissertation
Portion	figures/tables/illustrations
Number of figures/tables/illustrations	1
Format	electronic
Are you the author of this Elsevier article?	No
Will you be translating?	No

About Your Work

Title of new work	Regulating Interlayer Spacing and Defects on Nitrogen-Doped Hard Carbon Anodes from Waste Plastic for Sodium-Ion Batteries
Institution name	University of Waterloo
Expected presentation date	Aug 2025

Additional Data

Portions	Fig. 5
The Requesting Person / Organization to Appear on the License	Qiran Lu

Requestor Location

Requestor Location	Ms. Qiran Lu 305-2, 266 Phillip Street Waterloo, ON N2L 6B6 Canada

Tax Details

Publisher Tax ID	GB 494 6272 12

Order Date	12-Jul-2025	Type of Use	Republish in a thesis/dissertation
Order License ID	1629889-1	Publisher	Royal Society of Chemistry
ISSN	2050-7496	Portion	Chart/graph/table/figure

LICENSED CONTENT

Publication Title	Journal of materials chemistry. A, Materials for energy and sustainability	Publication Type	e-Journal
Article Title	Structural design of biomass-derived hard carbon anode materials for superior sodium storage via increasing crystalline cellulose and closing the open pores †	Start Page	21176
		End Page	21189
		Issue	32
		Volume	12
Author / Editor	Royal Society of Chemistry (Great Britain)	URL	http://pubs.rsc.org/en/journals/journaliss...
Date	01/01/2013		
Language	English		
Country	United Kingdom of Great Britain and Northern Ireland		
Rightsholder	Royal Society of Chemistry		

REQUEST DETAILS

Portion Type	Chart/graph/table/figure	Distribution	Canada
Number of Charts / Graphs / Tables / Figures Requested	1	Translation	Original language of publication
		Copies for the Disabled?	No
Format (select all that apply)	Electronic	Minor Editing Privileges?	No
Who Will Republish the Content?	Academic institution	Incidental Promotional Use?	No
Duration of Use	Current edition and up to 5 years	Currency	CAD
Lifetime Unit Quantity	Up to 499		
Rights Requested	Main product		

NEW WORK DETAILS

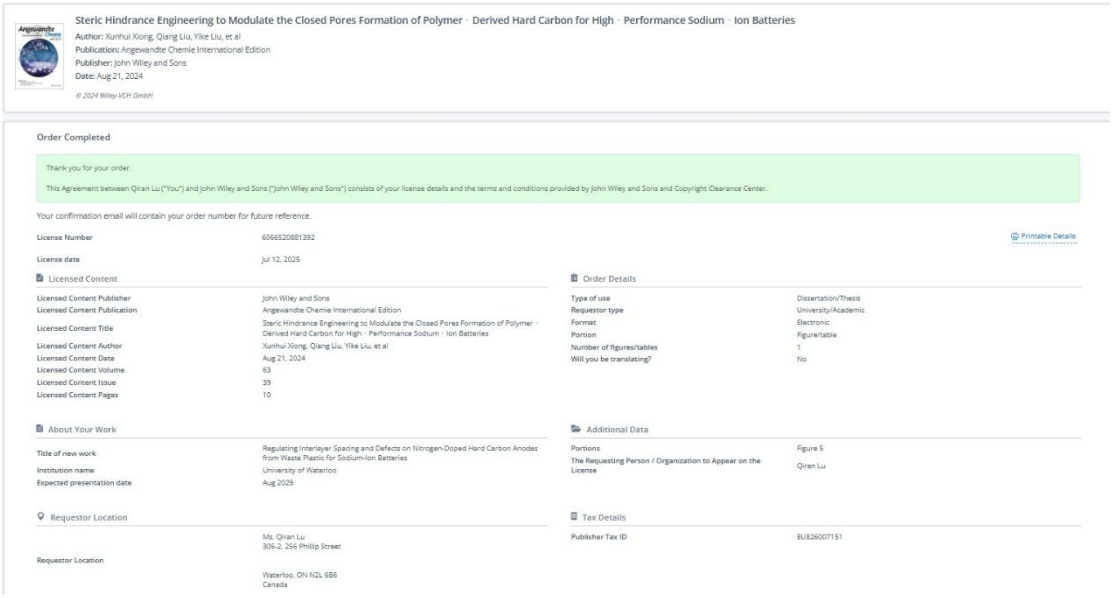
Title	Regulating Interlayer Spacing and Defects on Nitrogen-Doped Hard Carbon Anodes from Waste Plastic for Sodium-Ion Batteries	Institution Name	University of Waterloo
		Expected Presentation Date	2025-08-31
Instructor Name	Aiping Yu		

ADDITIONAL DETAILS

Order Reference Number	N/A	The Requesting Person / Organization to Appear on the License	Qiran Lu

REQUESTED CONTENT DETAILS

Title, Description or Numeric Reference of the Portion(s)	Fig. 5	Title of the Article / Chapter the Portion Is From	Structural design of biomass-derived hard carbon anode materials for superior sodium storage via increasing crystalline cellulose and closing the open pores †
Editor of Portion(s)	Li, Xiaoying; Zhang, Sijing; Tang, Jingjing; Yang, Juan; Wen, Kang; Wang, Jiong; Wang, Peng; Zhou, Xiangyang; Zhang, Yaguang	Author of Portion(s)	Li, Xiaoying; Zhang, Sijing; Tang, Jingjing; Yang, Juan; Wen, Kang; Wang, Jiong; Wang, Peng; Zhou, Xiangyang; Zhang, Yaguang
Volume / Edition	12	Issue, if Republishing an Article From a Serial	32
Page or Page Range of Portion	21176-21189	Publication Date of Portion	2024-08-13



Steric Hindrance Engineering to Modulate the Closed Pores Formation of Polymer - Derived Hard Carbon for High - Performance Sodium - Ion Batteries

Author: Xunhui Xiong, Qiang Liu, Yike Liu, et al
Publication: Angewandte Chemie International Edition
Publisher: John Wiley and Sons
Date: Aug 21, 2024

© 2024 Wiley-VCH GmbH

Order Completed

Thank you for your order.

This Agreement between Qiran Lu ("You") and John Wiley and Sons ("John Wiley and Sons") consists of your license details and the terms and conditions provided by John Wiley and Sons and Copyright Clearance Center.

Your confirmation email will contain your order number for future reference.

Printable Details

License Number	6066520881392
License date	Jul 12, 2025

Licensed Content

Licensed Content Publisher	John Wiley and Sons
Licensed Content Publication	Angewandte Chemie International Edition
Licensed Content Title	Steric Hindrance Engineering to Modulate the Closed Pores Formation of Polymer - Derived Hard Carbon for High - Performance Sodium - Ion Batteries
Licensed Content Author	Xunhui Xiong, Qiang Liu, Yike Liu, et al
Licensed Content Date	Aug 21, 2024
Licensed Content Volume	63
Licensed Content Issue	39
Licensed Content Pages	10

Order Details

Type of use	Dissertation/Thesis
Requestor type	University/Academic
Format	Electronic
Portion	Figure/table
Number of figures/tables	1
Will you be translating?	No

About Your Work

Title of new work	Regulating Interlayer Spacing and Defects on Nitrogen-Doped Hard Carbon Anodes from Waste Plastic for Sodium-Ion Batteries
Institution name	University of Waterloo
Expected presentation date	Aug 2025

Additional Data

Portions	Figure 5
The Requesting Person / Organization to Appear on the License	Qiran Lu

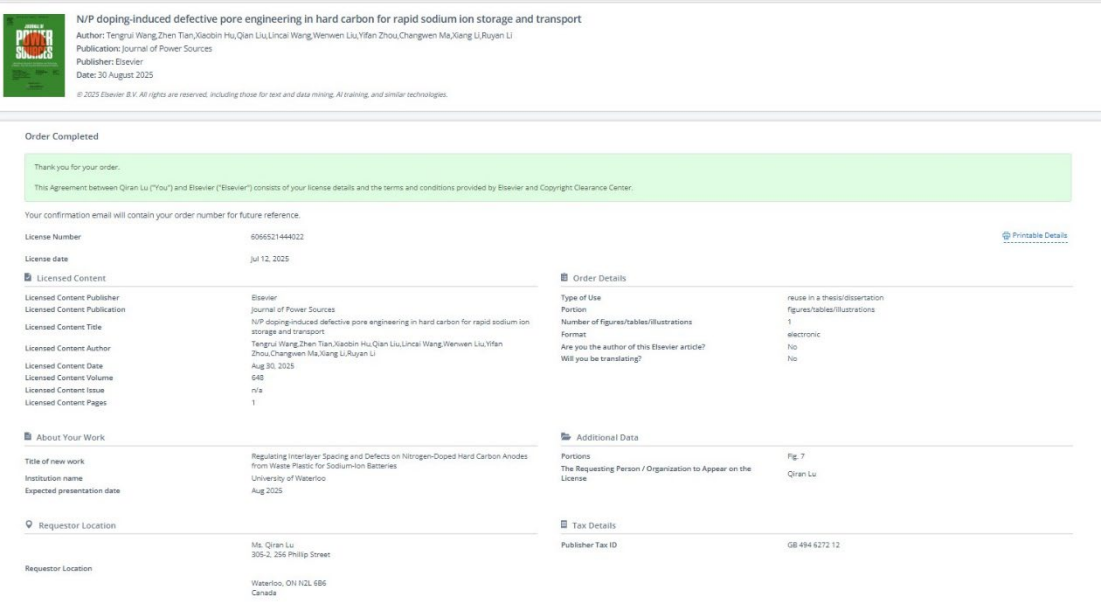
Requestor Location

Ms. Qiran Lu
305-2, 256 Phillip Street
Waterloo, ON N2L 6B6
Canada

Tax Details

Publisher Tax ID	EU826007151

Figure 8:



N/P doping-induced defective pore engineering in hard carbon for rapid sodium ion storage and transport

Author: Tengrui Wang,Zhen Tian,Xiaobin Hu,Qian Liu,Lincai Wang,Wenwen Liu,Yifan Zhou,Changwen Ma,Xiang Li,Ruyan Li
Publication: Journal of Power Sources
Publisher: Elsevier
Date: 30 August 2025

© 2025 Elsevier B.V. All rights are reserved, including those for text and data mining, AI training, and similar technologies.

Order Completed

Thank you for your order.

This Agreement between Qiran Lu ("You") and Elsevier ("Elsevier") consists of your license details and the terms and conditions provided by Elsevier and Copyright Clearance Center.

Your confirmation email will contain your order number for future reference.

Printable Details

License Number	606652144402 2
License date	Jul 12, 2025

Licensed Content

Licensed Content Publisher	Elsevier
Licensed Content Publication	Journal of Power Sources
Licensed Content Title	N/P doping-induced defective pore engineering in hard carbon for rapid sodium ion storage and transport
Licensed Content Author	Tengrui Wang,Zhen Tian,Xiaobin Hu,Qian Liu,Lincai Wang,Wenwen Liu,Yifan Zhou,Changwen Ma,Xiang Li,Ruyan Li
Licensed Content Date	Aug 30, 2025
Licensed Content Volume	648
Licensed Content Issue	n/a
Licensed Content Pages	1

Order Details

Type of Use	reuse in a thesis/dissertation
Portion	figures/tables/illustrations
Number of figures/tables/illustrations	1
Format	electronic
Are you the author of this Elsevier article?	No
Will you be translating?	No

About Your Work

Title of new work	Regulating Interlayer Spacing and Defects on Nitrogen-Doped Hard Carbon Anodes from Waste Plastic for Sodium-Ion Batteries
Institution name	University of Waterloo
Expected presentation date	Aug 2025

Additional Data

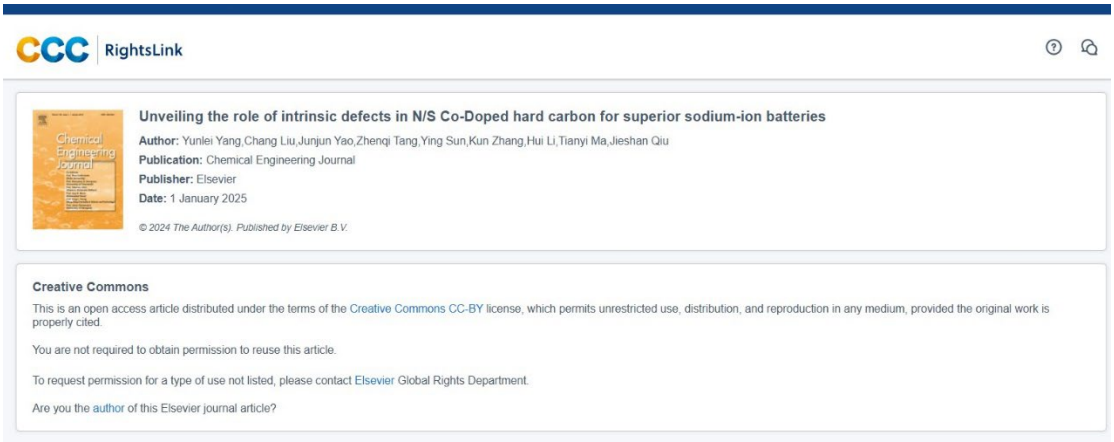
Portions	Fig. 7
The Requesting Person / Organization to Appear on the License	Qiran Lu

Requestor Location

Requestor Location	Ms. Qiran Lu 305-2, 256 Phillip Street Waterloo, ON N2L 6B6 Canada

Tax Details

Publisher Tax ID	GB 494 6272 12



CCC RightsLink

Unveiling the role of intrinsic defects in N/S Co-Doped hard carbon for superior sodium-ion batteries

Author: Yunlei Yang,Chang Liu,Junjun Yao,Zhenqi Tang,Ying Sun,Kun Zhang,Hui Li,Tianyi Ma,Jieshan Qiu
Publication: Chemical Engineering Journal
Publisher: Elsevier
Date: 1 January 2025

© 2024 The Author(s). Published by Elsevier B.V.

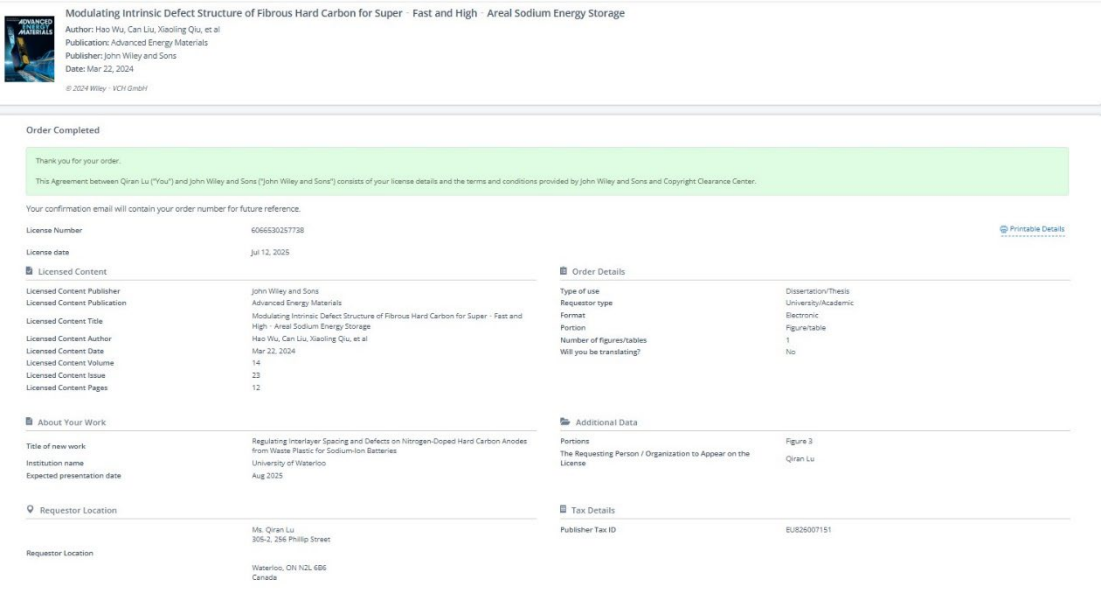
Creative Commons

This is an open access article distributed under the terms of the Creative Commons CC-BY license, which permits unrestricted use, distribution, and reproduction in any medium, provided the original work is properly cited.

You are not required to obtain permission to reuse this article.

To request permission for a type of use not listed, please contact Elsevier Global Rights Department.

Are you the author of this Elsevier journal article?



Modulating Intrinsic Defect Structure of Fibrous Hard Carbon for Super‐Fast and High‐Areal Sodium Energy Storage

Author: Hao Wu, Can Liu, Xiaoling Qiu, et al
Publication: Advanced Energy Materials
Publisher: John Wiley and Sons
Date: Mar 22, 2024

© 2024 Wiley‐VCH GmbH

Order Completed

Thank you for your order.

This Agreement between Qiran Lu ("You") and John Wiley and Sons ("John Wiley and Sons") consists of your license details and the terms and conditions provided by John Wiley and Sons and Copyright Clearance Center.

Your confirmation email will contain your order number for future reference.

Printable Details

License Number	6066530257738
License date	Jul 12, 2025

Licensed Content

Licensed Content Publisher	John Wiley and Sons
Licensed Content Publication	Advanced Energy Materials
Licensed Content Title	Modulating Intrinsic Defect Structure of Fibrous Hard Carbon for Super‐Fast and High‐Areal Sodium Energy Storage
Licensed Content Author	Hao Wu, Can Liu, Xiaoling Qiu, et al
Licensed Content Date	Mar 22, 2024
Licensed Content Volume	14
Licensed Content Issue	23
Licensed Content Pages	12

Order Details

Type of use	Dissertation/Thesis
Requestor type	University/Academic
Format	Electronic
Portion	Figure/table
Number of figures/tables	1
Will you be translating?	No

About Your Work

Title of new work	Regulating Interlayer Spacing and Defects on Nitrogen-Doped Hard Carbon Anodes from Waste Plastic for Sodium-Ion Batteries
Institution name	University of Waterloo
Expected presentation date	Aug 2025

Additional Data

Portions	Figure 3
The Requesting Person / Organization to Appear on the License	Qiran Lu

Requestor Location

Requestor Location	Ms. Qiran Lu 305-2, 256 Phillip Street Waterloo, ON N2L 6B6 Canada

Tax Details

Publisher Tax ID	EU826007151



Defect-rich hard carbon designed by heteroatom escape assists sodium storage performance for sodium-ion batteries

Author: Yongxin Wang,Meng Li,Yu Zhang,Naiqing Zhang
Publication: Chemical Engineering Journal
Publisher: Elsevier
Date: 1 November 2024

© 2024 Published by Elsevier B.V.

Order Completed

Thank you for your order.

This Agreement between Qiran Lu ("You") and Elsevier ("Elsevier") consists of your license details and the terms and conditions provided by Elsevier and Copyright Clearance Center.

Your confirmation email will contain your order number for future reference.

Printable Details

License Number	6066530555287
License date	Jul 12, 2025

Licensed Content

Licensed Content Publisher	Elsevier
Licensed Content Publication	Chemical Engineering Journal
Licensed Content Title	Defect-rich hard carbon designed by heteroatom escape assists sodium storage performance for sodium-ion batteries
Licensed Content Author	Yongxin Wang,Meng Li,Yu Zhang,Naiqing Zhang
Licensed Content Date	Nov 1, 2024
Licensed Content Volume	499
Licensed Content Issue	n/a
Licensed Content Pages	1

Order Details

Type of Use	reuse in a thesis/dissertation
Portion	figures/tables/illustrations
Number of figures/tables/illustrations	1
Format	electronic
Are you the author of this Elsevier article?	No
Will you be translating?	No

About Your Work

Title of new work	Regulating Interlayer Spacing and Defects on Nitrogen-Doped Hard Carbon Anodes from Waste Plastic for Sodium-Ion Batteries
Institution name	University of Waterloo
Expected presentation date	Aug 2025

Additional Data

Portions	Fig. 3
The Requesting Person / Organization to Appear on the License	Qiran Lu

Requestor Location

Requestor Location	Ms. Qiran Lu 305-2, 256 Phillip Street Waterloo, ON N2L 6B6 Canada

Tax Details

Publisher Tax ID	GB 494 6272 12



Interfacial - Catalysis - Enabled Layered and Inorganic - Rich SEI on Hard Carbon Anodes in Ester Electrolytes for Sodium - Ion Batteries

Author: Yuteng Gong, Ying Bai, Chuan Wu, et al
Publication: Advanced Materials
Publisher: John Wiley and Sons
Date: May 28, 2023

© 2023 Wiley - VCH GmbH

Order Completed

Thank you for your order.

This Agreement between Qiran Lu ("You") and John Wiley and Sons ("John Wiley and Sons") consists of your license details and the terms and conditions provided by John Wiley and Sons and Copyright Clearance Center.

Your confirmation email will contain your order number for future reference.

Printable Details

License Number	6066530757243
License date	Jul 12, 2025

Licensed Content

Licensed Content Publisher	John Wiley and Sons
Licensed Content Publication	Advanced Materials
Licensed Content Title	Interfacial - Catalysis - Enabled Layered and Inorganic - Rich SEI on Hard Carbon Anodes in Ester Electrolytes for Sodium - Ion Batteries
Licensed Content Author	Yuteng Gong, Ying Bai, Chuan Wu, et al
Licensed Content Date	May 28, 2023
Licensed Content Volume	35
Licensed Content Issue	29
Licensed Content Pages	12

Order Details

Type of use	Dissertation/Thesis
Requestor type	University/Academic
Format	Electronic
Portion	Figure/table
Number of figures/tables	1
Will you be translating?	No

About Your Work

Title of new work	Regulating Interlayer Spacing and Defects on Nitrogen-Doped Hard Carbon Anodes from Waste Plastic for Sodium-Ion Batteries
Institution name	University of Waterloo
Expected presentation date	Aug 2025

Additional Data

Portions	Figure 2
The Requesting Person / Organization to Appear on the License	Qiran Lu

Requestor Location

Requestor Location	Ms. Qiran Lu 305-2, 256 Phillip Street Waterloo, ON N2L 6B6 Canada

Tax Details

Publisher Tax ID	EU826007151



Simple and cost-effective method for engineering tunable defects and functional groups for high-performance coal-derived hard carbon anodes in sodium-ion batteries

Author: Xiaohu Wang,Jie Ren,Yi Zhu,Gai Lan,Yaxin Huang,Jianfang Wang,Jun Liu,Junhui Dong,Chunguang Wei,Na Huang,Ding Nan
Publication: Electrochimica Acta
Publisher: Elsevier
Date: 10 July 2025

© 2025 Published by Elsevier Ltd.

Order Completed

Thank you for your order.

This Agreement between Qiran Lu ("You") and Elsevier ("Elsevier") consists of your license details and the terms and conditions provided by Elsevier and Copyright Clearance Center.

Your confirmation email will contain your order number for future reference.

Printable Details

License Number	6066531046573
License date	Jul 12, 2025

Licensed Content

Licensed Content Publisher	Elsevier
Licensed Content Publication	Electrochimica Acta
Licensed Content Title	Simple and cost-effective method for engineering tunable defects and functional groups for high-performance coal-derived hard carbon anodes in sodium-ion batteries
Licensed Content Author	Xiaohu Wang,Jie Ren,Yi Zhu,Gai Lan,Yaxin Huang,Jianfang Wang,Jun Liu,Junhui Dong,Chunguang Wei,Na Huang,Ding Nan
Licensed Content Date	Jul 10, 2025
Licensed Content Volume	528
Licensed Content Issue	n/a
Licensed Content Pages	1

Order Details

Type of Use	reuse in a thesis/dissertation
Portion	figures/tables/illustrations
Number of figures/tables/illustrations	1
Format	electronic
Are you the author of this Elsevier article?	No
Will you be translating?	No

About Your Work

Title of new work	Regulating Interlayer Spacing and Defects on Nitrogen-Doped Hard Carbon Anodes from Waste Plastic for Sodium-Ion Batteries
Institution name	University of Waterloo
Expected presentation date	Aug 2025

Additional Data

Portions	Fig. 5
The Requesting Person / Organization to Appear on the License	Qiran Lu

Requestor Location

Requestor Location	Ms. Qiran Lu 305-2, 256 Phillip Street Waterloo, ON N2L 6B6 Canada

Tax Details

Publisher Tax ID	GB 494 6272 12

References

[1] M. Jiang, N. Sun, R. Ali Soomro, B. Xu, *Journal of Energy Chemistry* **2021**, *55*, 34-47.

[2] D. Larcher, J. M. Tarascon, *Nature Chemistry* **2015**, *7*, 19-29.

[3] aG. H. Newman, L. P. Klemann, *Journal of The Electrochemical Society* **1980**, *127*, 2097; bK. M. Abraham, *Solid State Ionics* **1982**, *7*, 199-212.

[4] N. Yabuuchi, K. Kubota, M. Dahbi, S. Komaba, *Chemical Reviews* **2014**, *114*, 11636-11682.

[5] X. Pu, H. Wang, D. Zhao, H. Yang, X. Ai, S. Cao, Z. Chen, Y. Cao, *Small* **2019**, *15*, 1805427.

[6] S. Qiao, Q. Zhou, M. Ma, H. K. Liu, S. X. Dou, S. Chong, *ACS Nano* **2023**, *17*, 11220-11252.

[7] W. Shao, H. Shi, X. Jian, Z.-S. Wu, F. Hu, *Advanced Energy and Sustainability Research* **2022**, *3*, 2200009.

[8] L.-F. Zhao, Z. Hu, W.-H. Lai, Y. Tao, J. Peng, Z.-C. Miao, Y.-X. Wang, S.-L. Chou, H.-K. Liu, S.-X. Dou, *Advanced Energy Materials* **2021**, *11*, 2002704.

[9] aX. Ji, Y. Wei, H. Yang, Z. Lu, S. Jin, H. Jin, X. Kong, H. Ji, *Small* **2024**, *20*, 2402616; bX. Zhang, Z. Hou, M. Jiang, J. Peng, H. Ma, Y. Gao, J.-G. Wang, *Small* **2024**, *20*, 2311778.

[10] H. Liu, M. Jia, M. Wang, R. Chen, N. Sun, Q. Zhu, F. Wu, B. Xu, *RSC Advances* **2016**, *6*, 78235-78240.

[11] aY. Li, Y. Lu, Q. Meng, A. C. S. Jensen, Q. Zhang, Q. Zhang, Y. Tong, Y. Qi, L. Gu, M.-M. Titirici, Y.-S. Hu, *Advanced Energy Materials* **2019**, *9*, 1902852; bC. Qiu, A. Li, D. Qiu, Y. Wu, Z. Jiang, J. Zhang, J. Xiao, R. Yuan, Z. Jiang, X. Liu, X. Chen, H. Song, *ACS Nano* **2024**, *18*, 11941-11954.

[12] C. Matei Ghimbeu, J. Górka, V. Simone, L. Simonin, S. Martinet, C. Vix-Guterl, *Nano Energy* **2018**, *44*, 327-335.

[13] X. Guo, Y. Xue, H. Zhou, Y. Weng, J. Zhou, *ACS Applied Materials & Interfaces* **2020**, *12*, 2407-2416.

[14] J. S. Weaving, A. Lim, J. Millichamp, T. P. Neville, D. Ledwoch, E. Kendrick, P. F. McMillan, P. R. Shearing, C. A. Howard, D. J. L. Brett, *ACS Applied Energy Materials* **2020**, *3*, 7474-7484.

[15] B. Wang, J. R. Fitzpatrick, A. Brookfield, A. J. Fielding, E. Reynolds, J. Entwistle, J. Tong, B. F. Spencer, S. Baldock, K. Hunter, C. M. Kavanagh, N. Tapia-Ruiz, *Nature Communications* **2024**, *15*, 3013.

[16] aD. A. Stevens, J. R. Dahn, *Journal of The Electrochemical Society* **2000**, *147*, 1271; bD. A. Stevens, J. R. Dahn, *Journal of The Electrochemical Society* **2001**, *148*, A803.

[17] S. Komaba, W. Murata, T. Ishikawa, N. Yabuuchi, T. Ozeki, T. Nakayama, A. Ogata, K. Gotoh, K. Fujiwara, *Advanced Functional Materials* **2011**, *21*, 3859-3867.

[18] aS. Qiu, L. Xiao, M. L. Sushko, K. S. Han, Y. Shao, M. Yan, X. Liang, L. Mai, J. Feng, Y. Cao, X. Ai, H. Yang, J. Liu, *Advanced Energy Materials* **2017**, *7*, 1700403; bJ. Ding, H. Wang, Z. Li, A. Kohandehghan, K. Cui, Z. Xu, B. Zahiri, X. Tan, E. M.

Lotfabad, B. C. Olsen, D. Mitlin, *ACS Nano* **2013**, *7*, 11004-11015; cL. Xiao, H. Lu, Y. Fang, M. L. Sushko, Y. Cao, X. Ai, H. Yang, J. Liu, *Advanced Energy Materials* **2018**, *8*, 1703238; dY. Cao, L. Xiao, M. L. Sushko, W. Wang, B. Schwenzer, J. Xiao, Z. Nie, L. V. Saraf, Z. Yang, J. Liu, *Nano Letters* **2012**, *12*, 3783-3787.

[19] P. Bai, Y. He, X. Zou, X. Zhao, P. Xiong, Y. Xu, *Advanced Energy Materials* **2018**, *8*, 1703217.

[20] Z.-E. Yu, Y. Lyu, Y. Wang, S. Xu, H. Cheng, X. Mu, J. Chu, R. Chen, Y. Liu, B. Guo, *Chemical Communications* **2020**, *56*, 778-781.

[21] aY. Jin, S. Sun, M. Ou, Y. Liu, C. Fan, X. Sun, J. Peng, Y. Li, Y. Qiu, P. Wei, Z. Deng, Y. Xu, J. Han, Y. Huang, *ACS Applied Energy Materials* **2018**, *1*, 2295-2305; bC. Bommier, T. W. Surta, M. Dolgos, X. Ji, *Nano Letters* **2015**, *15*, 5888-5892; cS. Alvin, H. S. Cahyadi, J. Hwang, W. Chang, S. K. Kwak, J. Kim, *Advanced Energy Materials* **2020**, *10*, 2000283.

[22] X.-X. He, J.-H. Zhao, W.-H. Lai, R. Li, Z. Yang, C.-m. Xu, Y. Dai, Y. Gao, X.-H. Liu, L. Li, G. Xu, Y. Qiao, S.-L. Chou, M. Wu, *ACS Applied Materials & Interfaces* **2021**, *13*, 44358-44368.

[23] N. Sun, J. Qiu, B. Xu, *Advanced Energy Materials* **2022**, *12*, 2200715.

[24] D. Saurel, B. Orayech, B. Xiao, D. Carriazo, X. Li, T. Rojo, *Advanced Energy Materials* **2018**, *8*, 1703268.

[25] N. Sun, Z. Guan, Y. Liu, Y. Cao, Q. Zhu, H. Liu, Z. Wang, P. Zhang, B. Xu, *Advanced Energy Materials* **2019**, *9*, 1901351.

[26] A. Rützler, J. Büttner, J. Oechsler, S. E. Balaghi, S. Küspert, N. Ortlieb, A. Fischer, *Advanced Functional Materials* **2024**, *34*, 2401188.

[27] aZ. Han, T. Wang, Y. Cai, S. Rong, J. Ma, L. Hou, Y. Ji, *Carbon* **2024**, *222*, 118969; bB. Zhang, C. M. Ghimbeu, C. Laberty, C. Vix-Guterl, J.-M. Tarascon, *Advanced Energy Materials* **2016**, *6*, 1501588.

[28] Q. Meng, Y. Lu, F. Ding, Q. Zhang, L. Chen, Y.-S. Hu, *ACS Energy Letters* **2019**, *4*, 2608-2612.

[29] Z. Liang, X. Fan, W. Zheng, D. J. Singh, *ACS Applied Materials & Interfaces* **2017**, *9*, 17076-17084.

[30] L. Dai, O. Karakas, Y. Cheng, K. Cobb, P. Chen, R. Ruan, *Chemical Engineering Journal* **2023**, *453*, 139725.

[31] X. Yang, C. Li, G. Zhang, C. Yang, *Journal of Materials Science* **2015**, *50*, 6649-6655.

[32] S. C. Dey, B. Worfolk, L. Lower, W. J. Sagues, M. R. Nimlos, S. S. Kelley, S. Park, *ACS Energy Letters* **2024**, *9*, 2590-2614.

[33] K. Tang, A. Zhang, T. Ge, X. Liu, X. Tang, Y. Li, *Materials Today Communications* **2021**, *26*, 101879.

[34] C. Fan, R. Zhang, X. Luo, Z. Hu, W. Zhou, W. Zhang, J. Liu, J. Liu, *Carbon* **2023**, *205*, 353-364.

[35] J. Lin, Q. Zhou, Z. Liao, Y. Chen, Y. Liu, Q. Liu, X. Xiong, *Angewandte Chemie International Edition* **2024**, *63*, e202409906.

[36] A. Beda, P.-L. Taberna, P. Simon, C. Matei Ghimbeu, *Carbon* **2018**, *139*, 248-257.

[37] D. Chen, K. Luo, Z. Yang, Y. Zhong, Z. Wu, Y. Song, G. Chen, G. Wang, B. Zhong, X. Guo, *Carbon* **2021**, *173*, 253-261.
[38] P. Zhang, Y. Shu, B. Zhong, L. Yang, X. Guo, *Chemical Engineering Journal* **2024**, *498*, 155231.
[39] L. Liu, X. Sun, Y. Dong, D. Wang, Z. Wang, Z. Jiang, A. Li, X. Chen, H. Song, *Journal of Power Sources* **2021**, *506*, 230170.
[40] Z.-h. Ma, T. Yang, Y. Song, X.-d. Tian, Z.-y. Liu, X.-j. Gong, Z.-j. Liu, *Journal of Colloid and Interface Science* **2024**, *661*, 436-449.
[41] B. Zhong, C. Liu, D. Xiong, J. Cai, J. Li, D. Li, Z. Cao, B. Song, W. Deng, H. Peng, H. Hou, G. Zou, X. Ji, *ACS Nano* **2024**, *18*, 16468-16488.
[42] P. Yu, W. Tang, F.-F. Wu, C. Zhang, H.-Y. Luo, H. Liu, Z.-G. Wang, *Rare Metals* **2020**, *39*, 1019-1033.
[43] M. Thompson, Q. Xia, Z. Hu, X. S. Zhao, *Materials Advances* **2021**, *2*, 5881-5905.
[44] T. Zhang, L. Yang, X. Yan, X. Ding, *Small* **2018**, *14*, 1802444.
[45] X. Du, Z. Zhang, W. Liu, Y. Deng, *Nano Energy* **2017**, *35*, 299-320.
[46] J.-B. Kim, G.-H. Lee, V. W.-h. Lau, J. Zhang, F. Zou, M. Chen, L. Zhou, K.-W. Nam, Y.-M. Kang, *The Journal of Physical Chemistry C* **2021**, *125*, 14559-14566.
[47] H. Wang, F. Sun, Z. Qu, K. Wang, L. Wang, X. Pi, J. Gao, G. Zhao, *ACS Sustainable Chemistry & Engineering* **2019**, *7*, 18554-18565.
[48] B. Zhao, X. Li, L. Shang, C. Qiu, R. Yuan, H. Liu, T. Liu, A. Li, X. Chen, H. Song, *Journal of Materials Chemistry A* **2024**, *12*, 5834-5845.
[49] X. Zhang, R. Duan, T. Zheng, P. Chen, X. Yu, Z. Qiao, D. Ruan, *Chemical Engineering Journal* **2024**, *498*, 155232.
[50] A. Wang, G. Zhang, M. Li, Y. Sun, Y. Tang, K. Sun, J.-M. Lee, G. Fu, J. Jiang, *Progress in Materials Science* **2025**, *152*, 101452.
[51] J. Zhang, B. Yu, Y. Zhang, C. Wang, *Energy Technology* **2020**, *8*, 1901423.
[52] F. Luo, T. Lyu, J. Liu, P. Guo, J. Chen, X. Feng, D. Wang, Z. Zheng, *Journal of Energy Chemistry* **2024**, *92*, 404-413.
[53] X. Lin, Y. Liu, H. Tan, B. Zhang, *Carbon* **2020**, *157*, 316-323.
[54] L. Fan, X. Zhang, L. Fan, L. Yan, Z. Wang, W. Lei, D. Ruan, Z. Shi, *ACS Applied Energy Materials* **2021**, *4*, 11436-11446.
[55] I. El Moctar, M. Diawara, M. Seydou, J. Yu, Y. Ma, H. Huang, S. Li, *Carbon Letters* **2025**.
[56] L. Zhou, Y. Cui, P. Niu, L. Ge, R. Zheng, S. Liang, W. Xing, *Carbon* **2025**, *231*, 119733.
[57] S. Guo, Y. Chen, L. Tong, Y. Cao, H. Jiao, Z. long, X. Qiu, *Electrochimica Acta* **2022**, *410*, 140017.
[58] P. Keerthana, R. Sivasubramanian, N. Priyadharsini, *Inorganic Chemistry Communications* **2025**, *178*, 114417.
[59] T. Zhang, T. Zhang, C. Zhao, F. Wang, L. Zhang, Y. Li, L. Zhang, F. Ran, *Advanced Functional Materials* **2025**, *n/a*, 2425234.
[60] Y.-M. Cao, X. Li, J. Peng, B.-S. Chen, N. Dang, J. Zhang, J.-Y. Xie, T.-B. Zhao, *Langmuir* **2025**, *41*, 9559-9566.

[61] C. Li, L. Yan, M. Wang, J. Kong, W. Bao, L. Chang, *The Chemical Record* **2023**, *23*, e202200216.
[62] S. Liu, J. Zhou, H. Song, *Advanced Energy Materials* **2018**, *8*, 1800569.
[63] J. Shao, X. Wang, G. Shen, P. Xu, L. Xiao, Z. Su, *Applied Surface Science* **2025**, *703*, 163423.
[64] H. Cheng, N. Garcia-Araez, A. L. Hector, *ACS Applied Energy Materials* **2020**, *3*, 4286-4294.
[65] Z. Yan, R. Liu, Z. Long, R. Zhang, K. Liu, W. Li, K. Wang, H. Qiao, *Materials Chemistry Frontiers* **2025**.
[66] M. Wang, Y. Zhu, Y. Zhang, J. Duan, K. Wang, R. Wang, G. Sun, C. Wang, *Journal of Power Sources* **2021**, *481*, 228902.
[67] C. Banerjee, V. K. Chandaliya, P. S. Dash, *Journal of Analytical and Applied Pyrolysis* **2021**, *158*, 105272.
[68] Y. Xue, Z. Ge, F. Li, S. Su, B. Li, *Fuel* **2017**, *207*, 64-70.
[69] Y. Li, W. Yang, Z. Tu, S. Che, C. Xu, H. Liu, G. Huang, Y. Li, *Carbon* **2021**, *182*, 700-710.
[70] T. Zhao, L. Wang, C. Zhang, N. Liu, C. Ouyang, Z. Wang, L. Chen, *Carbon Energy* **2025**, *n/a*, e649.
[71] Y. Li, Y. Yang, R. Lin, C. Zhang, T. Xiao, Z. Ma, Q. Zhang, X. Ma, *Fuel* **2025**, *381*, 133397.
[72] X. Zhang, Z. Yi, Y. Tian, L. Xie, F. Su, X. Wei, J. Chen, C.-M. Chen, *Carbon* **2024**, *226*, 119165.
[73] A. Vasileiadis, Y. Li, Y. Lu, Y.-S. Hu, M. Wagemaker, *ACS Applied Energy Materials* **2023**, *6*, 127-140.
[74] D. Chen, W. Zhang, K. Luo, Y. Song, Y. Zhong, Y. Liu, G. Wang, B. Zhong, Z. Wu, X. Guo, *Energy & Environmental Science* **2021**, *14*, 2244-2262.
[75] J. Zhao, X. Liu, H. Yuan, S. Feng, K. Xiong, X. Xu, Y. Li, G. Yang, *Journal of Power Sources* **2025**, *647*, 237367.
[76] Z. Tang, R. Zhang, H. Wang, S. Zhou, Z. Pan, Y. Huang, D. Sun, Y. Tang, X. Ji, K. Amine, M. Shao, *Nature Communications* **2023**, *14*, 6024.
[77] S. Alvin, C. Chandra, J. Kim, *Chemical Engineering Journal* **2021**, *411*, 128490.
[78] Y. Du, B. Chen, J. Xie, K. Du, *Industrial & Engineering Chemistry Research* **2025**, *64*, 6487-6499.
[79] H. Zhang, W. Zhang, F. Huang, *ACS Applied Materials & Interfaces* **2021**, *13*, 61180-61188.
[80] Z. Hou, D. Lei, M. Jiang, Y. Gao, X. Zhang, Y. Zhang, J.-G. Wang, *ACS Applied Materials & Interfaces* **2023**, *15*, 1367-1375.
[81] Z. Li, C. Bommier, Z. S. Chong, Z. Jian, T. W. Surta, X. Wang, Z. Xing, J. C. Neuefeind, W. F. Stickle, M. Dolgos, P. A. Greaney, X. Ji, *Advanced Energy Materials* **2017**, *7*, 1602894.
[82] A. Patel, R. Mishra, R. K. Tiwari, A. Tiwari, Samriddhi, S. P. Singh, V. Yadav, R. K. Singh, *Energy & Fuels* **2024**, *38*, 11262-11274.
[83] Y. Tang, X. Wang, J. Chen, X. Wang, D. Wang, Z. Mao, *Carbon* **2021**, *174*, 98-109.

[84] Y. Zhao, Z. Hu, C. Fan, P. Gao, R. Zhang, Z. Liu, J. Liu, J. Liu, *Small* **2023**, *19*, 2303296.
[85] Y. Chen, G. Peng, M. Zhao, Y. Zhou, Y. Zeng, H. He, J. Zeng, *Carbon* **2025**, *238*, 120269.
[86] F. Wu, L. Liu, Y. Yuan, Y. Li, Y. Bai, T. Li, J. Lu, C. Wu, *ACS Applied Materials & Interfaces* **2018**, *10*, 27030-27038.
[87] Y. Chu, J. Zhang, Y. Zhang, Q. Li, Y. Jia, X. Dong, J. Xiao, Y. Tao, Q.-H. Yang, *Advanced Materials* **2023**, *35*, 2212186.
[88] P. Fu, S. Hu, J. Xiang, L. Sun, S. Su, S. An, *Journal of Analytical and Applied Pyrolysis* **2012**, *97*, 130-136.
[89] W. Deng, H. Yang, H. Huo, Y. Yu, *Advanced Functional Materials* **2025**, *n/a*, 2504168.
[90] Q. Li, X. Liu, Y. Tao, J. Huang, J. Zhang, C. Yang, Y. Zhang, S. Zhang, Y. Jia, Q. Lin, Y. Xiang, J. Cheng, W. Lv, F. Kang, Y. Yang, Q.-H. Yang, *National Science Review* **2022**, *9*.
[91] A. Kamiyama, K. Kubota, D. Igarashi, Y. Youn, Y. Tateyama, H. Ando, K. Gotoh, S. Komaba, *Angewandte Chemie International Edition* **2021**, *60*, 5114-5120.
[92] W. Li, J. Li, B. W. Biney, Y. Yan, X. Lu, H. Li, H. Liu, W. Xia, D. Liu, K. Chen, A. Guo, *Energy Storage Materials* **2025**, *74*, 103867.
[93] W. Deng, Y. Wang, Z. Chen, H. Huang, C. Chen, B. Pan, Y. Yang, S. He, H. Pan, H. Yang, Y. Yu, *Advanced Functional Materials* **2025**, *n/a*, 2501721.
[94] L. Guo, C. Qiu, H. Liu, R. Yuan, X. Li, X. Li, K. Li, W. Zhu, M. Tabish, X. Liu, A. Li, X. Chen, H. Song, *Chemical Engineering Journal* **2025**, *512*, 162478.
[95] X. Li, S. Zhang, J. Tang, J. Yang, K. Wen, J. Wang, P. Wang, X. Zhou, Y. Zhang, *Journal of Materials Chemistry A* **2024**, *12*, 21176-21189.
[96] E. Olsson, J. Cottom, Q. Cai, *Small* **2021**, *17*, 2007652.
[97] R. Guo, C. Lv, W. Xu, J. Sun, Y. Zhu, X. Yang, J. Li, J. Sun, L. Zhang, D. Yang, *Advanced Energy Materials* **2020**, *10*, 1903652.
[98] F. Wu, R. Dong, Y. Bai, Y. Li, G. Chen, Z. Wang, C. Wu, *ACS Applied Materials & Interfaces* **2018**, *10*, 21335-21342.
[99] Y. Ding, Z.-A. Qiao, *Advanced Materials* **2022**, *34*, 2206025.
[100] Q. Li, J. Zhang, L. Zhong, F. Geng, Y. Tao, C. Geng, S. Li, B. Hu, Q.-H. Yang, *Advanced Energy Materials* **2022**, *12*, 2201734.
[101] E. Memarzadeh Lotfabad, P. Kalisvaart, A. Kohandehghan, D. Karpuzov, D. Mitlin, *Journal of Materials Chemistry A* **2014**, *2*, 19685-19695.
[102] T. Wang, Z. Tian, X. Hu, Q. Liu, L. Wang, W. Liu, Y. Zhou, C. Ma, X. Li, R. Li, *Journal of Power Sources* **2025**, *648*, 237369.
[103] Y. Yang, C. Liu, J. Yao, Z. Tang, Y. Sun, K. Zhang, H. Li, T. Ma, J. Qiu, *Chemical Engineering Journal* **2025**, *503*, 158441.
[104] L. Yuan, Q. Zhang, Y. Pu, X. Qiu, C. Liu, H. Wu, *Advanced Energy Materials* **2024**, *14*, 2400125.
[105] Y. Wang, M. Li, Y. Zhang, N. Zhang, *Chemical Engineering Journal* **2024**, *499*, 156115.

[106] M. Wang, Z. Yang, W. Li, L. Gu, Y. Yu, *Small* **2016**, *12*, 2559-2566.
[107] H. Zhao, J. Ye, W. Song, D. Zhao, M. Kang, H. Shen, Z. Li, *ACS Applied Materials & Interfaces* **2020**, *12*, 6991-7000.
[108] M. Liu, F. Wu, Y. Gong, Y. Li, Y. Li, X. Feng, Q. Li, C. Wu, Y. Bai, *Advanced Materials* **2023**, *35*, 2300002.
[109] X. Wang, J. Ren, Y. Zhu, G. Lan, Y. Huang, J. Wang, J. Liu, J. Dong, C. Wei, N. Huang, D. Nan, *Electrochimica Acta* **2025**, *528*, 146236.
[110] Y. Chen, F. Li, Z. Guo, Z. Song, Y. Lin, W. Lin, L. Zheng, Z. Huang, Z. Hong, M.-M. Titirici, *Journal of Power Sources* **2023**, *557*, 232534.
[111] T. Qi, X. Zhang, K. Xiong, H. Yang, S. Zhang, H. Chen, *Journal of Materials Chemistry A* **2025**.
[112] M. Ma, H. Cai, C. Xu, R. Huang, S. Wang, H. Pan, Y.-S. Hu, *Advanced Functional Materials* **2021**, *31*, 2100278.
[113] aH. Lu, X. Chen, Y. Jia, H. Chen, Y. Wang, X. Ai, H. Yang, Y. Cao, *Nano Energy* **2019**, *64*, 103903; bY. Wang, J. Lu, W. Dai, X. Cheng, J. Zuo, H. Lei, W. Liu, Z. Fu, *Advanced Functional Materials* **2024**, *34*, 2403841.
[114] A. Ponrouch, E. Marchante, M. Courty, J.-M. Tarascon, M. R. Palacín, *Energy & Environmental Science* **2012**, *5*, 8572-8583.
[115] Q. Liu, X. Zhao, Q. Yang, L. Hou, D. Mu, G. Tan, L. Li, R. Chen, F. Wu, *Advanced Materials Technologies* **2023**, *8*, 2200822.
[116] C. Matei Ghimbeu, A. Beda, B. Réty, H. El Marouazi, A. Vizintin, B. Tratnik, L. Simonin, J. Michel, J. Abou-Rjeily, R. Dominko, *Advanced Energy Materials* **2024**, *14*, 2303833.
[117] aM. Qin, W. Ren, R. Jiang, Q. Li, X. Yao, S. Wang, Y. You, L. Mai, *ACS Applied Materials & Interfaces* **2021**, *13*, 3999-4007; bY. Li, S. Xu, X. Wu, J. Yu, Y. Wang, Y.-S. Hu, H. Li, L. Chen, X. Huang, *Journal of Materials Chemistry A* **2015**, *3*, 71-77.
[118] J. S. Gaffney, N. A. Marley, *Atmospheric Environment* **2009**, *43*, 23-36.
[119] P. K. Nayak, L. Yang, W. Brehm, P. Adelhelm, *Angewandte Chemie International Edition* **2018**, *57*, 102-120.
[120] J.-Y. Hwang, S.-T. Myung, Y.-K. Sun, *Chemical Society Reviews* **2017**, *46*, 3529-3614.
[121] D. Schäfer, K. Hankins, M. Allion, U. Krewer, F. Karcher, L. Derr, R. Schuster, J. Maibach, S. Mück, D. Kramer, R. Mönig, F. Jeschull, S. Daboss, T. Philipp, G. Neusser, J. Romer, K. Palanisamy, C. Kranz, F. Buchner, R. J. Behm, A. Ahmadian, C. Kübel, I. Mohammad, A. Samoson, R. Witter, B. Smarsly, M. Rohnke, *Advanced Energy Materials* **2024**, *14*, 2302830.
[122] T. Perveen, M. Siddiq, N. Shahzad, R. Ihsan, A. Ahmad, M. I. Shahzad, *Renewable and Sustainable Energy Reviews* **2020**, *119*, 109549.
[123] Y. Liu, B. V. Merinov, W. A. Goddard, 3rd, *Proceedings of the National Academy of Sciences of the United States of America* **2016**, *113*, 3735-3739.
[124] aX.-F. Luo, C.-H. Yang, Y.-Y. Peng, N.-W. Pu, M.-D. Ger, C.-T. Hsieh, J.-K. Chang, *Journal of Materials Chemistry A* **2015**, *3*, 10320-10326; bL. Xie, C. Tang, Z. Bi, M.

Song, Y. Fan, C. Yan, X. Li, F. Su, Q. Zhang, C. Chen, *Advanced Energy Materials* **2021**, *11*, 2101650.
[125] C. Wu, Y. Yang, Y. Zhang, H. Xu, X. He, X. Wu, S. Chou, *Chemical Science* **2024**, *15*, 6244-6268.
[126] Z. Chen, W. Wei, B.-J. Ni, H. Chen, *Environmental Functional Materials* **2022**, *1*, 34-48.
[127] J. Zhu, C. Chen, Y. Lu, Y. Ge, H. Jiang, K. Fu, X. Zhang, *Carbon* **2015**, *94*, 189-195.
[128] Z. Song, M. Di, S. Chen, Y. Bai, *Chemical Engineering Journal* **2023**, *470*, 144237.
[129] D. C. Marcano, D. V. Kosynkin, J. M. Berlin, A. Sinitskii, Z. Sun, A. Slesarev, L. B. Alemany, W. Lu, J. M. Tour, *ACS Nano* **2010**, *4*, 4806-4814.
[130] R. Blanchard, T. H. Mekonnen, *Journal of Environmental Chemical Engineering* **2022**, *10*, 108810.
[131] R. Nölle, K. Beltrop, F. Holtstiege, J. Kasnatscheew, T. Placke, M. Winter, *Materials Today* **2020**, *32*, 131-146.
[132] K. Wang, Y. Xu, Y. Li, V. Dravid, J. Wu, Y. Huang, *Journal of Materials Chemistry A* **2019**, *7*, 3327-3335.
[133] M. Thommes, K. Kaneko, A. V. Neimark, J. P. Olivier, F. Rodriguez-Reinoso, J. Rouquerol, K. S. W. Sing, *Pure and Applied Chemistry* **2015**, *87*, 1051-1069.
[134] C. Chen, Y. Huang, Y. Zhu, Z. Zhang, Z. Guang, Z. Meng, P. Liu, *ACS Sustainable Chemistry & Engineering* **2020**, *8*, 1497-1506.
[135] H. Ai, J. Qin, Q. Zhou, W. Zhou, J. Xie, K. Du, *Industrial & Engineering Chemistry Research* **2025**.
[136] D. Sun, L. Zhao, P. Sun, K. Zhao, Y. Sun, Q. Zhang, Z. Li, Z. Ma, F. Zheng, Y. Yang, C. Lu, C. Peng, C. Xu, Z. Xiao, X. Ma, *Advanced Functional Materials* **2024**, *34*, 2403642.
[137] Y. Yin, Y. Tan, Y. Lu, Y. Wang, J. Yang, Y. Li, B. Huang, *Journal of Energy Storage* **2025**, *113*, 115649.
[138] Y. Qiu, Y. Su, X. Jing, H. Xiong, D. Weng, J.-G. Wang, F. Xu, H. Wang, *Advanced Functional Materials* **2025**, *n/a*, 2423559.
[139] W. Nie, H. Cheng, X. Liu, Q. Sun, F. Tian, W. Yao, S. Liang, X. Lu, J. Zhou, *Journal of Power Sources* **2022**, *522*, 230994.
[140] H. Zhang, Z. Chen, Z. Sun, M. Cai, W. Liu, W. Ye, H. Gao, J. Han, Y. Cheng, Q. Zhang, M.-S. Wang, *Advanced Functional Materials* **2023**, *33*, 2300769.
[141] K. C. Wasalathilake, G. A. Ayoko, C. Yan, *Carbon* **2018**, *140*, 276-285.
[142] H. Kammoun, B. D. Ossonon, A. C. Tavares, *Nanomaterials* **2024**, *14*, 123.
[143] X. Wang, J. Dong, J. Ren, K. Wang, X. Li, J. Li, J. Tao, *Electrochimica Acta* **2025**, *536*, 146731.
[144] X. Wang, Q. Hu, J. Cui, J. Hou, Y. Huang, X. Liu, *ACS Applied Materials & Interfaces* **2025**, *17*, 12004-12013.
[145] N. Li, H. Li, H. Huang, *Materials* **2025**, *18*, 2397.
[146] S. Li, J. Qiu, C. Lai, M. Ling, H. Zhao, S. Zhang, *Nano Energy* **2015**, *12*, 224-230.
[147] K. Li, J. Zhang, D. Lin, D.-W. Wang, B. Li, W. Lv, S. Sun, Y.-B. He, F. Kang, Q.-H. Yang, L. Zhou, T.-Y. Zhang, *Nature Communications* **2019**, *10*, 725.

[148] Y. Fang, M. Lu, H. Qian, J. Xiang, F. Tu, Y. Jiang, Y. Gan, X. He, H. Huang, X. Xia, Y. Xia, W. Zhang, J. Zhang, *ACS Applied Energy Materials* **2025**, *8*, 8320-8330.
[149] D. Ledwoch, L. Komsiyska, E. M. Hammer, K. Smith, P. R. Shearing, D. J. L. Brett, E. Kendrick, *Electrochimica Acta* **2022**, *401*, 139481.